Study of solar chromosphere: Variation of Calcium K line profiles with solar cycle

A Thesis

Submitted for the Award of the Degree of

Doctor of Philosophy in Physics

To

Mangalore University

by

G. Sindhuja

Under the Supervision of

Prof. Jagdev Singh (Guide)

Indian Institute of Astrophysics

Bangalore - 560 034

India

July 2015

Declaration of Authorship

I hereby declare that the matter contained in this thesis is the result of the investigations carried out by me at Indian Institute of Astrophysics, Bangalore, under the supervision of Prof. Jagdev Singh. This work has not been submitted for the award of any other degree, diploma, associateship, fellowship, etc. of any other university or institute.

Signed: _____

Date: _____

Certificate

This is to certify that the thesis entitled **'Study of solar chromosphere: Variation of Calcium K line profiles with solar cycle'** submitted to the Mangalore University by Mrs. G. Sindhuja for the award of the degree of Doctor of Philosophy in the faculty of Science, is based on the results of the investigations carried out by her under my supervision and guidance, at Indian Institute of Astrophysics, Bengaluru. This thesis has not been submitted for the award of any other degree, diploma, associateship, fellowship, etc. of any other university or institute.

Signed: _____

Date: _____

Dedicated to

my

family and friends...

Acknowledgements

I feel immense pleasure in expressing my sincere gratitude to my supervisor, Prof. Jagdev Singh, for his invaluable guidance throughout the tenure. I am indebted to Prof. Jagdev Singh, for all the wonderful discussions we had and for his patience in explaining me simpler things and his support, without which much of the work in this thesis would not have reached the stage of completion. My special thanks are due to Prof. K. E. Rangarajan, for his guidance and constant encouragement. It was all my pleasure to work with them.

I would like to thank Prof. S. Muneer for supporting me right from the beginning of my career. My special thanks to Dr. Ravindra and Dr. Sankar Subramanian for their support and help in my thesis work. I thank Prof. Dipankar Banerjee and Prof. Ramesh. K.B. for their valuable suggestions. I also thank M. L. Azad for reading the manuscript carefully and making useful suggestion.

I am thankful to the Director, Dean and BGS of our institute for providing me with all the necessary facilities for my research work. I thank Dr. Christina Birdie, Mr. B. S. Mohan, Mr. Prabhahar and the other staff of library for assisting me in accessing books and journals. I thank Dr. Baba Varghese, Mr. Fayaz and Mr. Ashok for their help in computer related issues.

I thank our administrative officer Dr. P. Kumaresan, personnel officer Mr. Narasimha Raju, Accounts officer, Mr. S. B. Ramesh and all other administrative staff for their timely help in completing the admin related work. I would like to thank all kodaikanal observatory staff for their support during my stay at kodaikanal for observations.

I would like to thank all my seniors Bharat, Ramya.S, Ananth, Madhu, Nagaraju, Vigeesh, Blesson, Sreeja. Especially S. Krishna prasad and Girjesh Gupta in helping me learning the solar physics basics and idl basics. I would like to specially thank my dear friends Indu. G and Drisya. K for all their support both personally and academically, whenever needed.

I would like to specially thank my batchmates Arya, Ramya P., Hema, Rathna, Prashanth, Dinesh, Sudha for their help and support during course work and whenever needed. I would like to thank all my juniors Arun, Sasi, Suresh, Manpreet, Susmitha, Honey, Tanmoy. Especially Sajal and Anantha for their help and support and all those who made my stay at IIA memorable.

My sincere thanks are due to Profs. Balakrishna, Vijayakumar, Dharmaprakash of department of physics at Mangalore University, for their help in registration, arranging the colloquium and assisting me in other University related formalities. I also thank Mrs. Anita for providing the required information on official procedures with her prompt responses.

Last but not the least, I would like to thank my parents T. Gunaseelan and G. victoria, my husband Avinash. T.R, my dear little daughter Adithi. A.S and all those who extended their support for the successful completion of this project.

List of Publications

1. Study of meridional flow using Ca-K line profiles during solar cycle 22 and 23
   G. Sindhuja; Singh, Jagdev; Ravindra, B., 2014, *ApJ*, **792**, 22 – 29.

2. Chromospheric variations with solar cycle phase using imaging and spectroscopic studies
   G. Sindhuja; Singh, Jagdev; Priyal, Muthu, 2015, *MNRAS*, **448**, 2798 – 2809.

3. Temporal Variation of Ca-K line profile of the Sun during the solar cycle 22 and 23
   G. Sindhuja.; Singh, Jagdev, 2015, *JA& A*, DOI ,10.1007/s12036-015-9330-4, **36**, 81 – 101

4. Multi-slit spectroscopic observations of the solar corona during total solar eclipse of 11 July 2010
   Samanta. T; Singh, Jagdev;**G. Sindhuja**; Banerjee, D., 2015, Submitted

Presentations

1. Poster presentation in the *Astronomical Society of India meeting 2013*, held at Trivandrum, India, during 21-23 February 2013.

2. Poster presentation in 39^{th} *COSPAR Scientific Assembly*, held at Mysore, India during 14-22 July 2012.

3. Poster presentation in 3^{rd} *Indo-China workshop and* 1^{st} *Asia-Pacific solar physics meeting*, held at Bangalore, India, during 21-24 March, 2011.

4. Poster presentation in the *Astronomical Society of India meeting 2011*, held at Raipur, India, during 23-25 February 2011.

5. Poster presentation in 13^{th} *Young Astronomers Meet*, held at Physical Research Laboratory, Ahmedabad, during 3-5 September 2010.

Abstract

The various features on the solar surface like sunspots, plages, network, active network play a main role in the solar variability. This thesis uses observations which were started in an effort to delineate the role of various features such as plages and networks in the variations of Sun with solar cycle. During 1970s, a new programme to study long term variability of solar chromosphere was started by several researchers. They used Ca-K line profiles of Sun as a star as diagnostic tool to study the long term variability of solar chromosphere. Skumanich *et al.* (1984) proposed a three component model using cell, network and plage areas and using extant laws of limb darkening. During minimum phase of the Sun they were able to reconstruct the observed Ca-K line profile with the contribution from cell and network. But during active phase, the addition of plage component was found to be insufficient to fit the model with observed profiles. Therefore, existence of excess component called as 'Active network' component was introduced during the active phase. Whereas White and Livingston (1978) found no variation in the centre of solar disc with respect to solar cycle phase. Hence, this excess component may be from higher latitudes. In view of the differences in the results of model for the variation of solar activity and observations, a new technique of observing the Sun was planned to take Ca-K line profiles as a function of latitude and integrated over visible longitude since 1986 at kodaikanal Solar Tunnel Telescope on day to day basis for the long period. Which means at each latitude we get the integrated flux over the 180 degree longitudes from all the features like cell, network, plage and active network. The spectra obtained on 807 days were found to be useful and rest of the observations for about 400 days were discarded due to existence of passing clouds which effected the profiles due to scattering of light. On some days spectra of Sun as a star have also been obtained. The variations in sky transparency are compensated by normalizing the profiles. The K_1 and K_2 widths of the Sun as a star, derived for the kodaikanal data agree well with those of Kitt Peak and NSO/Sac Peak on day to day basis with small scatter due to time difference of $\sim$ 12 hours in observation due to location of these observatories.

Further, we found that the average values of K_1 width of Sun as a star during the minimum period of solar cycle 23 are smaller than those during 22 and the K_2 width appear to show an opposite trend. The lower values of K_1 width during the period of 2010 -11 indicating the lower chromospheric emission in Ca-K line during the extended minimum period of solar cycle 23.

The plot of day to day variations in the K_1 and K_2 widths versus plage areas determined from the Ca-K spectrohelio-grams shows that irradiance variations occur not only due to large scale solar activity but also because of variations in some of the three types of network in quiet regions of the Sun. The variation in intensity of the plages can also cause day to day variations in widths that has not been considered at present due to observational limitations.

Further, We have derived Ca-K line parameters such as K_1 and K_2 widths and K-index averaged over regions of 10° latitude and 180° longitudes from the spectroscopic observations and plage areas in these regions from the images of the Sun in Ca-K line. The comparison of Ca-K line widths with plage areas in respective latitude belts shows that small-scale activity due to network areas is very important in the study of irradiance variation with solar cycle phase.

The Ca-K line spectra as a function of solar latitude, indicates that K_1 width attains maximum amplitude at various latitude belts at different phases of the solar cycle.

The FWHM of K_1 distribution at different latitudes shows that its width varies by about 30% for the equatorial belts (<30°) and 11% for the polar regions (>70°) latitude. Interestingly, K_1 width varies by ∼6% only in the 40 - 60° latitude belts during the solar cycle. The analysis of cross-correlation coefficients of K_1 width between 35° latitude and other latitude belts as a function of phase differences indicates that the activity representing toroidal field shifted at a uniform rate of about 5.1 m s^{-1} in northern hemisphere from mid latitudes towards equator. In the southern hemisphere activity shifted at faster rate 14 m s^{-1} in the beginning of the cycle and the speed decreased with time, yielding an average speed of 7.5 m s^{-1}, towards the equator. The shift of activity in the higher latitude belts showed a complex behaviour indicating pole-ward and equator-ward migration.

The K_1 and K_2 widths around 60° latitude belt show far less variation, almost negligible, during the solar cycle 22 and 23 as compared to other latitude belts and polar regions. These variations with latitude and time indicate the presence of two types of activity or flows. We infer the presence of counter flows in the polar regions and probably the existence of multi-cells for the meridional flow.

These findings, less variations in mid latitude belts as compared to polar regions, asymmetry in speed of shift in activity in both hemispheres and complex variation in the direction of shift in the activity representing poloidal fields in mid latitude belts will have important implications on the modelling of solar dynamo. We, recommend that such type of analysis with better resolution and frequent observations will be very useful for solar cycle studies.

Ca-K line profile modelling is one of the method to understand the Ca-K observations quantitatively. We have used RH code by Uitenbroek to model the observed line profiles. The observed line profiles are taken with high resolution spectrograph mainly to study the core of the line profiles and it covers only about 2 Å from the line centre. We tried different atmospheric models (these models were used in solar irradiance modelling to compute the Ca-K line profile). We have determined the Ca-K line parameters from the model Ca-K line profile to compare with the observed. The models FALXCO (cell interior) and FALF (bright network) with assumed contribution were used to model quiet Sun line profiles. For active Sun line profile plage model FALP is used additionally, with contribution of plages measured from Ca-K images taken from kodaikanal observatory. The quiet Sun line profile matches with the model profile [FALXCO + FALF]. But active Sun line profile does not match with the model profile [FALXCO + FALF + FALP]. So the excess component, that is the model profile subtracted from observed profile gives the active network contribution. This measurement of active network contribution will help in solar irradiance modelling.

Contents

Declaration of Authorship ii

Certificate iii

Acknowledgements v

List of Publications vii

Presentations viii

Abstract ix

List of Figures xvi

List of Tables xxi

Abbreviations xxii

1 Introduction 1

1.1 Sun as a variable star 4

1.1.1 Short term variations due to life of features 4

1.1.2 Long term variations due to activity on the Sun 6

1.1.3 Solar UV irradiance variations 7

1.2 Variation due to quiet Sun 8

1.3 Variations in the chromosphere using Ca-K line as a diagnostic tool . . 9

1.3.1 Ca-K line structure 10

1.4 Comparison of Ca-K line features with photospheric structures 13

1.4.1 Ca-K Network and Supergranulation cells 13

1.4.2 Correlation between Ca-K line and photospheric magnetic field 14
1.5 Motivation for the current studies 16
1.6 Outline of the thesis 17

2 Observations and Data analysis **21**
2.1 Introduction 21
2.2 Earlier Observations of Sun as a star 22
2.3 Present Observations as a function of latitude 22
2.4 Data Analysis 26
2.4.1 Analysis of photographic film data 27
2.4.2 Conversion of density to intensity values 27
2.4.3 Comparison of data with three detectors 32
2.4.4 Determination of parameters of Ca-K line 33

3 Temporal Variation of Ca-K line profile of the Sun as a star during the solar cycle 22 and 23 **39**
3.1 Introduction 39
3.2 Determination of Ca-K profiles of the Sun as a star 43
3.3 Comparison of K_1 and K_2 widths of the Sun as a star with those obtained at Sac Peak and Kitt Peak 45
3.4 K_1 and K_2 widths of Ca-K profile and plage areas 49
3.5 Variation of K_1 and K_2 width with solar cycle 50
3.6 Results and Discussions 52

4 Variations as a function of Latitude **57**
4.1 Introduction 57
4.2 Variation of Ca-K line profile with latitude 58
4.2.1 Variation of Ca-K line parameters during Minimum and Active phase 59
4.2.2 North-South asymmetry in K_1 width during minimum phase . . 62
4.2.3 North-South asymmetry in K_2 width during minimum phase . . 63
4.3 Comparison of K_1, K_2 widths variations with other measurements . . . 64
4.4 Variation of K_1 and K_2 widths with latitude and time 66
4.5 Comparison of K_1 and K_2 line widths with Ca-K plage area 71
4.6 Results and discussions 76

5 Study of meridional flow **79**
5.1 Introduction 79
5.2 Further analysis of K_1 and K_2 widths to study meridional flow 81
5.3 Results 82
5.3.1 Long term variation in K_1 and K_2widths at all latitudes 82
5.3.2 Differences in the distribution of K_1 and K_2 widths at equatorial and high latitude belts 83

5.3.3 Phase difference in the maximum activity at different latitude belts 86
5.4 Discussions and Conclusions 90

6 Ca-K line profile modelling **97**
6.1 Introduction 97
6.2 Method 98
6.3 Results and Discussions 100
6.3.1 Model 100
6.3.2 Active network contribution 104

7 Conclusion and Future work **109**
7.1 Important Results 110
7.2 Future direction 113

Bibliography **115**

List of Figures

1.1 A cartoon image showing the different layers of Sun from the central core to outer corona. *Image credit:* `http://astro.unl.edu` 2

1.2 A large sunspot group, observed by the Total Irradiance Monitor (TIM) radiometer in 2003, caused irradiance to decrease by 0.34 percent. Credit: University of Colorado/Laboratory for Atmospheric and Space Physics/Greg Kopp *Image credit:* `http://spacefellowship.com/news` . . 5

1.3 This graph shows the position of sunspots on the Sun during the period from 1870 to 1995. Notice that the centerline, from left to right, is the equator of the Sun and that sunspots happen north and south, above and below this line. Courtesy of NASA. 7

1.4 The Variation of temperature with height in the solar atmosphere. The height ranges over which H-α & Lyman-α, Ca-K & Ca-H and Mg II h and k lines are formed have also been shown in the figure (Vernazza *et al.* 1981a) *courtesy* From the book Guide to Sun by Kenneth Phillips 11

1.5 Ca-K line profile taken using Kodaikanal tunnel telescope. The K line parameters are marked on the line profile. 12

1.6 Plot of non-sunspot pixels as a function of magnetic flux density at disk center ($0.9 < \mu < 1.0$) versus Ca-K emission. 14

1.7 The filter-gram in Ca-K line taken on June 10, 2007 during the declining phase of the solar cycle, using the SOLIS- PSPT telescope. *Courtesy* SOLIS-PSPT images 15

2.1 An example of a sunchart for the heliographic latitude (B_0) of 5.5° showing the latitudes marked at an interval of 10° 24

2.2 The histogram indicates the number of days of observations made in each year. 27

2.3 *Top*: Raw image of the step wedge taken for 20 second exposure. *Bottom*: The selected box region for calculation of the average density values for each step. 28

2.4 *Left*: After taking average along the rows (wavelength axis) of Figure 2.3 *Right*: The diamond symbols show the distribution of density difference obtained by subtracting adjacent values of average density represented by the curve in the left panel to find the beginning and end of each step. The multiple Gaussian fit to the distribution is over plotted to determine the six steps and their average density values. 29

2.5 *Left*: The steps are extracted using Gaussian fitting. The brighter region has more % of density and intensity as compared with the darker region. *Right*: The intensity vs density plots for step wedge calibrations for the exposures 6,10,15 and 20 seconds. 30
2.6 The plot shows final and extended density versus intensity values for the data taken on January 20, 1997 along with a polynomial fit(solid line) 31
2.7 *Left*: shows the typical observed spectrum on density scale taken on January 20,1997 after the dark and flat field correction and *Right*: shows the same spectrum in the intensity scale obtained using the coefficients of polynomial fit of the calibration curve for that day. 31
2.8 The figure shows the averaged Ca-K line profiles for the 0.25 and 10° spatial intervals for the three types of detectors used, The intensity values in case of averaging over 0.25° spatial locations have been decreased by 0.02 to separate out two line profiles. *Top Left*: data taken on march 15, 2006 using Photometrics CCD, *Top Right*: data taken on March 22, 2005 using Andor CCD, *Bottom*: data taken using the photographic film on January 05, 1994. 32
2.9 The solid line in top and bottom panel shows a normalized averaged observed Ca-K line profile taken on march 08, 2007 for 0-10° south latitude and integrated over the 180° longitude. *Top*: The chosen intervals to find the Ca-K line parameters are over plotted with the values obtained from the 3-degree polynomial fit in different colors The alternative minimum and maximum of these interval gives K_{1v}, K_{2v}, K_3, K_{2r} and K_{1r} locations on the profile respectively. *Bottom*: The crosses (stars) marked on the normalized average Ca-K line profile indicate the maxima and minima locations computed from the polynomial fits and the locations to derive the Wilson-Bappu width of the line. 34

3.1 Variation of Ca-K index with the phase of solar cycle during the period of 1974-80 as determined by White and Livingston (1981) from the spectroscopic observations of Sun as a star. *Courtesy*: White and Livingston (1981) 42
3.2 The observed Ca-K line profiles for the plage and quiet region of the Sun. *Courtesy*: White and Livingston (1981) 42
3.3 *Left*: Plot of average values of K_1 width derived from the values at all the latitudes vs values obtained from the observations of the Sun as a star shown along with linear fits(blue) and quadratic fits(red). *Right*: For K_2 width. The χ^2 test indicates that a quadratic fit represents a better relation. 45
3.4 *Top left*: shows the scatter plot of the residual values after removal of outliers and cyclic variations in the measurements of K_1 width for the Kodaikanal data vs that of NSO/Sac Peak data along with a linear fit. *Top right*: Residuals of K_1 width for Kodaikanal vs Kitt Peak and *Bottom*: for the data of Kitt Peak vs NSO/Sac Peak values along with linear fit. The values of correlation coeffcients (R) are written in each panel. . 47

3.5 Same as that for the Figure 3.4 but for the K_2 width of Ca-K line profile. 48
3.6 *Left*: Scatter plot of K_1 widths versus measured plage areas in millionth of the solar disc *Right*: Same for K_2 width 49
3.7 *Top left*: Variation of K_1 width with time after outliers removal. *Top right*: Variation of K_2 width with time after outliers removal. *Bottom*: Variation of K_1 to K_2 width ratio with time. The black circles show the day to day data and the red solid line shows the yearly mean values along with standard deviation by bars on yearly basis. 51

4.1 Figure shows the normalised Ca-K line profile averaged over 10° in latitude and 180° in longitude at an interval of 10° for Northern (blue) and southern latitudes (red). The bottom most curve at 80° south has the original normalized values and successive curves have been offset by 0.01 in intensity. The top most curve is for 80° north latitude. The separation between two astericks and two diamonds gives the K_1 and K_2 width, respectively 59
4.2 Average of Ca-K line parameters K_1, K_2, wilson-bappu widths, K1.0, K0.5 index, K_3 intensity and K_{2v}/K_3, K_{2v}/K_{2r} ratios for few days in March, 2007 (minimum phase of solar cycle) when no Sunspots or plages were visible. Standard deviation is shown as bars which is not due to the error but because of day to day variation in solar activity. . . 60
4.3 Average of Ca-K line parameters K_1, K_2, Wilson-Bappu widths, K1.0, K0.5 index, K_3 intensity and K_{2v}/K_3, K_{2v}/K_{2r} ratios for few days in March, 2000 (active phase of solar cycle). Standard deviation is shown as bars which is not due to the error but because of day to day variation in solar activity. 61
4.4 Figure shows average K_1 width over 10° latitude and 180° longitude as a function of latitude, separate polynomial fits to the southern and northern hemisphere is also shown in Figure. 62
4.5 Figure shows average K_2 width over 10° latitude and 180° longitude as a function of latitude, separate polynomial fits to the southern and northern hemisphere is also shown in Figure. 64
4.6 The figure shows the K_1 and K_2 widths of Ca-K line as a function of distance from disc center in degrees. Triangles show K_2 width at the central meridian as a function of latitude, diamonds show K_2 width for each latitude but integrated over the longitudes and asterisks indicates K_2 width determined by Engvold (1966) with longitude. K_1 width without and with integration over the longitudes are shown by squares and crosses , respectively. 65
4.7 Variation of K_1 width of Ca-K line with time for the period of 1985 -2011 shown by dots. Over plotted are half yearly mean data (red asterisk) and half yearly averaged sunspot number (black line) for the northern hemisphere. 66
4.8 Same as Figure 4.7 but for the southern hemisphere. 67

4.9 Distribution of K_1 width of Ca-K line profile for the active period for different latitude for both the hemispheres. Histograms in blue and red are for northern and southern hemispheres. Latitudes of histogram is noted in the top left corner of each panel. 68
4.10 Same as that of figure 4.9 but for minimum phase of the solar cycle. . . 69
4.11 *Left* shows most probable value of K_1 width defined by the peak of Gaussian fit for the active phase in red and for minimum phase in black. *Right* shows range of K_1 width defined by the FWHM of the Gaussian fit to the distribution of K_1 widths. 70
4.12 Same as that for figure 4.11 but for K_2 width 70
4.13 Mean K_1 width as a function of latitude for cycle 22 to see the yearly variation. The year for the plot is indicated in each panel. 72
4.14 Same as that of figure 4.13 but for cycle 23 73
4.15 *Left* Plot of K_1 width vs plage area in millionth of solar disc for 5°, 15°, 25° and 35° north latitudes for the years 1989 - 1992 and 2000 - 2005 around the active phase *Right* Same for southern hemisphere 74
4.16 Same as that for Figure 4.15 but for K_2 width. 75
4.17 *Left* K_1 - width of Ca-K line versus intensity ratio of K_{1v} / K_{1r} for all the data for latitude up to 40°n at an interval of 10° for the northern hemisphere. *Right* Same for southern hemisphere 76

5.1 The K_1 widths as a function of time are plotted for all the latitudes for period of 1989 - 2011, at an interval of 10° in the northern hemisphere on day to day basis (black dots). Half yearly mean values of K_1 width are shown as red asterisks and the half yearly Greenwich averaged Sunspot numbers (solid line) are also shown for comparison. Average latitude of the data is indicated at top right side in each panel. 83
5.2 Same as Figure 5.1 but for the southern hemisphere. 84
5.3 The K_2 widths as a function of time are plotted for all the latitudes for period of 1989 - 2011, at an interval of 10° in the northern hemisphere on day to day basis (black dots). Half yearly mean values of K_1 width are shown as red asterisks and the half yearly Greenwich averaged Sunspot numbers (solid line) are also shown for comparison. Average latitude of the data is indicated at top right side in each panel. 85
5.4 Same as Figure 5.3 but for the southern hemisphere. 86
5.5 Histograms of the distribution of K_1 widths in blue and red are for northern and southern hemispheres respectively with bin size of 0.015 Å . Gaussian fit curves are also plotted in respective colours. The mean latitude of the distribution is shown in each panel. 88
5.6 Histograms of the distribution of K_2 widths in blue and red are for northern and southern hemispheres respectively with bin size of 0.007 Å . Gaussian fit curves are also plotted in respective colours. The mean latitude of the distribution is shown in each panel. 89

5.7 The cross-correlation coefficients of K_1 width at 35° latitude with that at other latitude belt as a function of phase difference. *Top left* CCs is for 5° (blue), 15° (red), 25° (green) and 80° (purple) northern belts with 35° northern latitude belt and *Bottom left* CCs is for 45° (blue), 55° (red) and 65° (green) northern latitude belts. *Top and bottom right* are for southern hemisphere. Solid curves are polynomial fits to the coefficients. 90
5.8 The cross-correlation coefficients of K_1 width for various latitudes with K_1 width at adjacent latitude belts as a function of phase difference. *Top left* is for 15° (blue), 25° (red), 35° (green) and 45° (purple) northern belts with adjacent northern latitude belt and *Bottom left* for 55° (blue), 65° (red) and 80° (green) northern latitude belts. *Top and bottom right* are for southern hemisphere respectively. Solid curves are polynomial fits to the coefficients. 92

6.1 figure illustrating the geometry of the observing system. 99
6.2 *Top*: Temperature vs Column mass in log scale for the different models C, F and XCO *Bottom*: Similarly Electron density vs Column mass . . . 102
6.3 comparison of computed profile for different models with observed profile shown in different colours 103
6.4 Variation of K_1 width with latitude for model (FALXCO (75%) + FALF (25%)) and observed line profiles 105

List of Tables

2.1 Comparison of the data obtained with three different detectors 33

3.1 Statistics of the line parameters after removal of outliers considering the 2σ level variations. 46
3.2 RMS variations in the scatter plot of the K_1 and K_2 widths measured for three observatories. 48
3.3 Average K_1 and K_2 widths during minimum and maximum phase . . . 52

4.1 The most probable values of K_1 width defined by the peak of Gaussian fit to the frequency distribution of widths and range of the values defined by the FWHM of Gaussian fit for K_1 and K_2 widths for minimum and active phase as a function of latitude. 68
4.2 Remnant K_1 and K_2 width representing the plage free chromosphere . . 74

5.1 List of mean $\pm$ σ values and range of widths (maximum - minimum) derived from daily data after removal of outliers with 2σ level cutoff and FWHM derived from the Gaussian fit to the distribution of K_1 and K_2 width for various latitudes. 87
5.2 Table lists the maximum value of cross-correlation coefficients between two belts, significance level in % and the phase difference in months. . 91
5.3 Table lists the maximum value of cross-correlation coefficients between two belts, significance level in % and the phase difference in months. . 91

6.1 The Table shows the computed K_{2v}/K_{1v} ratio and K_{2v}/K_3 ratio from the model profile, the fifth row of the table shows the ratios for observed profile 104
6.2 Contribution of model used 106
6.3 Calculated active network contribution using K_1 width (in Å) 106

Abbreviations

NASA	**N**ational **A**eronautics and **S**pace **A**dministration
SOLIS	**S**ynoptic **O**ptical **L**ong-term **I**vestigations of the **S**un
PSPT	**P**recision**S**olar **P**hotometric **T**elescope
NSO	**N**ational **S**olar **O**bservatory
TSI	**T**otal **S**olar **I**rradiance
CCD	**C**harge **C**oupled **D**evice
UT	**U**niversal **T**ime
UV	**U**ltra **V**iolet
MDI	**M**ichelson **D**oppler **I**nterferometer
KTT	**K**odaikanal **T**unnel **T**elescope
SOHO	**SO**lar and **H**eliospheric **O**bservatory

Chapter 1

Introduction

The Sun is a main sequence star of average mass, luminosity and effective temperature - one of about 10^{11} stars in our milky way galaxy. The Sun, like any other main sequence stars, supplies its energy needs by conversion of hydrogen to helium. Although the Sun is in the gaseous state completely but density and temperature of the gas change drastically as you travel from the center to the outermost regions. Figure 1.1 shows the internal structure of the Sun, which has been modelled from different observations of the solar surface and different features of the solar surface and its atmosphere.

The CORE starts from the center and extends outward up to 25% of Sun's radius. The Sun's core has a very high temperature about 15 million degrees Kelvin and density is as high as 150 gcm^{-3} because of high pressure from the outer layers. The high temperature and density provide the core an environment for nuclear reactions. The conversion of four protons to Helium nucleus in the nuclear reactions produces high energy photons, the energy source of the Sun.

Then the high energy photons travel from core to the outer part of the Sun through radiative transfer process. In this process, photons are absorbed and re-emitted and their energy decreases. Approximately 10^{25} absorptions and re-emissions take place in this zone before a photon reaches the surface. Therefore, there is a significant time

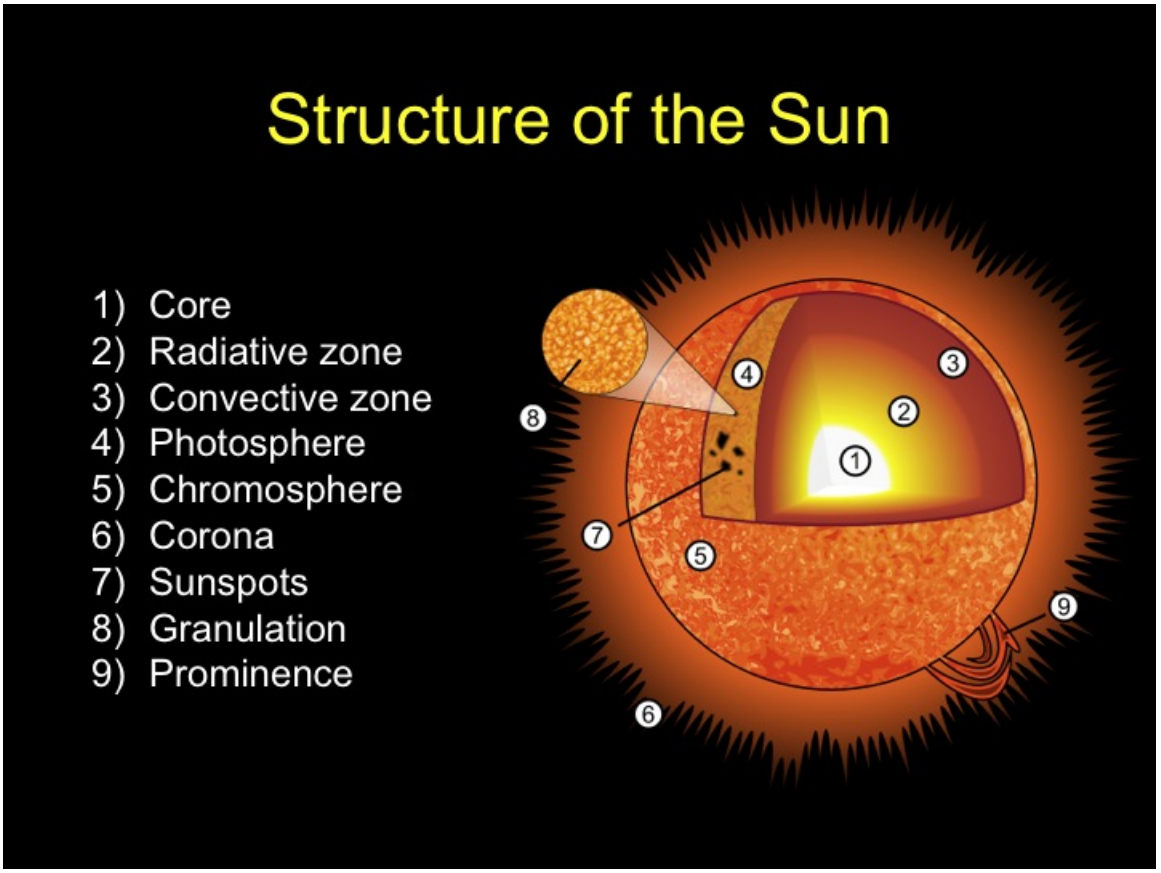

FIGURE 1.1: A cartoon image showing the different layers of Sun from the central core to outer corona. *Image credit:* http://astro.unl.edu

delay between a photon generated in the core and one that reaches the surface. The region surrounding the core of the Sun is called RADIATION ZONE. This layer is not as dense as the core, and the temperature is also relatively cooler (about 5 million degrees kelvin). This Zone extends outward from the core, accounting for 45% of the Sun's radius.

The temperature goes on decreasing as one moves away from the core to the surface. Outside the radiation zone the temperature is relatively cooler and decreases to ~2 million degrees Kelvin. Due to decrease in temperature more elements are able to hold more number of electrons and make it difficult for the photons to travel outward. Therefore, the plasma gets heated up and the heated plasma starts to move up beginning the convection. The zone between the radiation zone and surface is dominated by convective currents that carry the energy outward to the surface. This zone known as CONVECTION ZONE extends outward from the Radiative zone and accounts for

the final 30% of the Sun's radius.

The core, the radiation and the convection zones make up the interior of the Sun. The Sun's atmosphere is composed of photosphere, chromosphere and corona.

The PHOTOSPHERE is the lowest region of the Sun's atmosphere visible to our eyes. The photosphere is also known as surface of the Sun. It has an average temperature of 5800 degrees Kelvin. The rising and falling of hot and cool bubbles are called convective cells. These cells produce a pattern on the surface of Sun known as GRANULATION. The dark spots observed on surface called SUNSPOTS are relatively cooler than the surrounding gas. The number of sunspots seen on the surface of the Sun increases and decreases in a regular pattern known as the solar cycle. The inner-most portion of the sunspots is known as Umbra and surrounding region is called Penumbra. These regions have large magnetic field of a few thousand Gauss.

The CHROMOSPHERE begins outward after the photosphere has an average thickness of about 2000 kms. The temperature starts rising with distance and rises to about 10000 degree K at the top of the chromosphere from 4500 degrees K at the base of the chromosphere. Chromosphere can be easily observed through a filter that isolates H-alpha, Ca-K lines, etc and during the total solar eclipse. The larger scale convection called super-granulation can be seen in the chromosphere by observing in Ca-K line or in Dopplar-grams taken in number of lines such as NaD, MgI and some others. The vertical velocity ~2 km/s dominates in the granulation whereas horizontal velocity of about 0.3 km/s from the centre of the cell to its boundary exists in the super-granules. Many features can be seen in this layer which include chromospheric network of magnetic elements, bright plages around sunspots, dark filaments across the disk and PROMINENCE above the limb.

CORONA is the outermost atmosphere of the Sun and is about million times fainter than the center of the solar disc. It can be observed during total solar eclipse and by using Coronagraph telescopes, which simulates an eclipse by covering the bright solar disk. Coronal gas is super heated to temperatures greater than 1 million degrees kelvin. The corona displays a variety of features including streamers, plumes and loops. These structures are formed as a result of movement of the electrons along the

magnetic field lines.

1.1 Sun as a variable star

The Sun is one of the major players in driving global change, through the variation of its total brightness, its spectrum and magnetic field. In 1843 Schwabe was the first to recognize the variability of the Sun in the form of 11 year variation in sunspot number. In 1934 Abbot tried to study the variability of the Sun by ground based solar radiometry but day to day variation in the sky transparency made it difficult to get the reliable results. However, measurements of 10.7 cm radio flux in the mid-20th century opened what might be called the modern era in the study of solar variability. Total irradiance means that the solar flux has been integrated over all wavelengths to include the contributions from ultraviolet, visible and infrared radiation. The reliable measurements of total solar irradiance started with various space programs to perform the radiometry from space base instruments such as ACRIM, SMM and others (Willson 1989). The ultimate goal is to uncover how and why the Sun is changing, in order to reconstruct and predict the solar-induced climate changes (Pap *et al.* 1997).

The variations at the Sun occur at all time scales from seconds to years. The dynamics and life time of short lived features of the Sun produce short term variations whereas solar activity and dynamo processes are responsible for the long term variations of the Sun. The solar rotation also introduces periodicity of $\sim$ 27 days, rotation period of the Sun.

1.1.1 Short term variations due to life of features

on the Sun Variation in the intensity of small scale features and their limited life time produces short term variations. For example, the granulation life of $\sim$ 10 minutes, meso-granulation life of few hours, average life of super-granulation of $\sim$ 20 hours and sunspots with lifetime ranging from few hours to months, produces variations

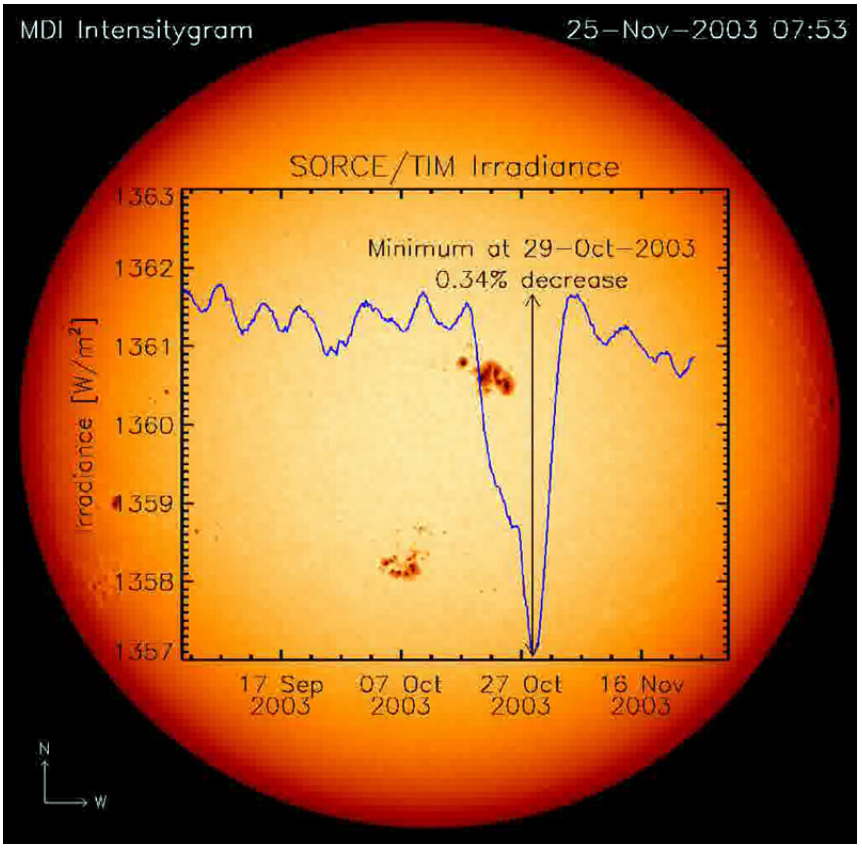

FIGURE 1.2: A large sunspot group, observed by the Total Irradiance Monitor (TIM) radiometer in 2003, caused irradiance to decrease by 0.34 percent. Credit: University of Colorado/Laboratory for Atmospheric and Space Physics/Greg Kopp *Image credit:* http://spacefellowship.com/news

with times according to their lifetimes locally. Some of these average out on global scale but a few of these show effects on the global scale also. For example it has been found that a sunspot when crosses the solar meridian, causes a dip in the solar irradiance as seen from Figure 1.2. On November 27, 2003 a radiometer aboard NASA's Solar Radiation and Climate Experiment (SORCE) satellite observed large sunspot patches that caused irradiance to drop by as much 0.34 percent, the largest short-term decrease ever recorded. The sunspots are cooler than the surrounding regions of Sun's surface at a temperature of 3000-4000K. Another contributor for the short term variation of the Sun are the faculae. The faculae are bright regions surrounding the dark sunspots and have lifetime of several days to months. The sunspots decrease the solar radiation output, whereas faculae increase the solar radiation output, relatively, to a large extent causing net increase in the solar radiation output during active phase (Foukal and Lean 1988). The magnetic network and the related features are

also likely to cause short term variations in the Sun ranging between seconds to days (Foukal *et al.* 2006).

1.1.2 Long term variations due to activity on the Sun

Even though each sunspot lives for short duration of few days to few months but their numbers visible on the solar surface at any given time vary with an average period of 11 years popularly known as solar cycle. The sunspots appear at the mid latitude around 40 degrees in the beginning of cycle and then appear at lower and further lower latitudes as the cycle progresses. This behaviour of appearance of sunspots at latitude is called Sporer's law and its regularity is best demonstrated in the butter-fly diagram as seen in Figure 1.3. Hale discovered the magnetic fields of sunspots by observing the Zeeman splitting in some of the solar absorption (Fraunhoffer) lines . Hale (1919) showed that in the 11 period of the solar cycle, all the sunspot groups in a given hemisphere, have one magnetic polarity that leads and the opposite follows, while in the other hemisphere the situation is reversed. The solar cycle related variation of total solar irradiance is attributed mainly due to the appearance of sunspots and related activity (Foukal and Lean 1988). The variation in the chromospheric irradiance is mainly caused by (1) plages surrounding sunspots, (2) changing emission of bright magnetic elements and a third component, the so called 'active network', which was introduced to explain the long term variation in the Ca-K line (Foukal and Lean 1988). After a solar cycle, the polarity at both the solar poles and that of leading and following sunspots in both the hemispheres reverses during the next solar cycle. This means north magnetic field becomes the south, and vice versa. Thus the magnetic cycle has a period of about 22 years whereas the sunspot cycle is of half of this period $\sim$ 11 years.

Apart from these periodicities in the Sun, some very long period variations in the sunspots' numbers have been observed such as Maunder's minimum. During the beginning of seventeenth century, for about 50 years the sunspots did not appear on the solar surface. The variation in the surface magnetic field is the major cause in the variations in the appearance of the Sun and solar features. These variations are likely to be triggered by the variation in the characteristics of solar interior. The variations

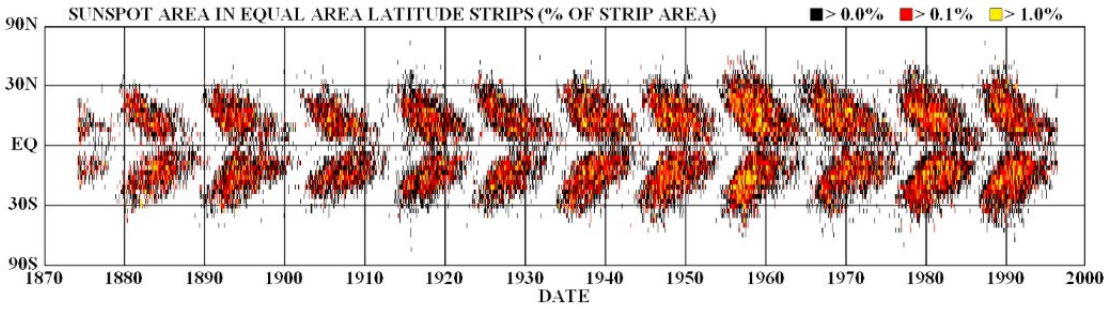

FIGURE 1.3: This graph shows the position of sunspots on the Sun during the period from 1870 to 1995. Notice that the centerline, from left to right, is the equator of the Sun and that sunspots happen north and south, above and below this line. Courtesy of NASA.

in the strength of magnetic fields may give rise to variations in the luminosity of the Sun.

1.1.3 Solar UV irradiance variations

Determining the details of the solar UV spectrum and its variability is important to our understanding of both the structure of the solar atmosphere and the impact of solar variability on the terrestrial climate. Number of experiments have been done to measure emission from the solar UV spectrum since the late 1970s (Woods *et al.* 1996; Cebula and Deland 1998; Thuillier 2004; Floyd *et al.* 1998). The empirical modelling of spectro-radiometric observations indicates that the variability of solar ultraviolet flux (FUV) at wavelengths shorter than approximately 250nm, is determined mainly by APN (Area of plages plus active network) alone (Lean 1989; Solanki and Unruh 1998; Lean 1997). The different behaviour occurs because, the photometric contrast of plages increases with decreasing wavelength and the contribution of the plages dominates in the UV wavelengths than that of sunspots. The bright magnetic features overcompensate the effect of sunspots and give the primary source of long term irradiance variations They are also of interest for climate studies because variations in the total solar irradiance measured from a satellite plat-form must be separated into different parts of the solar spectrum incident on the earth's surface and the solar UV spectrum at wavelengths less than 300 nm that is absorbed in the earth's atmosphere. Slightly more than 60% of the variation in total irradiance is in the UV region of the

spectrum (Morrill *et al.* 2011). This difference in variability suggests that although only 1% of the Sun's electromagnetic energy is radiated at wavelengths shorter than 300 nm, variations in these radiations may contribute significantly more than 1% of the variations to the Sun's total irradiance.

The magnitude of the Sun's UV irradiance variations over the 11-year cycle becomes approximately twice at Lyman-alpha (121.6 nm), decreasing to 10% at 200 nm, 5% at 250 nm, and less than 1% at wavelengths longer than 300 nm (SME instrument). The measurements of irradiance variations at wavelengths from 300 to 400 nm, which may account for some 13% of the total irradiance variability, have yet to be made with sufficient precision to permit a reliable evaluation of the contribution of this spectral region to total irradiance variability or to establish the relative roles of sunspots and faculae for understanding either the day-to-day variations or the solar cycle trends (Lean 1989). Krivova and Solanki (2005) empirically found that around 60% of the total irradiance change between solar minimum and maximum is produced in the UV part of the spectrum, i.e., short-ward of 400nm, although only 8% of the radiations are emitted at these wave-lengths (Solanki and Krivova 2006). This result suggests that more attention should be paid to the influence of the Sun's varying UV radiation on the Earth's atmosphere (Haigh and Blackburn 2006; Schmidt and Brasseur 2006).

1.2 Variation due to quiet Sun

Measurements with radiometers on board satellites launched during the last three decades (NIMBUS-7, SMM, UARS, EURECA, SOHO) have revealed that the total irradiance, also referred to as the solar constant, changes on a variety of time-scales. Solar irradiance variations on scales of up to the solar activity cycle length are closely related to the evolution of the solar surface magnetic field, because the emergence and evolution of active regions on the surface cause changes in irradiance (Lean *et al.* 1998; Fligge and Solanki 2000b). Sunspots and active region faculae are considered to be the dominant contributors to solar irradiance changes on time scales of days to weeks. Space-based irradiance records have also established variation of about 0.1% of the irradiance in phase with 11-year solar activity cycle, irradiance being more

during the maximum phase. Thus, the net increase in irradiance caused by the active regions results in a brighter Sun around activity maximum (Chapman 1987; Willson and Hudson 1988). The origin of the long-term variation of the irradiance between activity minimum and maximum is still widely debated. In addition to contribution from large scale activity, the observations indicate that small-scale magnetic elements that compose the enhanced and quiet network contribute substantially to the observed irradiance increase during activity maximum (Foukal and Lean 1988; Solanki *et al.* 2001; Fligge and Solanki 2000a; Ortiz *et al.* 2002). White (1996) showed that lyman-α irradiance come from less active solar areas and contribute 80% to the spectral irradiance in this line. Ermolli *et al.* (1999) found that contribution to TSI due to quiet network is about 10^{-4}, assuming a constant network contrast over the disk. There is a small increase in the quiet region magnetic field 2.8 G at minimum to 3.8 G at solar maximum Withbroe (2006). This causes the change in the intensity of bright points in the quiet regions due to the evolution of the network as the magnetic elements in active regions faculae break up and disperse over the disk (Skumanich *et al.* 1984). Further, the study by Withbroe (2006) using the spatially resolved measurements of the intensity of the photospheric continuum by MDI onboard SOHO, shows that 50% or more of the long term variations in TSI is due to changes in the brightness of the quiet Sun. The weak changes in the irradiance levels at minima are believed to be occuring due to the changes in the weak background magnetic flux (Solanki and Fligge 2002; Krivova *et al.* 2007). Number of network bright points during solar maximum exceeds that during solar minimum on an average by about 30% (Sivaraman 1984).

1.3 Variations in the chromosphere using Ca-K line as a diagnostic tool

The Ca-K line profiles and images are one of the best diagnostic tools to study the solar chromosphere and its variability with space and time. Irradiance variations in Ca-K line have been studied by many researchers using long series of spectroheliograms obtained at Kodaikanal, Mount Wilson, Sac Peak and other observatories (Tlatov *et al.* 2009; Foukal *et al.* 2009; Ermolli *et al.* 2009b; Priyal *et al.* 2014)[and

references therein] using plage areas as a proxy to the chromospheric irradiance variation. Worden *et al.* (1998) analyzed 1400 spectroheliograms obtained at the National Solar Observatory, Sac Peak spread between the period of 1980 -1996 to identify the different features such as plages, enhanced, active and quiet network using the intensity contrast technique to study the rotational modulation and solar cycle variations in the chromosphere. Walton *et al.* (2003) concluded that faculae are responsible for 80% of the solar cycle variations whereas Ermolli *et al.* (2003) estimated that during the ascending phase of the solar cycle (1996-2002) the network contributed 40-50% to the solar cycle variations. Following this work Priyal *et al.* (2014) digitized the spectroheliograms obtained at Kodaikanal Observatory and analyzed the data for three solar cycles (1955- 1985) and found good correlation with the Mount Wilson data and sunspot number. The various properties of the line and how it can be used for the long term variability studies of the chromosphere are described in the following:

1.3.1 Ca-K line structure

The Ca-K line is one of the strongest absorption lines in the visible wavelength part of the solar spectrum. Popularly known as Ca-K and Ca-H lines are the resonance doublet lines due to singly ionized calcium at 3933.6 Å and 3967.7 Å , respectively. These are the strongest spectral lines of the optically accessible part of the solar spectrum because of abundance of calcium at the solar surface and most of calcium element resides in the singly ionized ground state throughout the photosphere and lower chromosphere. First observed by Joseph Fraunhofer in 1814, this line was designated as K in his catalogue of prominent absorption features. Hale and Ellerman (1904) introduced the designations K_3 for the central absorption, and K_2 for the emission features on both sides of the central absorption, and K_1 for the minimum in the profile wings beyond the emission as seen in Figure 1.5. The different parts of these lines represent different depths of the chromosphere because of optical depth and temperature. The core of the Ca-K line (K_3) is formed at a height of $\sim$ 1900 km, above the base of photosphere as shown in Figure 1.4 for the modelled 'average quiet Sun'. It shows the temperature variation with height from the base of the photosphere to the beginning of the transition region, about 2300 km height above the

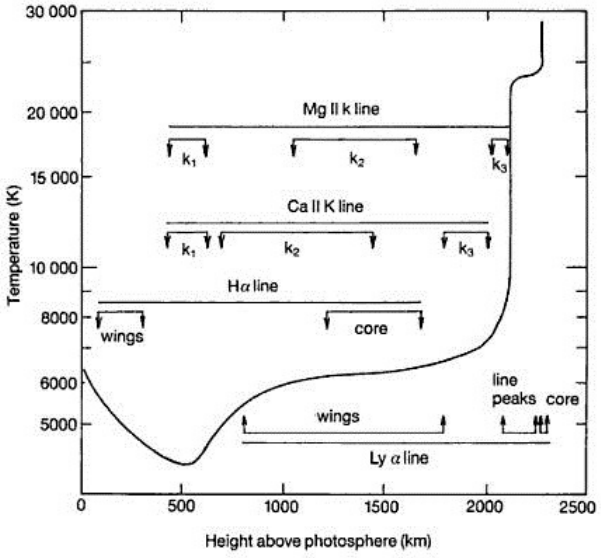

FIGURE 1.4: The Variation of temperature with height in the solar atmosphere. The height ranges over which H-α & Lyman-α, Ca-K & Ca-H and Mg II h and k lines are formed have also been shown in the figure (Vernazza *et al.* 1981a) *courtesy* From the book Guide to Sun by Kenneth Phillips

photosphere. The temperature minimum at 500 km height is evident, as is the rise above this level to the chromosphere and the extremely rapid rise at a height of 2000 km or so. The chromospheric regions where various parts of the line profiles of Hα, Ca-K, Mg-k and Lyman-α lines are formed have been indicated in the Figure 1.4. The kinetic temperatures describing the motion of particles representing different lines are at higher than the photospheric temperature of $\sim$ 6000 K by few hundred to few thousands degrees. The source function for the K line reflects the value of local temperature of the region. The temperature rises with height from the temperature minimum out into the chromosphere. This results in an increase in the K line source function, at least over a certain height range. Eventually at a height of about 1900 km, the source function again decreases owing to the effects of the scattering terms in the source function. The increase in the source function at chromospheric heights causes existence of two bumps in the line profile near its core (Figure 1.5). For the K line, these emission peaks are called K_{2v} (on the violet side of the line core) and K_{2r} (red side). Their prominence is strongly related to solar activity, since in case of activity on the Sun, the collisional terms of the source function increase. The 'self-reversal' core called K_3, is formed highest in the chromosphere (altitude of about 1900 km, where the source function again decreases). The wings called K_1, are formed near the temperature minimum. They extend over a wide wavelength range

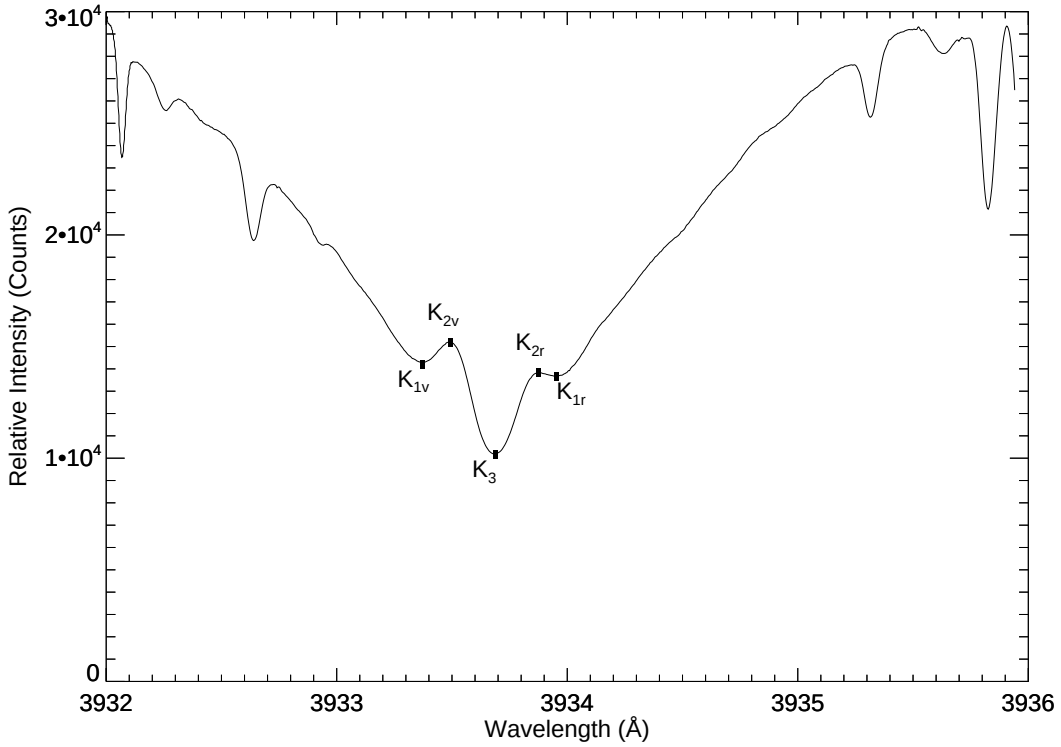

FIGURE 1.5: Ca-K line profile taken using Kodaikanal tunnel telescope. The K line parameters are marked on the line profile.

(392-395 nm) such that many other absorption lines due to other elements are superimposed on the K line profile. Images taken at K_2 emission peaks and the K_3 core show the mid-chromosphere, and the K_1 wings show the region of the temperature minimum. Smith (1960) finds that although the separation of the K_1 features is larger in plage profiles, the separation of the K_2 peaks is narrower. In the asymmetric Ca-K line profile, the K_{2v} emission is usually greater than K_{2r} emission and the intensity fluctuations increase with spatial locations from K_1 to K2 and K_3 images of the Sun Jewell (1896). The broader profiles of Ca-K in plages suggest an increase in the turbulent broadening due to larger temperature of plage regions than those of quiet Sun. Athay and Thomas (1961) suggest that perturbations in the physical properties of plages relative to the quiet chromosphere are probably due to a coupling of the kinetic energy of the gas with the enhanced magnetic field observed to be as large as 200G Leighton (1959). Liu and Smith (1972) found about 80% of the area in the

chromosphere produces profiles with K_2 emission peaks and 20% of it produces virtually un-reversed absorption profiles of the K line. Statistically they found that 50% of the profiles (K_{232}) are double peaked with the preferred location at the network boundary. Further, 20% have K_{2v} single peak with preferred location of bright points in network cells and 10% have K_{2r} single peak, preferably from bright points in cells and the remaining profiles $\sim$ 20% are without emission peaks with preferred location in dark region of network cells. The reason for the asymmetry of the K_2 emission peaks is due to the non-homogenous and non-static nature of the solar chromosphere. For a double reversed profile to happen temperature rise is very important as in case of network boundaries.

1.4 Comparison of Ca-K line features with photospheric structures

The structures seen in the Ca-K line images have counterparts at the photospheric levels. The bright regions seen in the Ca-K images known as plages are associated with filigree's and relatively large magnetic field regions around sunspots at photospheric level. The small bright structures of 5 - 10$''$ seen in Ca-K images are related with the bipoles seen in quiet region in magnetograms. In the following we discuss their association in detail.

1.4.1 Ca-K Network and Supergranulation cells

Ca-K Network was discovered by Hale in 1892 is like a honey comb in appearance with characteristic cells of 10-40$''$ sizes. The chromospheric network is co-spatial with Super-granules at the photospheric level observed in Doppler-grams (Leighton 1959; Leighton *et al.* 1962). Super-granulation cells formed as a result of large scale convective motions in the He ionization zone. The plasma moves from cell centre to the cell boundary with a velocity of about 0.3 Km/ sec. The average lifetime and average size of super-granulation cells are about 20 hours and 30000 km respectively.

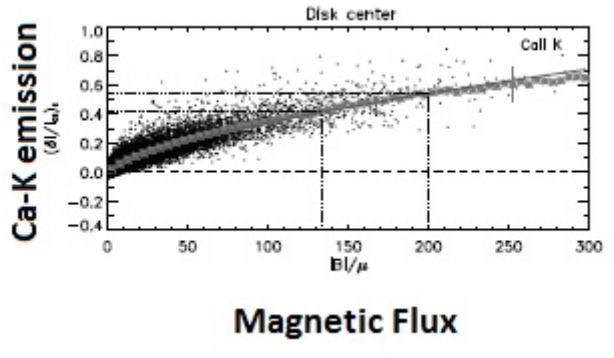

FIGURE 1.6: Plot of non-sunspot pixels as a function of magnetic flux density at disk center ($0.9 < \mu < 1.0$) versus Ca-K emission.
Courtesy Ortiz and Rast (2005)

Sheeley (1967) noted that the chromospheric network appears wider and more complete at the time of sunspot maximum than at minimum. After analyzing the Ca-K spectro-heliograms for the period of seven solar cycles obtained at Kodaikanal observatory, Singh and Bappu (1981) found that the average cell size in the quiet region varies with the phase of solar cycle being 5% smaller during the maximum phase of the Sun. Comparison between Ca-K line images and magneto-grams shows strong correlation between bright features in Ca-K line and strong magnetic fields. (Ortiz and Rast 2005) have found a relation between Ca-K emission and magnetic flux density using SOLIS longitudinal magnetogram and the corresponding PSPT images as seen in Ca-K Figure 1.6. The flow in the supergranules causes flux tubes to move to the boundaries of cells and the concentration of magnetic field shows as outline of Ca-K network boundaries. At the super-granular boundaries, the magnetic field appears concentrated in patches with an average magnetic flux of 2.5 x 10^{18} Mx.

1.4.2 Correlation between Ca-K line and photospheric magnetic field

The regions of high magnetic field are correlated with enhanced emission in Ca-K (Babcock and Babcock 1955; Leighton 1959). Filter-grams obtained in the K-line of Ca II studied for many years showed that the solar chromosphere is highly structured

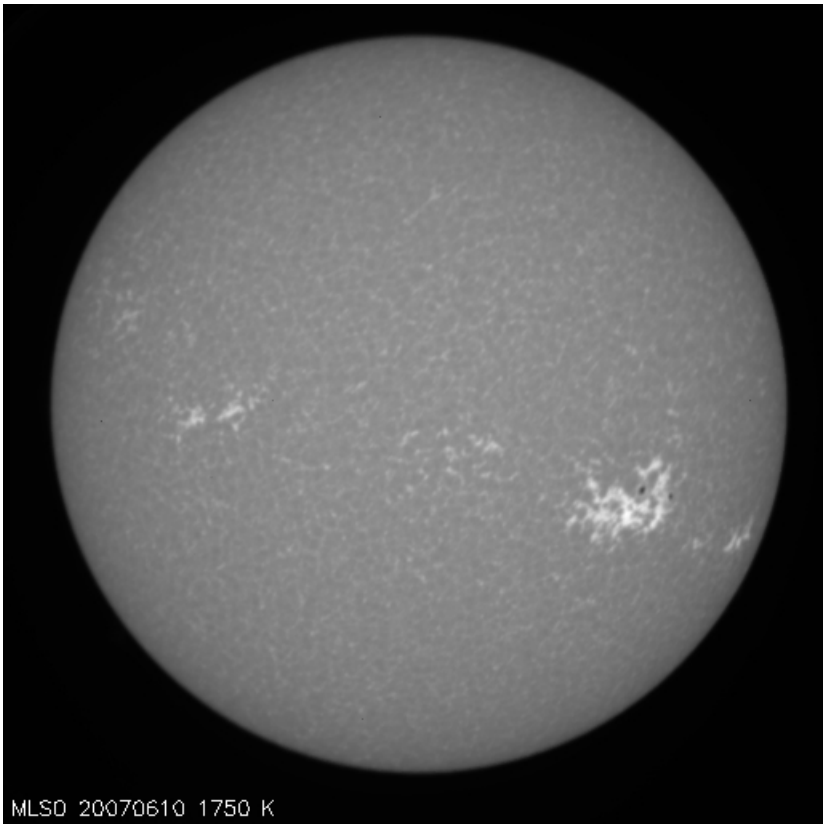

FIGURE 1.7: The filter-gram in Ca-K line taken on June 10, 2007 during the declining phase of the solar cycle, using the SOLIS- PSPT telescope. *Courtesy* SOLIS-PSPT images

(Zirin 1974). The in-homogeneities seen in emission are because of plages, the network and the bright points that populate the interior of the network. Sivaraman and Livingston (1982) showed that concentration of magnetic field plays a major role in the formation of K-line intra-network elements. By comparing magneto-grams in Fe I 868.8 nm line and K-line spectro-heliograms obtained with an 1.1 Å band pass filter, they found that there was a one-to-one correlation between K-line intra-network (IN) bright elements and magnetic elements of 10-80 G without any exception. Nindos and Zirin (1998) verified that the magnetic field plays an important role in the temporal evolution of the K-line bright features. This is especially true when new bipoles are formed, their formation was always followed by enhanced K-line emission. This finding implies that the heating becomes more efficient due to the trapping of hot electrons in the closed magnetic loops. The correlation between the K-line intensity and the magnetic field strength was found to be linear for the stronger network elements. The different features seen in Ca-K line images have been shown on the grey scale

shown in Figure 1.7, the thick grey shows the internetwork region, grey shows the network region, light grey enhanced network and white plages. Similarly, magnetic field data of the Sun has been analyzed by many researchers to study the variations in the strong magnetic field representing toroidal as well as weak field representing poloidal field with solar cycle (Jin and Wang 2011; Sheeley *et al.* 1989; Wang *et al.* 2002).

1.5 Motivation for the current studies

In 1970's several astronomers started monitoring the Ca-K line spectra to study the long term variability of the solar chromosphere. White and Livingston (1978); Oranje (1983); Keil and Worden (1984); Sivaraman *et al.* (1987) used different techniques to record Ca-K line profiles of the Sun as a star. Most of the variations in the Ca-K line profiles of Sun as a star are attributed to active regions like plages on the Sun. Skumanich *et al.* (1984) proposed a three component model of the solar cycle variability of the Ca-K emission using extant contrast and fractional area parameters for cell, network and plage. They were able to fit computed line profile with the observed one at the solar minimum by taking the contribution of only cell and network feature and using extant limb darkening laws. The occurrence of plages during the growth of the solar cycle was found to be insufficient to account for the increase in Ca-K emission and therefore, they introduced an additional network component, 'active network' in excess during maximum phase. On the contrary, measurements made by White and Livingston (1978) over the centre of disc integrated over $1' \times 3'$ boxed region do not show any change in K-index with the solar cycle phase. It may be possible that contribution to 'active network' comes from the higher latitude belts. Therefore, a new technique has been developed which will give information about the 'active network' contribution during different phases of solar cycle, at various latitude belts with the phase of solar cycle. Using this kind of observation, long term variability of solar chromosphere, study of polar regions, quiet regions and meridional flow can be studied.

1.6 Outline of the thesis

In this thesis I would like to address the variation of solar Ca-K line profiles of the Sun as a star and as a function of latitude with time and investigate their implications on the physical and dynamical characteristics of the Sun. Analysis of the Ca-K profiles obtained using the newly developed technique of observations, as a function of latitude and integrated over visible 180° longitude was done to determine the various parameters of the line profiles. The detailed results of data have yielded new information about contribution of the quiet and active regions, polar regions to irradiance variations with solar cycle and meridional flow in the chromosphere. In the following we give the description of each chapter:

The Sun and, in particular, chromosphere and its variation with time have been described in chapter 1. The work done by various authors in the visible as well as in the UV and EUV wavelength band have been reported in detail. It was noted that various proposed models do explain the variations in the Sun up to some extent but are unable to address some day to day variations in the Sun and exact magnitude of the variation with time and solar cycle. The spectroscopic observations of the Sun as a star in Ca-K line over the last 40 years and images of the Sun in Ca-K line over a century have provided lot of information about the solar variability but not complete. The need to improve the methodology of observations has been addressed to make observations for developing realistic models of solar variations. The sources that cause these variations and to estimate the magnitude of the variations by each change, detailed high resolution spectroscopic observations with spatial information may lead to better understanding of these variations. The contribution of quiet and polar regions to these variations needs to be investigated apart from the variations caused by large scale activity such as sunspots, flares etc. The formation of Ca-K line, formation heights, and properties of various features such as plages, networks and the role of magnetic field in the formation of various features in the chromosphere have been discussed.

In chapter 2, I describe the optical design of the Solar Tower Telescope at Kodaikanal and the instrumental set up used to make the observations. Also described are the methodology and procedure adopted to make the observations on daily basis whenever the sky conditions permitted. The observational procedure to calibrate observed

data has also been given. The parameters of the instrumental set up are listed. The procedure followed to analyse the raw data and create set of uniform data for further analysis has been described. Then the details of the automatic software developed to average the profiles for the chosen region on the Sun, normalize the Ca-K profiles, derive the various parameters of the profile such as K_1 and K_2 widths and K-index and intensity ratios have been provided. Various parameters of Ca-K line as a function of latitude were determined for all the data and the procedure followed to reject the unreliable data due to poor sky conditions has been discussed.

The quality and uniformity of the data obtained for the long period of about 25 years have been described in chapter 3. The method to compute the Ca-K line parameters for the Sun as a star from the parameters as a function of latitude is discussed to compare the results of these observations with those obtained by other observatories such as Kitt Peak observatory and NSO/Sac Peak observatory. I compared the derived values of K_1 and K_2 widths from the KKL data with the values obtained from Kitt Peak and NSO/Sac Peak data. Results of this comparison and the long term variations of the Sun as a star using Ca-K line profiles for solar cycles 22 and 23 are presented.

In chapter 4, the data for the active and minimum phase have been analysed separately to compare the parameters during the active and minimum phase of solar cycle. Further, the variations in the Ca-K line parameters have been compared with the variations in the plage areas derived from the Ca-K images of the Sun. From these comparisons we tried to study the contribution of networks in the quiet regions of the Sun.

In chapter 5, data for both the cycles have been considered together but for all the latitudes separately to study the variations as a function of latitude. This chapter deals with the behaviour of K_1 width parameter of the Ca-K line profile at various latitude belts at different phases of the solar cycle. We show how the activity shift in the northern and southern hemisphere and compute the rate of shift in both the hemispheres and find asymmetric behaviour in both the hemispheres. The information about drift rate has been used to study the meridional flows in the Sun. The implications of the rate and direction of shift of the activity with latitude and random behaviour of shift around 60° latitude have been discussed. The variation of activity in polar region

with solar cycle phase has also been studied.

The procedure to model Ca-K line profiles at different latitude and then investigate the variation of K_1 width with latitude are described in Chapter 6. We have used Uitenbroek's RH code to model the Ca-K line profile. We have derived the path length at different μ in order to compute the profiles at different latitudes for the quiet chromosphere. We have attempted to compute the total network contribution to the line width by considering contribution due to plage areas determined from Ca-K images obtained at Kodaikanal. We found that large database is required to study the variation due to network over solar cycle phase.

Chapter 7 contains the summary of entire thesis work. The main conclusions drawn from our studies are outlined here. Some of the possible future prospects of these studies are also listed.

Chapter 2

Observations and Data analysis

2.1 Introduction

The Kodaikanal Observatory is Located on the Palni hills at (lat. 10° 14′ N; long. 77° 5′ E) an elevation of 2343 meters above mean sea level. At this observatory the Solar Tower Tunnel Telescope houses a two-mirror fused quartz coelostat 61 cm diameter, mounted on an 11 m tower. The first mirror of the coelostat system rotates at a speed ∼ 7.5 degree / hour to compensate the rotation of earth, collects the light from the Sun and reflects in the fixed direction, to the second mirror. The second mirror of the coelostat reflects light vertically down onto a third quartz flat, which sends the beam in the horizontal direction into a 60 m long underground tunnel. The parallel light falls on a 38 cm achromatic objective of 36 m focal length. The objective forms a 34 cm diameter solar image on the slit of the spectrograph with an image scale of 5.5 ″/mm. The spectrograph is of the Littrow type and utilizes a 20 cm aperture of, 18.3 m focal length, Hilger achromatic lens in conjunction with a 600 lines/mm Babcock grating of ruled area 200 x 135 mm and blazed in the fifth order at 5000 Å .The 50 mm length of the spectrograph slit provided 275 ″ coverage on the Sun. After the installation of telescope in 1962, examination of the iodine absorption spectrum near 5330 Å in the fifth order indicates, from the separation of the doublets, that the theoretical resolution has been attained.

2.2 Earlier Observations of Sun as a star

To study the long term behavior of solar chromosphere Late Vainu Bappu started an observing program at Kodaikanal to monitor the emission output from the solar chromosphere using the Ca-K line profile when the Sun is viewed as a star, since 1969. The methodology adopted at Kodaikanal observatory to take spectra of the Sun as a star was to cover the third mirror of the three mirror coelostat system by a metal cover painted with white pigment (TiO_2) that scatters the radiations with high efficiency. Later, Ca-K line profiles of the Sun as a star were obtained using high-resolution spectrograph at number of observatories around the world on a regular basis at Sacramento Peak observatory and for 4-6 days every month at Kitt peak (White and Livingston 1978; Keil and Worden 1984; Sivaraman *et al.* 1987). The observatories at Kitt Peak, Sacramento Peak and Kodaikanal adopted different procedures to obtain the Ca-K line profiles of the Sun as a star.

The spectra of the Sun as a star covering a spectral range of about 10 Å around Ca-K line were recorded using a Kodak 103-aO, 35 mm film with a large exposure time in the range of 120-180 minutes using the spectroscopic arrangement described above. The spectrograph provided a dispersion of 9.34 mm/Å in sixth order at the Ca-K wavelength. Observations were made on day to day basis when ever sky conditions permitted. It may be noted that most of the data obtained pertained to the months from December to May as the period from June to November remains cloudy and rains occur occasionally on most of the days.

2.3 Present Observations as a function of latitude

The Sun as a star studies provided information about the solar variability with time and its relation with earth's climate and relation with variability of other features and parameters of the Sun. While doing the analysis of the data, it was felt that information about the Ca-K line profiles as function of latitude can provide much more information about the solar dynamo and flows in the Sun by determining the

movement of the activity as a function of latitude and time. The observations may also help in estimating the variation in the background flux (network emission) with solar cycle phase, if any. This methodology also helps to study the variations in polar regions with time confidently.

We have, therefore, obtained the spectra of the Sun around Ca-K line wavelength as a function of latitude integrated over the longitude (starting from 1986 to 2011) in the following way. (1) A portion of the Sun's image is allowed to pass through the slit of the spectrograph. (2) While the Sun's image is moved with uniform speed from East end to the West end on the slit of the spectrograph at particular latitude, the spectra in Ca-K wavelength is obtained. (3) The procedure is repeated for each of 10° latitude belt while the spectra is integrated over the longitude belt. Here we enlist the salient features of the long time series of data obtained. Littrow arrangement using a 600 lines/mm grating blazed at 25000 Å at the first order, provides a dispersion of 9.34 mm/Å around Ca-K line in 6th order. An interference filter with pass band of 20 nm centered around Ca-K line was kept in front of slit to separate different orders of the spectrum. The slit width (0.1 mm) of the spectrograph is maintained throughout the observational period of 25 years. This provides the uniformity in the instrumental line profile whose width is much smaller, about 11 mÅ as compared to the Ca-K line. The 50 mm length of the slit covers about 16° near the equator but the 35 mm 103-aO Kodak film used to record the spectra covers about 11° of latitude near the equator and about 30° near the polar regions.

To obtain the spectra as a function of latitudes, we made the sun-chart (Figure 2.1) on a thick sheet of paper whose size is corresponding to the size of the Sun's image and the center is located at B_0 angle. Each sun-chart can be used for about 5-days when the B_0 angle varies with time relatively faster and for about 20 days when the B_0 varies slowly. The latitude lines at an interval of 5° are drawn on the sun-chart. The sun-chart is kept near focal plane of the Sun's image in such a way that N-S axis marked on sun-chart becomes parallel to the axis of rotation of image. The height of the sun-chart is adjusted in such a way that when North limb of the Sun's image is moved along a particular latitude line (say 30°N) on the sun-chart, the same latitude area of the solar image (30°N) falls on the centre of the slit. To integrate the spectrum over the 180° longitudes at that latitude, the image is moved in the E-W direction of

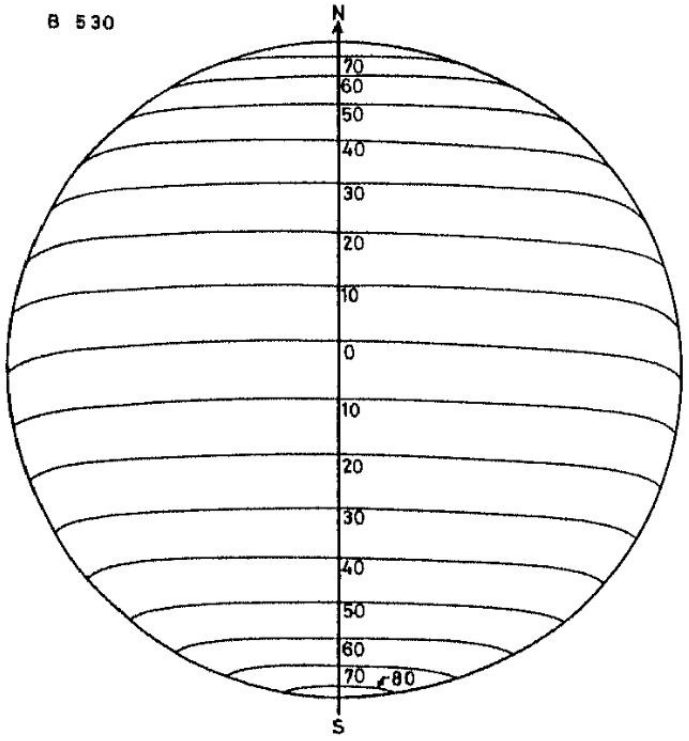

FIGURE 2.1: An example of a sunchart for the heliographic latitude (B_0) of 5.5° showing the latitudes marked at an interval of 10°

the Sun along the given latitude line at a uniform speed by moving the second mirror of the coelostat with the help of an electric motor. All the spectra were recorded on 35 mm Kodak 103-aO film till February 1997. The spectra were obtained at an interval of 10° latitude, because the 35 mm 103-aO Kodak film used to record the spectra covers about 11° of latitude near the equator, to cover whole of the Sun. The shadow caused by a wire kept in-front of the spectrograph slit serves as the reference to mark the latitude position on the spectra. After taking the 17 spectra covering all the latitudes of the Sun with an interval of 10° each, 5 calibration spectra with step wedge having 6 different density steps were recorded with different exposure times (5 - 30 seconds) in the nearby continuum to cover all the density range. In addition to this, a spectrum of Sun as a star around Ca-K line was obtained as explained below :

The use of a cover painted with white pigment to cover the third mirror to scatter the Sun-light requires a large exposure time to obtain the spectra of Sun as a star. Therefore, a different method was adopted to take the integrated spectrum of the Sun. That is instead of covering the third mirror by a lid painted with white pigment, the

objective lens was removed from the optical path and thus every point on the slit received light from whole of the Sun as the first mirror subtended an angle more than half a degree. This was done to decrease the exposure time from couple of hours to a few minutes in case of photographic observations, because on number of days the integrated spectrum remained underexposed due to appearance of clouds during the exposure.

Then the 103-aO film being used to record the spectra became unavailable. In view of the non-availability we procured a CCD camera of 1K $\times$ 1K format from Photometrics in 1997. A smaller CCD chip size of 24.6 mm $\times$ 24.6 mm as compared to the width of 35 mm film, restricted the spatial and spectral coverage of the spectrum. To overcome the limitation of spectral coverage, the spectrum around Ca-K was taken in the 5th order to cover a sufficient portion of the spectrum around the Ca-K line in case of observations with CCD. But the CCD chip is of smaller size and covers about 7° latitude spectra near the equator and about 20° near the polar region. Hence, we have obtained spectra at an interval of 5° latitude up to 30° latitude and at an interval of 10° beyond 30° latitude. Later, the spectra were combined to study the Ca-K line profiles averaged over 10° latitude and at an interval of 10° to maintain the uniformity throughout the period. Twenty three spectra at different latitudes and one spectra of the Sun as a star were obtained daily whenever the sky conditions permitted. On number of days spectra around Ca-K line were also obtained as a function of longitudes during the minimum phase of the Sun to compare line parameters at the different latitudes with those of longitudes, respectively. Using CCD in a binned mode of 2 $\times$ 2, the pixel size of 48 μm provides a spectral scale of 7.07 mÅ / pixel. The slit width of 100 μm, kept during the observations, gives a spectral resolution of 14.7 mÅ .

The use of CCD camera has necessitated to take the dark and flat field images to correct for the dark signal and pixel to pixel gain variations. We used the overlapping 3rd order continuum around 6000 Å for the flat field images using 8 mm slot instead of the slit and defocused solar image. In the year 1999, the CCD camera from Photometrics was replaced by the CCD camera of 2K $\times$ 2K format from ANDOR company having higher efficiency in the UV and smaller pixel size of 13.5 $\times$ 13.5 μm. Sometimes, when ANDOR camera was required for other solar observations, Photometrics

camera was used to make the observations. We have also determined the line profiles at different longitudes near zero degree latitude without scanning during the minimum phase of solar cycle. Sometimes we have obtained spectra at different latitudes near the central meridian without scanning during the minimum phase of the solar cycle, when there were no Ca-K plages on the visible part of the solar disc, so that the variations in the widths are due to latitude only. There are large data gaps during the monsoon months from June to November every year at Kodaikanal. This way we have collected the spectral data of the Ca-K line since the 1985 till 2011. In the next section we provide the details of observations at kodaikanal using high-resolution spectrograph and calibration of the data.

2.4 Data Analysis

The 23 years of data starting from 1989 to 2011 have been used to study the line width variation over the solar cycle. Most of the observations are made during the month of December to May as the period from June to November is mostly cloudy due to the monsoon at Kodaikanal observatory. Everyday data has been named as yymmdd for example if observations are taken on 2009, February 22, then it was named as 090222. Then the spectrum for each latitude is named as a, b, c,— beginning from the 90 degree northern latitude belt to 90 degree southern latitude. Observations were made on 1205 days during this period of 23 years, but we found that the data of 807 days to be useful for the study, other days of data sets were not complete or had the calibration problems. To complete the one set of observations we needed about one hour of clear sky without any type of clouds. But some times low or high clouds appeared in the sky disturbing the observations and the data set remained incomplete. In addition, sometimes step wedge or the flat field spectra could not be obtained due to clouds and thus making the data unusable. In Figure 2.2 we show the distribution of the number of days of observations in a year used in this analysis. The data are of three types, (i) data obtained using the photographic film, (ii) the data with the CCD camera with pixel size of 24×24 microns and (iii) spectra obtained with CCD camera having pixel size of 13.5×13.5 microns.

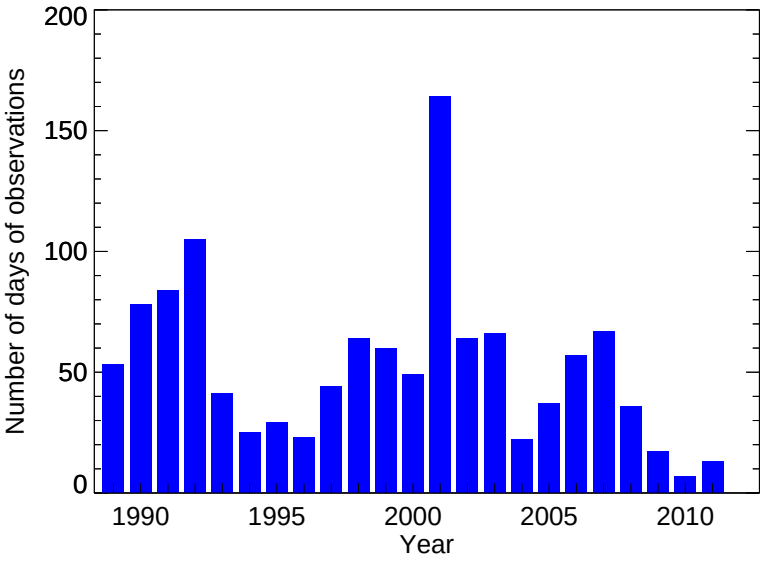

FIGURE 2.2: The histogram indicates the number of days of observations made in each year.

2.4.1 Analysis of photographic film data

To convert the analog photographic data to digital data we developed a digitizing unit using a uniform light source. A good camera lens is used to avoid any vignetting in the spectral data. The CCD camera used in the digitizing unit has pixel of 13.5 $\times$ 13.5 microns size with 16-bit read out. The unit was dedicated to digitize this data to maintain the same magnification and uniformity. All the data were digitized under uniform environment conditions. The data are corrected for the dark current and pixel to pixel variations of the CCD camera used. Software was developed to analyze the data in the semi-automatic mode.

2.4.2 Conversion of density to intensity values

For the photographic data, to convert density values to intensity values we used 5 step wedge (each step with known percentage of transmission) calibration spectra taken on each day of observations with different exposure times. Figure 2.3 shows the images of the calibration spectra taken with 20 second exposure time and the bottom panel of the figure shows the part of the calibration spectra free from the

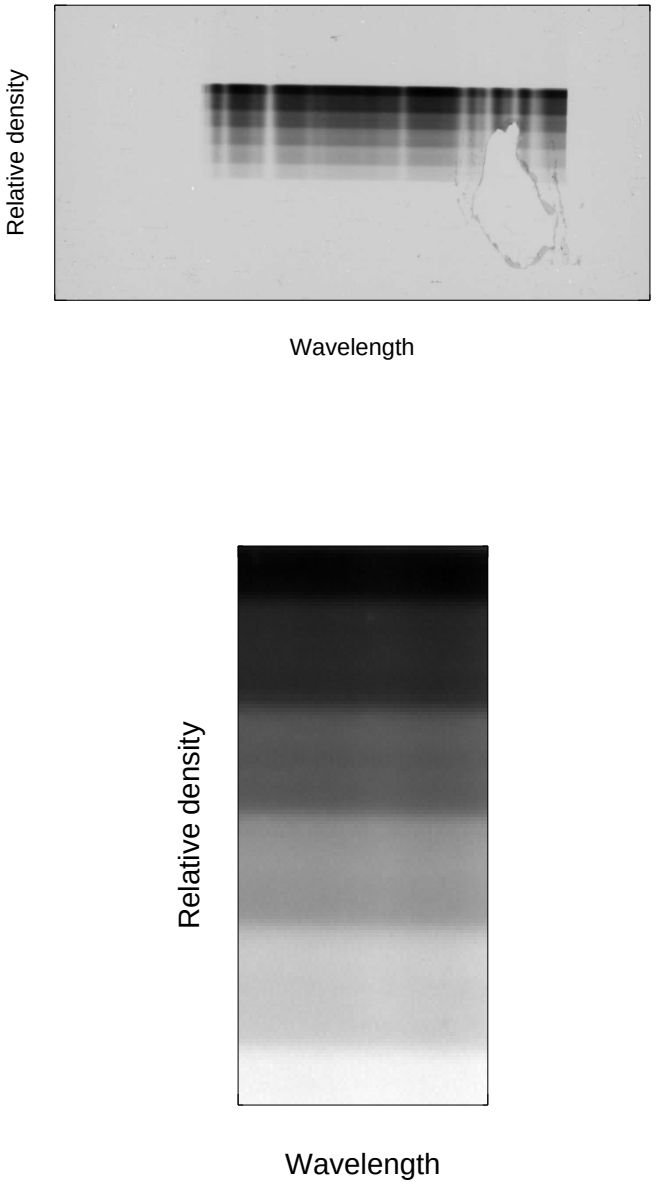

FIGURE 2.3: *Top*: Raw image of the step wedge taken for 20 second exposure. *Bottom*: The selected box region for calculation of the average density values for each step.

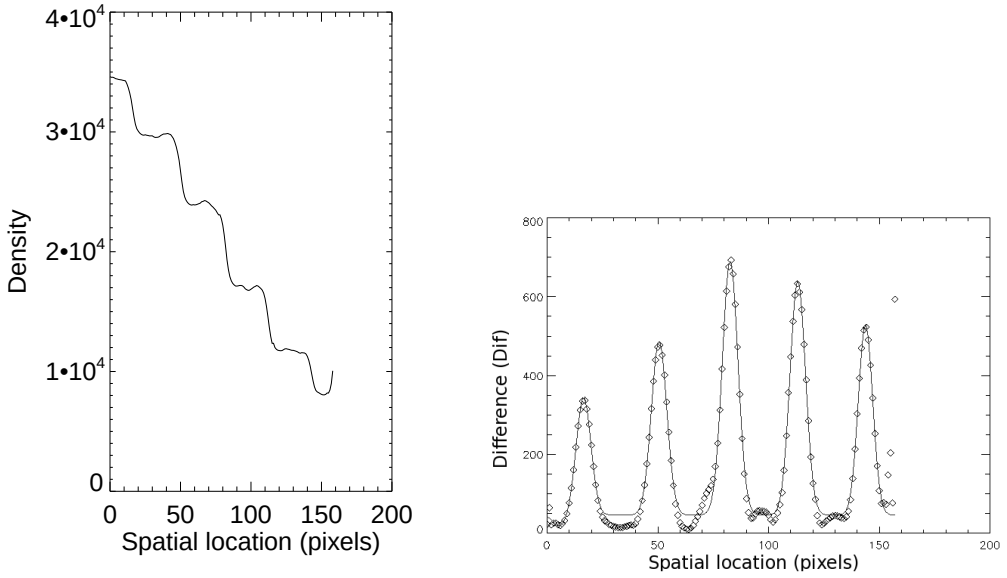

FIGURE 2.4: *Left*: After taking average along the rows (wavelength axis) of Figure 2.3 *Right*: The diamond symbols show the distribution of density difference obtained by subtracting adjacent values of average density represented by the curve in the left panel to find the beginning and end of each step. The multiple Gaussian fit to the distribution is over plotted to determine the six steps and their average density values.

absorption lines selected to calculate the average density value for each step. The left panel of Figure 2.4 shows the plot of density values as a function of pixel values and the right panel of the figure shows the method to extract number and location of pixels for each steps separately to compute the average density. The beginning of new step can be found by subtracting y axis value from the next adjacent y value, the maximum difference between the values will give the location of the beginning of the next step. The diamond symbol in the right panel of Figure 2.4 indicates the amplitude of the values of difference (Dif.) obtained by subtracting density value from the next adjacent value and the solid line corresponds to separate Gaussian fits for each step. The peak value of Gaussian gives the start of each step. After extracting each step, average density value was determined by neglecting the edges of each step. The intensity values (percentage transmission) of the steps on the log scale are 1.795, 1.590, 1.394, 1.199, 1.004 and 0.806 determined by the photometric methodology. The zero intensity value was measured from the clear region away from the step wedge as seen in top panel of Figure 2.3. The difference in the dark count and the clear count is named as CC. Then the % of density is calculated as for each step (CC- step value/CC)*100. This process was applied for all the other

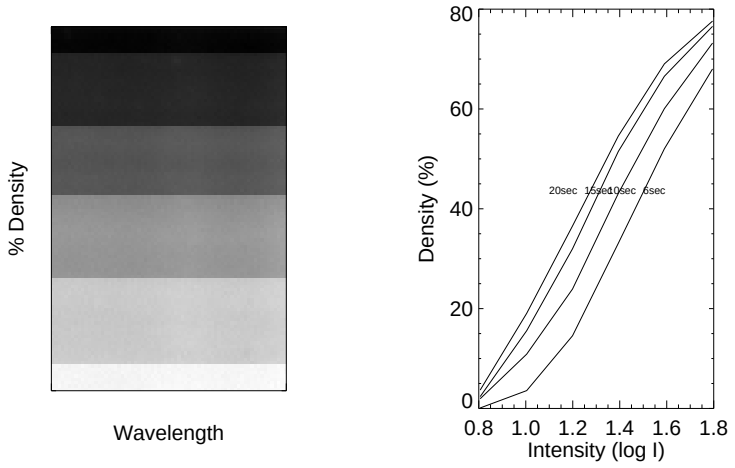

FIGURE 2.5: *Left*: The steps are extracted using Gaussian fitting. The brighter region has more % of density and intensity as compared with the darker region. *Right*: The intensity vs density plots for step wedge calibrations for the exposures 6,10,15 and 20 seconds.

calibration frames with 6, 10, 15 and 20 second exposure time. This methodology is adopted to achieve larger density coverage since spectra with shorter exposure time gives low density range and with larger exposure provides high density range. With different exposure times we get four plots of the density versus intensity as seen in Figure 2.5. The exposure with 10 seconds covers the average density range. Then we shift the low and high exposure curves in the intensity direction so that the mean value of % density coincides for all the curves. In the process, we get number of data points as compared to only 6 points for a single exposure. The large number of data points helps in making a polynomial fit to data points with better accuracy and to overcome the noise. The derived values of % density (D) versus intensity in (Log I) are plotted in Figure 2.6. A three degree polynomial fit to these data points found to represent best fit to density versus intensity values and is also shown in the Figure 2.6. The coefficients of the polynomial fit were computed for observations of each day and these coefficients have been used to determine the intensity values for the measured values of % density of each spectrum. Left panel of Figure 2.7 shows a typical flat field spectrum around Ca-K line the photographic density scale and the right side panel shows the spectrum after conversion of density values to intensity, on the intensity scale. The inversion of the gray scale is apparent in the intensity image. This procedure has been used for observations of each day.

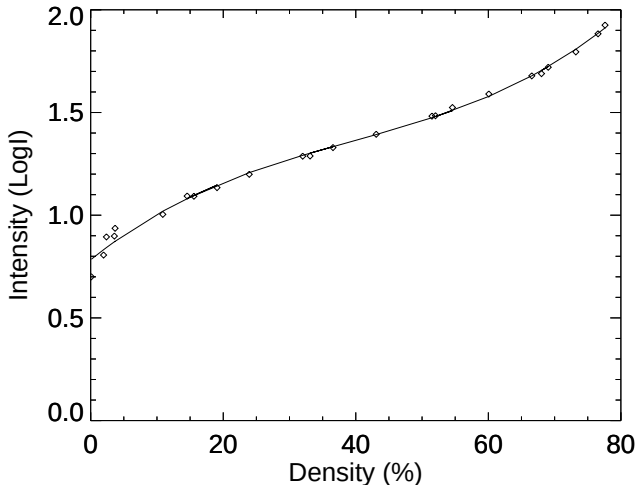

FIGURE 2.6: The plot shows final and extended density versus intensity values for the data taken on January 20, 1997 along with a polynomial fit(solid line)

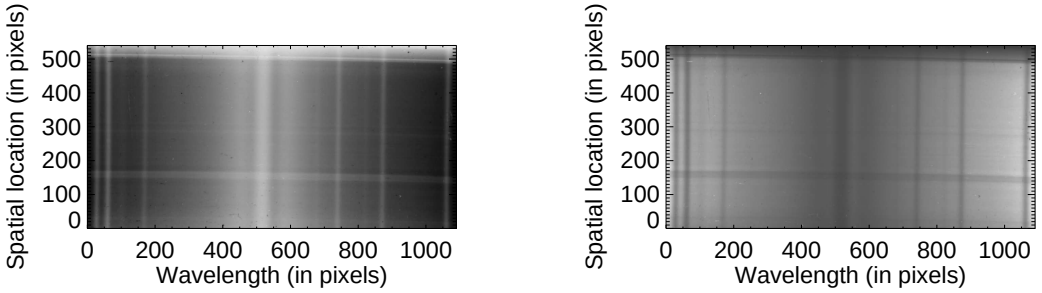

FIGURE 2.7: *Left*: shows the typical observed spectrum on density scale taken on January 20,1997 after the dark and flat field correction and *Right*: shows the same spectrum in the intensity scale obtained using the coefficients of polynomial fit of the calibration curve for that day.

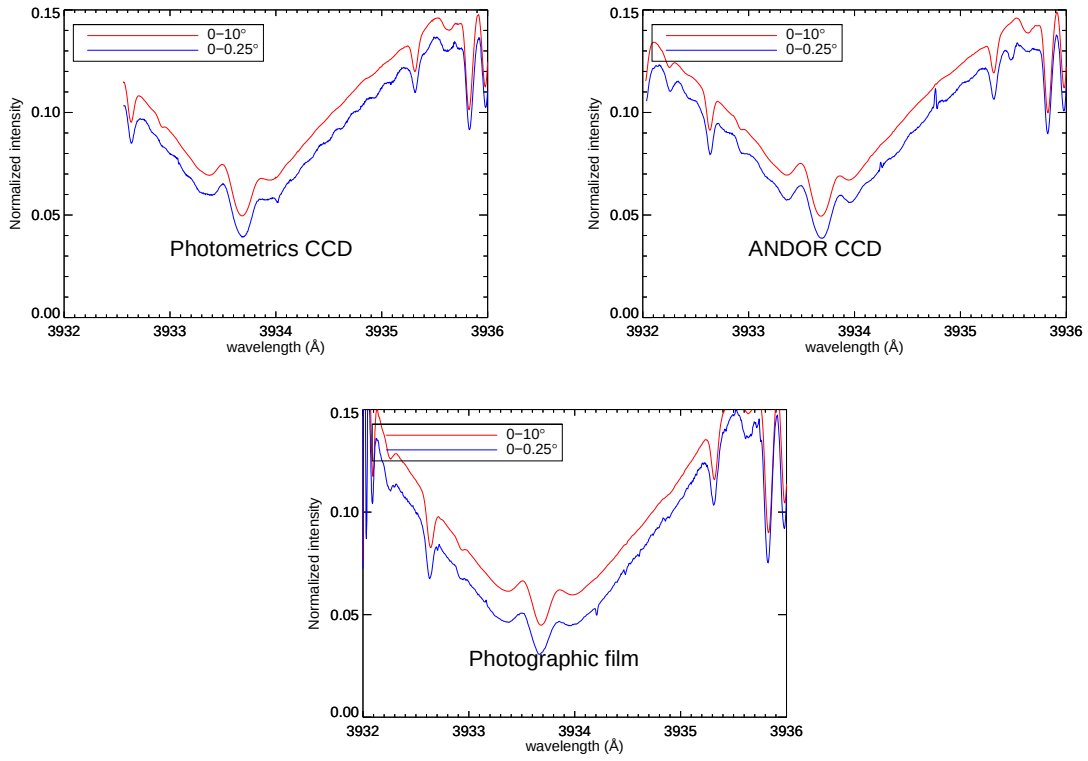

FIGURE 2.8: The figure shows the averaged Ca-K line profiles for the 0.25 and 10° spatial intervals for the three types of detectors used, The intensity values in case of averaging over 0.25° spatial locations have been decreased by 0.02 to separate out two line profiles. *Top Left*: data taken on march 15, 2006 using Photometrics CCD, *Top Right*: data taken on March 22, 2005 using Andor CCD, *Bottom*: data taken using the photographic film on January 05, 1994.

2.4.3 Comparison of data with three detectors

To study the effect of 3 different detectors in the data, first we computed the pixel resolution in each case and found that the values of dispersion per pixel are in the range of 0.0035 to 0.0046 Å better than the resolution due to the slit width (0.011 Å). In Figure 2.8 the normalized Ca-K profiles averaged over two spatial intervals indicate small scale variations in the average profile for shorter interval of 0.25° caused by dust particle or some other irregularity on the detector. These variations are averaged out in the average profile over 10° that is being used to derive the line parameters. Then to determine the rms variations in the line profile, we choose an interval of 3933.13 - 3933.27 Å where the intensity variation appears to be linear with wavelength. After normalization of the line profiles the residual intensity is around 0.05. In Table 2.1

TABLE 2.1: Comparison of the data obtained with three different detectors

Detector	Year of Observation	Pixel Resolution in Å	Rms variation in average profile over	
			0-10°	0-0.25°
Photographic film	1989 - 1996	0.0046	1.6e-04	5.4e-04
Photometrics	1997 - 1999	0.0035	7.7e-05	4.8e-04
Andor	2000 - 2011	0.0039	2.3e-04	2.1e-04

we list the pixel resolution, rms variation computed after subtracting the linear variation with wavelength for the average line profiles over 0.25° and 10° latitudes for all the three detectors. The similar values of pixel resolution and rms variations in the line profiles as listed in Table 2.1 indicate that the change in detector may not have any effect in the derived line parameters and determination of Ca-K line parameters.

2.4.4 Determination of parameters of Ca-K line

The data obtained with the CCD camera were corrected for the dark current and the pixel to pixel gain variations. Reference spatial position corresponding to the given latitude on the photographic spectrum and pixel position on the observed spectrum with the CCD camera were determined. The image size of the Sun and the B_0 angle of the Sun varies with time and thus extent of the interval between two latitudes varies. We computed the Ca-K line profile average parameters at an interval of 10° latitude up to 70° latitudes in both the northern and southern hemispheres. For the polar regions, we computed the Ca-K line profile parameters averaged over about 20° latitude starting from 70° to limb of the Sun.

In order to find out the number of spectra to be added in the spatial direction and to obtain the average spectra at each latitude interval we adopted the following procedure. The distances between the adjacent latitudes at the meridian at an interval of 10° were computed with respect to centre of the Sun. This has been done by considering the actual size of the solar image on that day. Knowing the radius of the Sun, the distance (D) between the two latitudes (say θ_1 & θ_2) is computed as
D = R*(sinθ_1- sinθ_2)
Then, we computed the number of spectral rows to be added to obtain the average spectrum at each latitude interval. For wavelength calibration of the averaged spectra

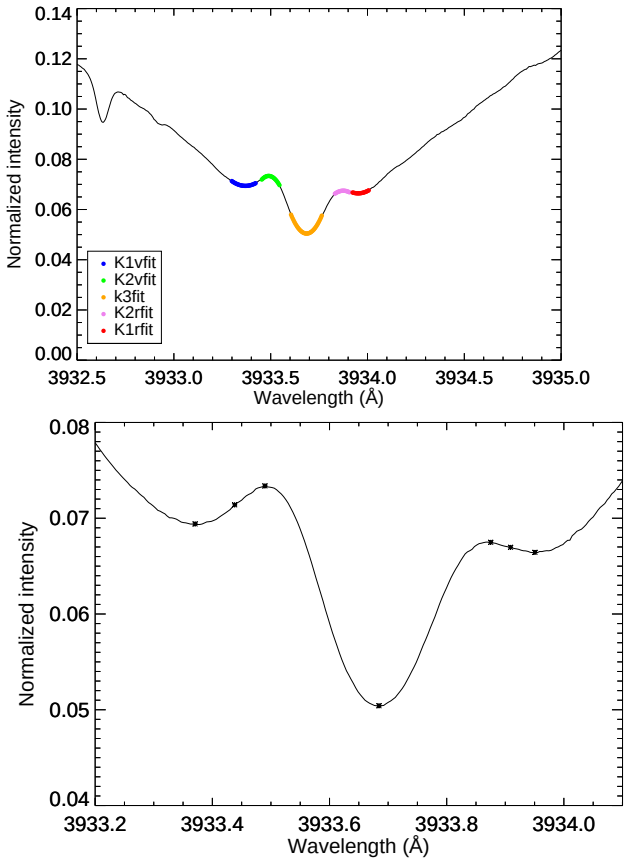

FIGURE 2.9: The solid line in top and bottom panel shows a normalized averaged observed Ca-K line profile taken on march 08, 2007 for 0-10° south latitude and integrated over the 180° longitude. *Top*: The chosen intervals to find the Ca-K line parameters are over plotted with the values obtained from the 3-degree polynomial fit in different colors The alternative minimum and maximum of these interval gives K_{1v}, K_{2v}, K_3, K_{2r} and K_{1r} locations on the profile respectively. *Bottom*: The crosses (stars) marked on the normalized average Ca-K line profile indicate the maxima and minima locations computed from the polynomial fits and the locations to derive the Wilson-Bappu width of the line.

we used two photospheric absorption lines of Fe I at 3932.640 Å and 3935.825 Å . The observed intensities were normalized using the residual intensity at 3935.16 Å on the red wing of the Ca-K line. This has been done as 13% of the continuum intensity of the photometrically calibrated Ca-K line profile (White and Suemoto 1968). In Figure 2.9, top panel shows a typical normalized average Ca-K line profile for the 0-10° latitude interval. Generally all the solar absorption lines show one dip in the intensity, but the Ca-K line shows double reversal in the profile. Bottom panel shows central part of the profile the double reversal, the occurrence of alternative minimum

and maximum. The first minimum and maximum intensity points are known as K_{1v} and K_{2v} locations of the profile. The minimum intensity point is called K_3 and maximum and minimum intensity points on the red side of K_3 are known as K_{2r} and K_{1r} locations on the Ca-K line profile. To determine the position and intensity values of these maxima and minima at the Ca-K line profiles we have carefully chosen 5 small wavelength intervals. These intervals consist of 20-50 points around the maximum and minimum locations without any cross-talk with the adjacent interval. The large number of points were chosen to accommodate the shift in the minimum and maximum locations in the profiles of different latitudes as the K_1 width is larger at higher latitudes compared with that for lower latitudes. Even though locations of the minima and maxima vary on the line profile with latitude, the chosen intervals are valid for all the line profiles at all the latitudes. We made an attempt to determine the minimum and maximum locations by three methods namely (i) comparing the adjacent values, (ii) Gaussian fit and (iii) 3-degree polynomial fit to each interval. The first and third methods were found to be suitable as compared to the Gaussian fit because of asymmetry in the profile. To avoid the dependence on a single point we chose to use a 3-degree polynomial fit method to locate the minimum and maximum as seen in top panel of Figure 2.9. The rms value of the difference in line-width measurements from the first and third method is about 0.002 Å for the spectra up to 60° latitudes and 0.004 Å for spectra greater than 60° latitudes. This is much smaller than the observed variation of 0.169 Å in K_1 and 0.049 Å in K_2 width (see Table 3.1) with time.

In the bottom panel of Figure 2.9, the location of minima and maxima are shown by crosses along with points to determine the Wilson-Bappu width of Ca-K line. After determining the minima and maxima intensity locations we can determine the K_1, K_2 widths of Ca-K line and intensity ratios as defined below:
K_1 width: K_1 width is defined as the wavelength separation between the K_{1v} and K_{1r} minima.
K_2 width: K_2 width is defined as the wavelength separation between the K_{2v} and K_{2r} emission peaks.
Wilson-Bappu width: The wavelength difference of the two wavelength positions corresponding to $(IK_{1r}+IK_{2r})/2$ and $(IK_{1v}+IK_{2v})/2$ gives the Wilson-Bappu width.
Other parameters of interest are the intensity ratios K_{2v}/K_{2r}, K_{2v}/K_3 and derivation of Ca-K line indices, namely 1 Å and 0.5 Å index to study the variation in solar radiance with time.

Following the analysis procedures for all the observations of 807 days, the computed parameters of the Ca-K profile have been used to study the long term variations as discussed in chapters 3, 4 and 5.

Chapter 3

Temporal Variation of Ca-K line profile of the Sun as a star during the solar cycle 22 and 23

3.1 Introduction

[1] The study of the variations in chromospheric flux using Ca-K spectral line at all time scales is important to study the solar dynamo because of relation between the Ca-K line and the magnetic fields on the Sun (Leighton 1964; Skumanich *et al.* 1975; Sivaraman and Livingston 1982; Ortiz and Rast 2005). Short time scale variations provide the information about the dynamics and energy transport in the chromosphere whereas the long period variations provide valuable knowledge about the dynamo process. The study that causes variation in solar irradiance is very important to understand the changes occurring in the earth's climatic conditions and weather. Total Irradiance variations of the Sun occurs on time scales of less than a day to solar cycle and very large periods such as centuries. Approximately 60% of the variation observed in TSI between solar minimum and maximum is produced by the UV part of the spectrum short ward of 400 nm (Solanki and Krivova 2006). Whereas the Ca-K

[1]The chapter is based on the paper Sindhuja and Singh (2015)

index varies by about 18% during the solar cycle (White and Livingston 1981) and amplitude of total irradiance variation measured radiometrically between minimum and maximum is only ~ 0.1% (Fröhlich and Lean 1998). The observations made during the period of 1981 to 1985 show that the contribution of the UV part of the spectrum to the total solar irradiance (TSI) is 19% (Lean 1989). The large variations in solar irradiance observed during maximum phase could be caused by the faculae brightness over large areas, part of these compensates the less radiations emitted from sunspot areas and part of additional brightness causes increase in the irradiance of the Sun during this period (Froehlich *et al.* 1991; Pap *et al.* 1997).

It is believed that the magnetic cycle is controlled by the dynamo processes occurring at the base of the convection zone. The variations in the magnetic field generally causes the variations in the appearance of various features on the solar surface, their intensity and irradiance of the Sun. Further, Nindos and Zirin (1998); Ortiz and Rast (2005) found a strong correlation between areas of Ca-K emission and underlying photospheric magnetic field. Therefore, the spectroscopic and photometric observations of the chromosphere in Ca-K line will be very valuable to study the irradiance variation and dynamo processes. The measured area of plages, active network and network depends on the intensity contrast of the features, threshold intensity value etc. which varies due to day to day variations in the sky conditions. Thus, there is always an uncertainty involved in identifying the extent of various features reliably. In spite of this limitation Worden *et al.* (1998); Tlatov *et al.* (2009); Foukal *et al.* (2009); Ermolli *et al.* (2009a); Priyal *et al.* (2014) have developed semi-automatic programs to determine the areas of these features on the images and study their contribution to the variation in solar irradiance with time from the Ca-K images of the Sun. In addition, the intensity of different Ca-K plages is likely to be different due to magnitude of underlying magnetic field and may vary with time or solar cycle phase. Therefore, the determination of irradiance from the areas of features has some uncertainty whereas measurements from the spectroscopic observations, variations in both the intensity and areas are considered automatically. In order to overcome this problem, Bappu (1974, personal communication with Singh) started monitoring the Ca-K line profiles of Sun as a star since 1969 to study the variation in Ca-K line emission with greater confidence. Further, the line profiles are normalized to the continuum or calibrated known intensity at a given wavelength to account for the day to day variations in sky transparency and any change in the instrumental set up. The

observations of the Ca-K line profiles of the Sun as a star were also started by other groups around the world White and Livingston (1978); Oranje (1983); Keil and Worden (1984). White and Livingston (1978) found that during 1977 (onset of cycle 21) the K-index increased by 2.7% while central intensity rose by 5.7%, Oranje (1983) found that the line core emission varies considerably on short term basis during the active phase, by nearly as much as the mean difference between the solar maximum and minimum values and Keil and Worden (1984) found that there is a good long term (6 months) correlation between K-line and the number of plages and sunspots but poor ($\sim$ 1 week) short term correlation. Ca-K index varied by about 20% over the solar cycle phase. Further, White and Livingston (1981) found that Ca-K index increases by about 17% at the maximum phase of the Sun around 1980 as compared to that during the minimum phase around 1974 as seen in Figure 3.1. We show in Figure 3.2 the Ca-K line profiles for the quiet Sun and the plage region as observed by White and Livingston (1981). The figure indicates that K_1 width and Ca-K line intensity are larger for the plages as compared to those for the quiet Sun region. This implies that when area of plages increases on the Sun during the active phase, the K_1 width and Ca-K index will be greater as compared to those for the Sun during the minimum phase for the Sun as a star.

Skumanich *et al.* (1984) proposed a three component model of cell, network and plage to explain the observed changes in Ca-K line profile, using the extant laws of limb darkening. They were able to fit the model profile with the observed one by considering the contribution of two components, namely cell and network during the minimum phase. But during the maximum phase the contribution due to plage component and networks were found to be insufficient to explain the observed profile. They, therefore, suggested an addition of excess contribution due to 'active network component' to achieve a good agreement between the model and observed Ca-K line profiles. This assumption explained the existence of extra emission during the maximum phase. But the measurements made over the centre of the solar disk over a region of $1' \times 3'$ showed no variation with solar cycle phase (White and Livingston 1981; Livingston *et al.* 2007a). Hence, it might imply that the extra emission originates from background component at high latitudes or additional brightness of networks at higher latitudes.

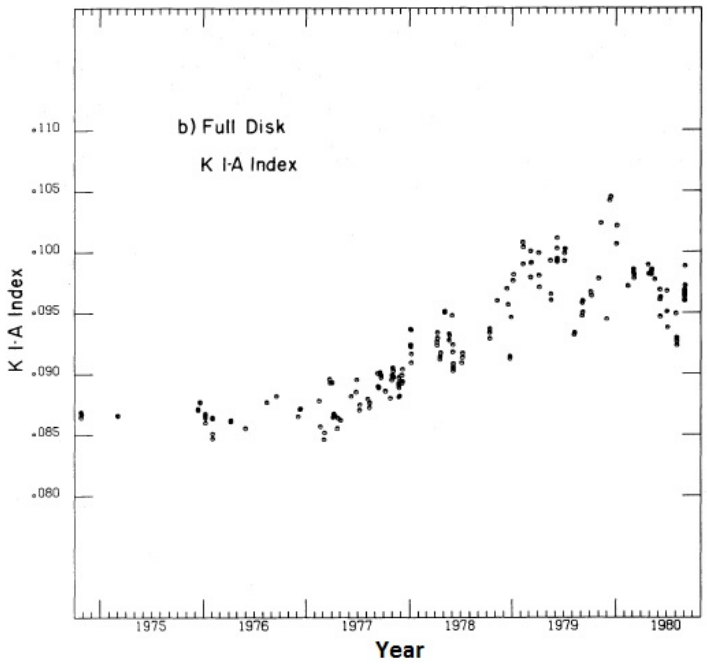

FIGURE 3.1: Variation of Ca-K index with the phase of solar cycle during the period of 1974-80 as determined by White and Livingston (1981) from the spectroscopic observations of Sun as a star. *Courtesy*: White and Livingston (1981)

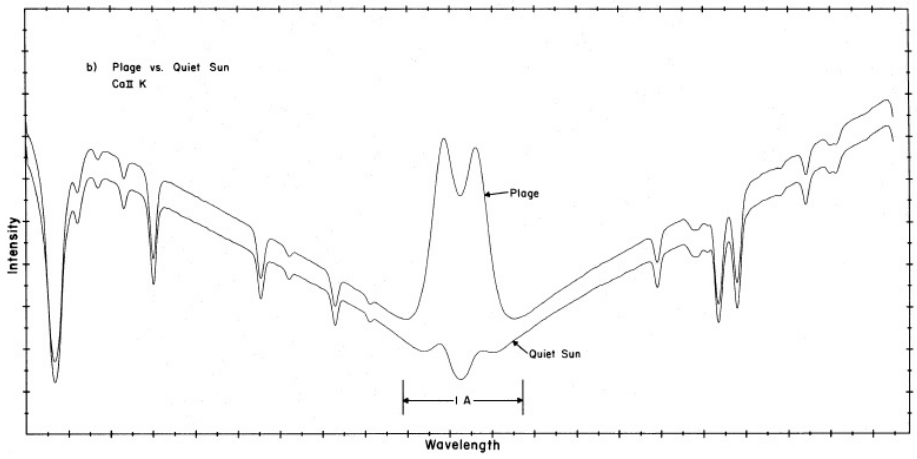

FIGURE 3.2: The observed Ca-K line profiles for the plage and quiet region of the Sun. *Courtesy*: White and Livingston (1981)

Pevtsov *et al.* (2013) using Ca-K line profiles made the effort to understand the variations of quiet chromosphere by removing K_2 components from the Ca-K line profiles, the resultant of which is also known as basal component. The basal profile originates from non-magnetic chromosphere and shows slight variation between minimum and rising phase of the sunspot cycle. It may be possible that the contribution of 'active network' component introduced by Skumanich *et al.* (1984) comes from different latitudes at different times, probably due to spread of decaying magnetic fields or some other reasons. To estimate the contribution of the active network component to chromospheric irradiance, a new technique of observations was developed by Singh in 1986, Singh (1989) at Kodaikanal Solar Tunnel Telescope which involves taking the spectra around Ca-K line as a function of latitude and integrated over the visible 180° longitude. Singh *et al.* (2004) analyzed data of 2 years, (1986-1987) of Ca-K line profile as a function of latitude and made initial study to determine the contribution of plages and network flux to the line width. In this chapter we studied the variations in the Ca-K line profiles of the Sun as a star and compared the results with the results obtained by White and Livingston (1978); Keil and Worden (1984) to establish the authenticity of our method of observations.

3.2 Determination of Ca-K profiles of the Sun as a star

We have made observations of the Ca-K line profiles as a function of latitudes and integrated over the visible longitudes on daily basis for about two solar cycles. Before we study variations in the Ca-K line profiles with latitude and time, it may be a good exercise to establish the methodology of observations by comparing the results of these observations with the results of similar observations of the Sun as a star carried out at other observatories. We have also made limited observations of the Sun as a star for about 20% of the days compared to the data taken as a function of latitude. For comparison with other observations of the Sun as a star, more data points are desired. We, therefore, planned to determine the average Ca-K line parameters by combining results of observations at all the latitudes and compare these with our observations of the Sun as a star. It is rather difficult to give the weightage factor to Ca-K line profiles of each latitude properly to combine all the observed profiles on a given day to study

the combined profile of the Sun as a star because of varying intensity due to limb darkening and area with latitude. The comparison of average values of parameters for Ca-K line and the integrated values for the Ca-K line profiles of the Sun as a star obtained on number of days will help to determine the factor that needs to be applied to average value to get the integrated value and thus enlarge the data base.

To begin with, we have considered only two parameters for the comparison, namely the K_1 and K_2 widths. From the comparison of day to day values, it appears that the computed average values of K_1 and K_2 widths are greater than those observed from the Sun as star. The large values of K_1 and K_2 widths as compared to the Sun as a star values are likely due to the different weightage factor. We have taken simple average of the K_1 and K_2 widths for all the latitudes whereas areas at each latitude observed are different, and it is maximum at the equator.

To determine the relation between the average values of K_1 and K_2 widths and observed values of the Sun as a star, we made the scatter plots for both of these parameters as seen in left and right panels of Figure 3.3. The plot of average K_1 width derived from values of all latitudes (Here after referred as average value) versus K_1 width of the Sun as a star (referred as integrated value) is shown in the left panel of Figure 3.3. The Figure indicates a relation between these two values. We fit a linear and various degree polynomial fits to these data points. The χ^2 test indicated that a quadratic fit matches well with the data points but it may be noted that the linear fit and the quadratic fit yield similar results. The quadratic fit shown in the plot gives the relation between the integrated K_1 widths and average widths. From the fit, we derived the relation between the K_1 widths shown in the plot. Using this relation, we computed the integrated values for K_1 widths for each day of observations to make a comparison with other similar observations. We also found that the derived values of integrated K_1 width from the linear and quadratic fits are similar for the middle values of average K_1 widths. A maximum difference of 0.025 Å was found for the small and larger values of average K_1 width. Similarly we derived the relation for K_2 width as shown in the right panel of Figure 3.3.

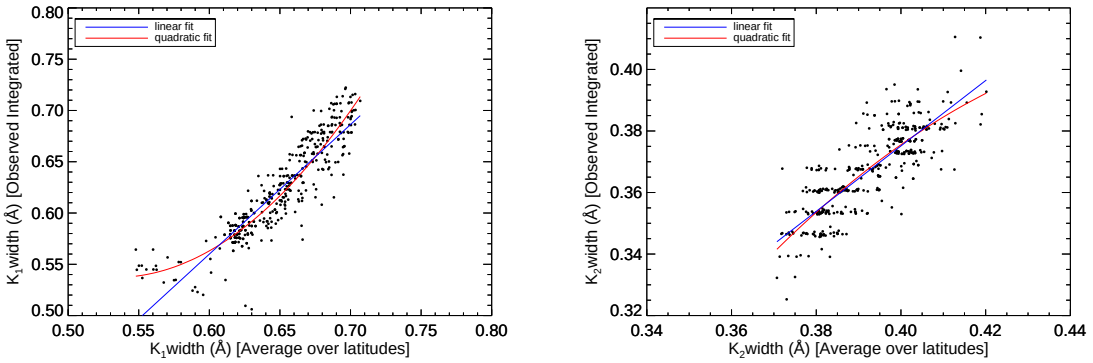

FIGURE 3.3: *Left*: Plot of average values of K_1 width derived from the values at all the latitudes vs values obtained from the observations of the Sun as a star shown along with linear fits(blue) and quadratic fits(red). *Right*: For K_2 width. The χ^2 test indicates that a quadratic fit represents a better relation.

3.3 Comparison of K_1 and K_2 widths of the Sun as a star with those obtained at Sac Peak and Kitt Peak

White and Livingston (1978) and Keil and Worden (1984) have made extensive observations of the Sun as a star using Mcmath telescope at Kitt Peak (KP) and NSO/Sac Peak observatories, respectively. It may be noted that observing facility at NSO/Sac Peak is dedicated to these observations whereas the facilities at Kodaikanal (KO) and Kitt Peak are being used for other type of observations too. This caused large gaps and less data sample of KO and KP as compared to that at NSO/Sac Peak observatory. Only 282 days of our observations are common with those of NSO/Sac Peak and 100 days of observations are common with those of KP due to availability of the telescope for this kind of observations and sky conditions. Also, time difference of about 12 hours exists between ours and their observations due to longitude difference between the locations of the observatories. We have three sets of data namely, from Kodaikanal, Kitt Peak and NSO/Sac Peak observatory but common days of observations are different in these three data sets.

To have a meaningful comparison between the three data sets, first we removed the outliers from all the three data sets by restricting the values up to 2σ level. After removing the outliers from all the three data sets, we computed the mean, standard

TABLE 3.1: Statistics of the line parameters after removal of outliers considering the 2σ level variations.

	Kodaikanal		Kitt Peak		NSO/Sac Peak	
	K_1 width (Å)	K_2 width (Å)	K_1 width (Å)	K_2 width (Å)	K_1 width (Å)	K_2 width (Å)
Mean	0.633	0.366	0.641	0.369	0.630	0.375
σ	0.039	0.011	0.040	0.010	0.048	0.017
$Width_{max}$-$Width_{min}$ (range)	0.169	0.049	0.166	0.039	0.221	0.130
Residual σ	0.022	0.007	0.016	0.005	0.026	0.013

deviation and difference in maximum and minimum values (range) as listed in Table 3.1. The means of K_1 and K_2 widths for all the three data sets are about 0.635 ± 0.005 Å and 0.370 ± 0.005 Å respectively indicating a correlation and accuracy in measurements made at all the three observatories. Standard deviation values of K_1 (0.039 ± 0.001 Å) and K_2 widths (0.011 ± 0.001 Å) for KO and KP data are in agreement as seen in Table 3.1. But those of NSO/Sac Peak differ being 0.048 and 0.017 Å respectively. In addition to this, Table 3.1 indicates that ranges of values of K_1 and K_2 widths for the KP and KO data agree but differ from the NSO/Sac Peak values. Table 3.1 shows generally an agreement in all the derived parameters, the small differences in values may be due to difference in time of observations. The smaller range and scatter in the width measured at KP and KO as compared to that for NSO/Sac Peak values may be because of difference in the resolution of the instruments (5, 6.5, 26 mÅ for the KP, KO and NSO/Sac Peak, respectively).

We have chosen yearly mean of the data due to limited number of observations to remove the cyclic variation in the K_1 and K_2 widths. Then we made scatter plots of the residuals of K_1 widths of the Sun as a star for the KO and NSO/Sac Peak values (Top left panel); KO and KP values (Top right panel) and KP and NSO/Sac Peak values (Bottom panel) of Figure 3.4 to study the correlation between three data sets. The figure shows good amount of scatter in the values which may be basically due to about 12 hours difference in the observation made on each day. The measurements of widths indicate significant variations in the day to day observations. In spite of these factors there appears correlation between all the data sets and it may be noted that significance level of the correlation coefficient is above 99% in all the three cases. Further, it may be noted that the mean values of K_1 and K_2 widths determined at KO agree well with KP than those of NSO/Sac Peak with KP. The values of rms

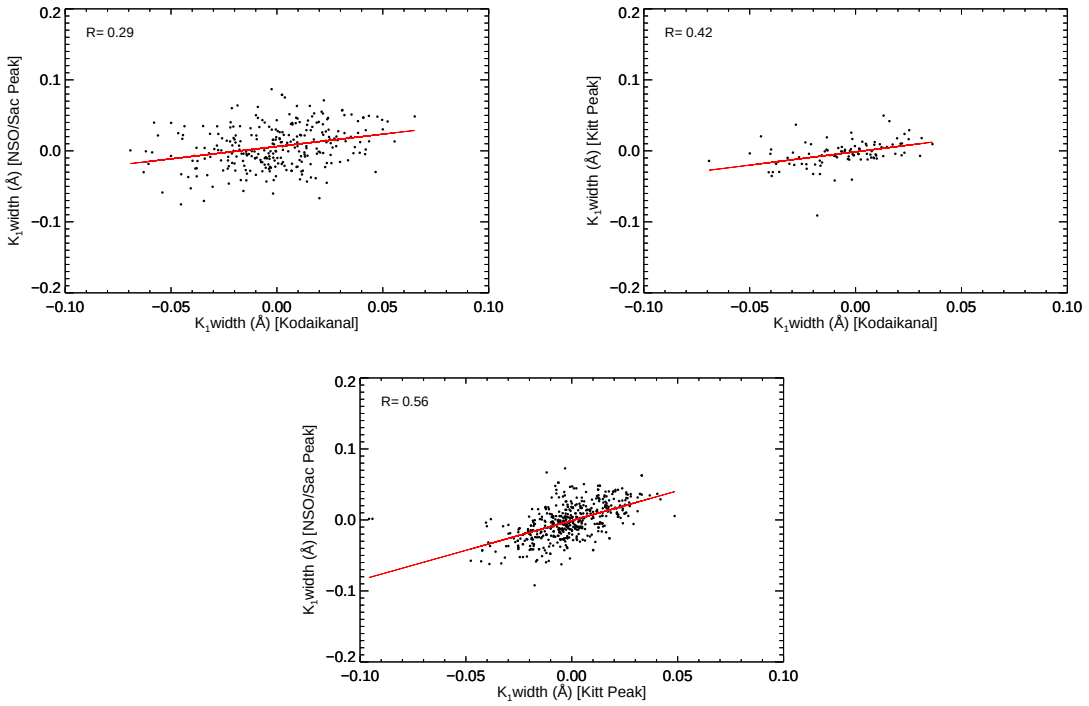

FIGURE 3.4: *Top left*: shows the scatter plot of the residual values after removal of outliers and cyclic variations in the measurements of K_1 width for the Kodaikanal data vs that of NSO/Sac Peak data along with a linear fit. *Top right*: Residuals of K_1 width for Kodaikanal vs Kitt Peak and *Bottom*: for the data of Kitt Peak vs NSO/Sac Peak values along with linear fit. The values of correlation coeffcients (R) are written in each panel.

variations for the scatter plots of all the three data sets are listed in Table 3.2. The listed values are close to the resolution limits of observations dominated by the slit width of the spectrograph (11 mÅ in case of KO and 26 mÅ for the NSO/Sac Peak). Similarly, the residuals for the K_2 widths for all the three data sets indicate correlation but apparently scatter in the values appear large as seen in Figure 3.5 because the variations in K_2 widths are much less as compared to variations in K_1 width. Further, it may be noted that scatter in the KO and KP values is less than that in the NSO/Sac Peak values. Even though the correlation coefficient is small their significance levels are above 98% in each case. It may be noted that average amount of scatter in the values of K_1 width is less than the resolution of the instrument for the KO and KP data.

Further, it may be recalled that the observations made during poor sky conditions

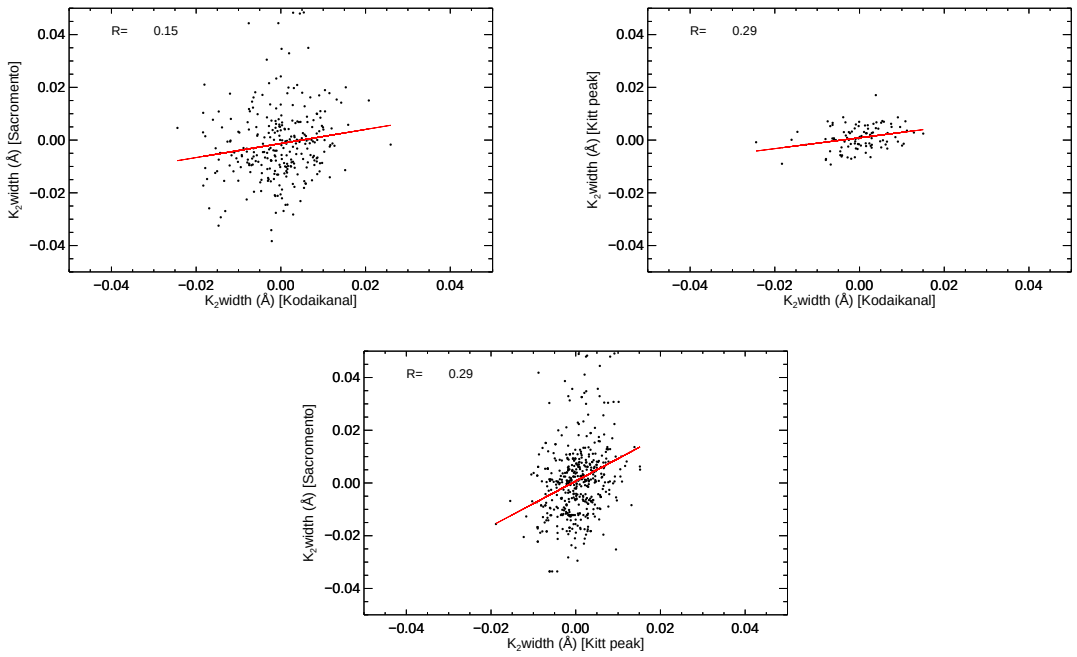

FIGURE 3.5: Same as that for the Figure 3.4 but for the K_2 width of Ca-K line profile.

TABLE 3.2: RMS variations in the scatter plot of the K_1 and K_2 widths measured for three observatories.

Observatory	K_1 width (mÅ)	K_2 width (mÅ)
Kodaikanal and NSO/Sac Peak	28.2	13.7
Kodaikanal and Kitt Peak	14.6	4.3
Kitt Peak and NSO/Sac Peak	20.7	13.7

and high clouds caused the intensity vignetting in the data. Using the record of sky conditions maintained in the logbook, we discarded all the data obtained on the days with poor sky conditions. Instrumental stray-light also affects the line profile but the agreement in parameters such as mean, range and standard deviation values for K_1 and K_2 widths for the Kodaikanal, Kitt peak and NSO/Sac Peak (Table 3.1) indicates that scattered light in the instruments at kodaikanal has been less or similar to in the instruments at other observatories.

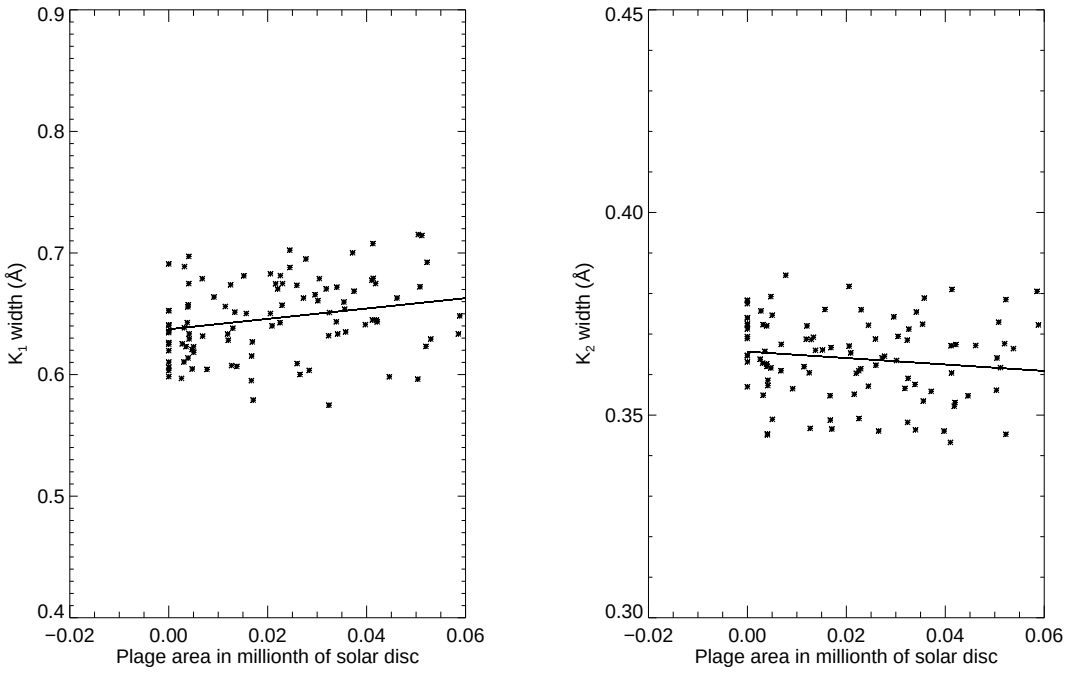

FIGURE 3.6: *Left*: Scatter plot of K_1 widths versus measured plage areas in millionth of the solar disc *Right*: Same for K_2 width

3.4 K_1 and K_2 widths of Ca-K profile and plage areas

The plages are the brightest among the Ca-K line features and affect the line profiles, relatively, by larger amount. The emission at K_{2v} and K_{2r} in case of Plages is much more than that in the networks. Therefore, variation in plage areas on the Sun is likely to cause large variations in K_1 and K_2 widths as compared to that in the networks. Hence, we have plotted in Figure 3.6 the K_1 and K_2 width versus plage areas determined from the Ca-K spectro-heliograms obtained at Kodaikanal observatory as described by Priyal *et al.* (2014). The plot shows that generally the K_1 width increases whereas K_2 width decreases with the increase in plage areas and the linear fits in the plot confirms the same. The scatter in the plot appears considerable, more than the uncertainty in the measurements of both the parameters. The uncertainty in measurement of width of the K_1 and K_2 is < 5 mÅ and the plage areas have been determined fairly well. It appears that plage areas are not able to account for the day to day variations in the K_1 width, assuming that intensity is same for all the plages

and remains the same during their growth and decay. The scatter can arise because of variations in the contribution of enhanced, active and quiet network towards the K_1 and K_2 widths. Therefore, day to day variations in the K_1 width may be due to variations in the contribution from networks in addition to variation in plage areas. The variation in intensity of plages at shorter time scales as well as solar cycle can also cause variation in K_1 and K_2 widths. The systematic measurements of intensity of plages with time have not been done and considered in modelling the solar irradiance which may cause day to day variations in widths. The K_1 width increases with increasing activity because higher temperature of active regions is likely to cause broadening of the Ca-K profile. The emission at K_{2v} and K_{2r} also increases in active regions. It is not clear why the K_2 width decreases with increasing activity? It may be due to asymmetry in the profile around K_{2v} and K_{2r} peaks.

3.5 Variation of K_1 and K_2 width with solar cycle

In the upper part of top-left panel of Figure 3.7 we plot the K_1 width of Ca-K line as a function of time (outliers are removed on all the days of observations made between years 1989 - 2011). The sky conditions do not permit the observations during the months from June to November which caused a gap every year in the plot. Yearly mean values of the K_1 width are indicated by the red dotted solid line in the figure. We also show the Standard deviation (SD) for the yearly mean by the length of the bar. It may be noted that this is not due to measurement error but because of actual variation in widths caused by variations in Ca-K features such as plages and networks. In the lower part of this panel, residuals of the K_1 width are plotted as a function of time (after the removal of cyclic variations). Similarly, top right-panel of Figure 3.7 shows the variation of K_2 width and residuals as a function of time. Both these panels indicate that a deviation of residuals are more at maximum and smaller at minimum phase of the solar cycle. These results agree with the findings of Scargle *et al.* (2013). The bottom panel shows the variation in the ratio of K_1 to K_2 width as a function of time. All the three panels indicate large variations in K_1, K_2 and their ratio at short as well as at long time scale, namely, days and solar cycle time scales. These might be caused by the rotational modulation or by other phenomena listed

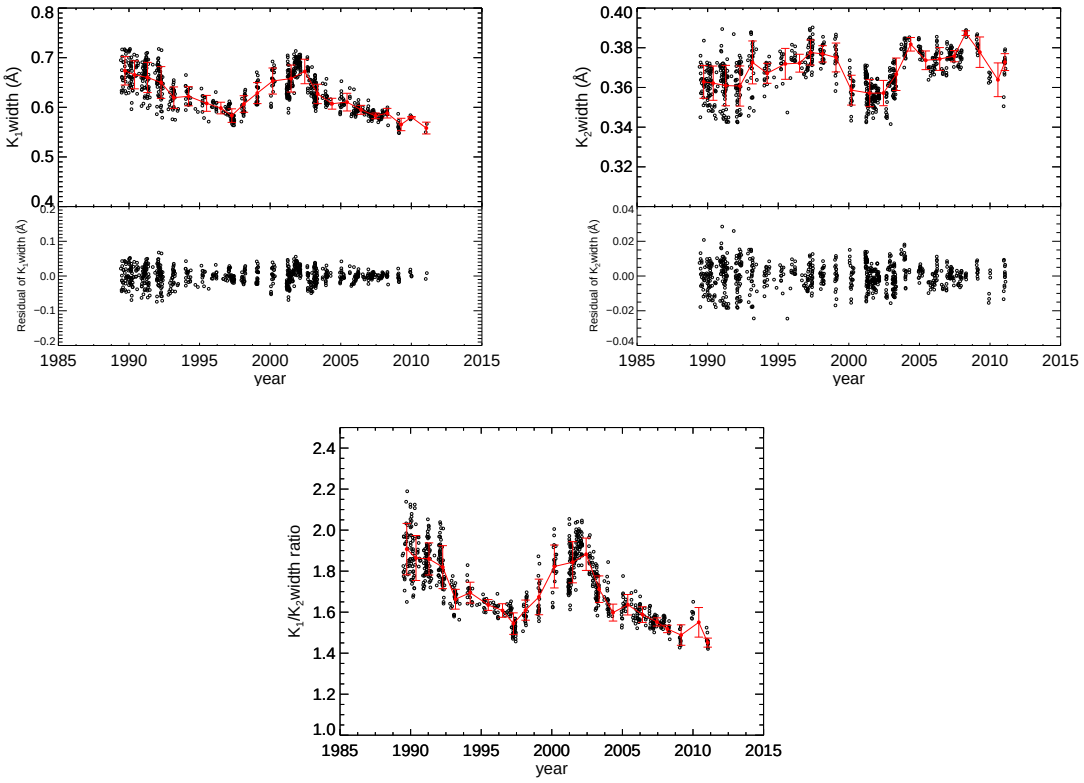

FIGURE 3.7: *Top left*: Variation of K_1 width with time after outliers removal. *Top right*: Variation of K_2 width with time after outliers removal. *Bottom*: Variation of K_1 to K_2 width ratio with time. The black circles show the day to day data and the red solid line shows the yearly mean values along with standard deviation by bars on yearly basis.

by Scargle *et al.* (2013) which cause variations in Ca-K line profile with different amplitude and periods. It is not possible to investigate the short period variations in widths because of large gaps in the data and hence, we discuss long period variations only. The top-left panel of Figure 3.7 indicates that K_1 width of Ca-K line varies with the solar cycle phase, being larger at the maximum phase of the solar cycle and smaller during the minimum phase, apart from the day to day variations due to changes in the plage areas. Similarly, K_2 width also varies with the solar cycle phase but its width is larger at the minimum phase as seen in the top-right panel of Figure 3.7. The ratio of K_1 to K_2 width also varies with the phase of the solar cycle being larger during the maximum phase of the solar cycle and it may be noted that the ratio has the lower value during cycle 23 as compared to that for cycle 22. The values of K_1 and K_2 widths during the minimum and maximum phases are given in Table 3.3 for solar cycle 22 and 23 for comparison.

TABLE 3.3: Average K_1 and K_2 widths during minimum and maximum phase

Period	K_1 width (Å)	K_2 width (Å)
Maximum (1991)	0.673±0.02	0.36±0.01
Minimum (1997)	0.58±0.01	0.38±0.01
Maximum (2003)	0.672±0.02	0.36±0.01
Minimum (2011)	0.55±0.01	0.37±0.004

3.6 Results and Discussions

From the observations of the Sun as a star, White and Livingston (1981) found that K_1 width of the Ca-K line increases with increasing activity whereas K_2 width decreases. They also reported that K_3 intensity and K-index increases by 30% and 18%, respectively, during the maximum as compared to those at minimum phase of the solar cycle. Worden *et al.* (1998) empirically found intensity threshold values to identify the Ca-K plages and networks to model the solar irradiance variations. They found that the plage and enhanced network typically cover about 13% and 10%, respectively, of the solar disk around solar-maximum and active network can cover large portion of the Sun during minimum period. Kariyappa and Pap (1996) reported that the variation in spatial index and full width at half maximum (FWHM) of the intensity distribution of the chromospheric features such as plages and networks observed from Ca-K spectroheliograms representing the activity agrees with the UV irradiance measured in MgII h and K lines. It is not clear from their paper, how the FWHM of the intensity distribution without the accounting for the limb darkening effect can be related with the solar cycle variations. The plages in the Ca-K images are most intense and therefore, lie at the edge of the intensity distribution curve. Hence the occurrence of the plages is not likely to contribute to the width of FWHM of the intensity distribution curve. Further, the FWHM of the distribution curve is effected by the contrast of the image due to seeing conditions during the observations. Poor seeing conditions diffuses the bright points and therefore, changes the intensity of bright points. In a Ca-K image where intensity due to limb darkening effect has not been corrected, part of the FWHM of the intensity distribution curve is because of background chromosphere coupled with limb darkening effect, which is likely to vary due to sky conditions and small changes in the observational set up such as minor shift in the Ca-K line on the exit slit incase of spectroheliograph or shift in the pass-band of the filter incase of filter-grams and some other effects. The intensity of the bright

points lies between that of background and plages. The number of bright points and intensity of bright points are likely to effect the width of FWHM of the distribution. The part of variations may be due to seeing condition. Hence, the variation in FWHM of the intensity distribution may not represent the solar cycle variatons. Further, Verbeeck *et al.* (2014); Kumara *et al.* (2014) have used segmentation method to identify the active regions, coronal holes and quiescent Sun (QS) to study the UV and EUV variability of the Sun. Identified active regions are likely to resemble with Ca-K plages. The coronal holes cannot be identified in the Ca-K images. The QS identified in EUV images is due to high temperature coronal plasma and the Ca-K emission is because of chromospheric plasma at relatively low temperature. The networks in Ca-K images appears distributed all over the solar surface during all phases of solar cycle. The boundaries of networks coincide with the boundaries of large convective cells seen in Dopplar-grams (Leighton 1959; Leighton *et al.* 1962) and the contribution to the solar irradiance due to networks vary by few percent with the solar cycle phase (Worden *et al.* 1998). Whereas quiet Sun (QS) identified by Kumara *et al.* (2014) represents solar corona and is the greatest contributor to solar irradiance, up to 63% in the EUV spectral irradiance in terms of intensity. The active regions contribute about 10% and off-limb features about 24%.

We have made observations of the Ca-K line profiles on a daily basis as a function of latitudes and integrated over the visible longitudes. This data can be used to study the variations in the various parameters with latitude and solar cycle phase for about two solar cycles. The analysis of the data was done to derive the K_1 and K_2 widths of the Sun as a star using the values of K_1 and K_2 widths computed for different latitudes at an interval of 10°. The values of K_1 and K_2 widths of Sun as a star obtained at KO shows good correlation with those obtained at KP and NSO/Sac Peak. The results discussed in section 3.4 indicate that the observed day to day variations in the K_1 and K_2 widths may be caused by not only the plage areas but also by variation in intensity of plages and variations in the enhanced, active and quiet networks and may be responsible for the day to day irradiance variations. To delineate the contribution of each feature to these variations, more systematic observations are required. It may be noted that the average value of K_1 width during the maximum phase of the solar cycle 22 is 0.673 Å and 0.672 Å for cycle 23 (obtained from the yearly mean data). In addition we find that yearly mean of K_1 width is larger (0.58 ± 0.01 Å) during the minimum phase of cycle 22 for the period of March - December 1997 as

compared to the average value (0.55 ± 0.01 Å) during the minimum phase (January - Februray 2011) of cycle 23. It may be noted that standard deviation (SD) is 0.01 Å whereas the difference in mean values at two minima is 0.03 Å and large variations are not expected during the minimum phase as seen in the residual plot of Figure 3.7. Further, the ratios of K_1/K_2 width are 1.54 and 1.45 during the minimum phase of cycle 22 and 23. The smaller value of K_1 width and K_1/K_2 ratio during the cycle 23 may be because of the extended minimum phase of this cycle. We speculate that the extended minimum phase may lead to lower temperature of the chromosphere or lower small scale chromospheric activity causing the K_1width to be smaller as compared to that for cycle 22. The plot of K_2 width versus plage areas indicates that K_2 decreases with increasing activity but it shows only ~ 10% variation in the width as compared ~ 20% variation in K_1 width during these two solar cycles. These findings have support from the fact that in 2010-11 when the sunspot activity has started appearing with sunspot number around 25, the K_1 width continues to be minimum implying less chromospheric emission in Ca-K. The effect of extended minimum on the emission in Ca-K line agrees well with the results obtained from the analysis of Ca-K images obtained at Kodaikanal by Singh *et al.* (2012).

Chapter 4

Variations as a function of Latitude

4.1 Introduction

[1] The Sun as a star has been investigated by many researchers, using spectroscopic method (Livingston *et al.* 2007b) and references there in, imaging mostly in Ca-K line (Priyal *et al.* 2014) and references there in, by measuring the integrated flux in visible, EUV X-ray, 10.7 cm and some other part of the electromagnetic spectrum. A large body of data have been collected and analysed to study the short as well as long term variability of the Sun. Various features of images have been identified to delineate the significance of various feature in the variability of the Sun. In spite of all these studies, number of questions need to be answered. Is there any variation in the background chromospheric emission with the phase of solar cycle? It is known that features in the mid latitude and equatorial belts vary with the phase of solar cycle and other periods but how the polar regions and high latitude regions behave with solar cycle still needs to be investigated reliably? Therefore, information about variation as a function of latitude and its variation with time will be very useful to understand the dynamo process and the variability of the Sun realistically. Engvold (1966) measured K_2 width of Ca-K line as a function of longitude to study the limb darkening but not much information is available about temporal variations at different latitudes.

[1]The chapter is based on the paper Sindhuja *et al.* (2015)

We, therefore, planned an experiment to monitor the Ca-K profiles to derive the information as a function of latitude and time. As discussed earlier, the observed K_1 and K_2 widths are more dependable than the K-index for the investigation of cyclic variations, especially for the study of variation of profiles as a function of latitude as the profile at a chosen latitude may have some contribution from other parts of the Sun because of increase in scattering in the presence of thin clouds or passing clouds.

Further, we have computed the plage areas as a function of latitude at an interval of 10° in millionth of the hemisphere in regions of 10° in latitude and 180° in longitude. We compare the variations in the K_1 and K_2 widths with those in plage areas and explore to estimate the contribution from other features for the solar cycle 22 and 23.

4.2 Variation of Ca-K line profile with latitude

We have determined the average Ca-K profiles over regions covering 10° in latitude and 180° in longitude at an interval of 10° up to 70° in both the hemispheres. The data over the remaining visible polar region up to solar limb is averaged as it is and referred it as an 80° latitude curve. The averaged region near poles has the seasonal variation over the year. Figure 4.1 shows these normalized Ca-K line profiles for different latitudes at an interval of 10° with each curve being offset by 0.01 in intensity along the y-axis with respect to the preceding curve to show all the profiles clearly in a single plot. A look at the profiles indicates that K_1 width (separation between the two valleys of K_{1v} and K_{1r}) and K_2 width (separation between the two peaks K_{2v} and K_{2r}) appear to increase with latitude continuously during the minimum phase of the solar cycle. Further, to study the variations in detail , the K_1 and K_2 widths and other parameters for each latitude were computed from these normalized profiles as explained earlier in chapter 3. In the following we discuss the variations in parameters of Ca-K line profile with latitude and time.

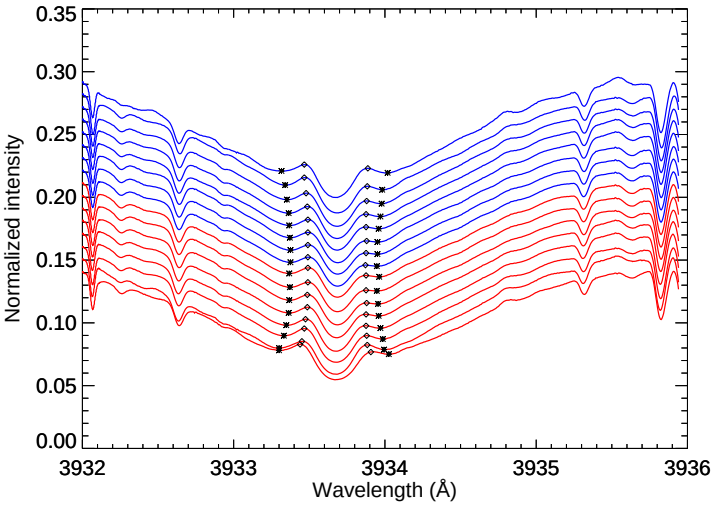

FIGURE 4.1: Figure shows the normalised Ca-K line profile averaged over 10° in latitude and 180° in longitude at an interval of 10° for Northern (blue) and southern latitudes (red). The bottom most curve at 80° south has the original normalized values and successive curves have been offset by 0.01 in intensity. The top most curve is for 80° north latitude. The separation between two astericks and two diamonds gives the K_1 and K_2 width, respectively

4.2.1 Variation of Ca-K line parameters during Minimum and Active phase

To study the average variations of all the parameters of Ca-K line profile during the minimum and active phase of the solar cycle we have chosen few days during the period of March 2007 when no sunspots were visible on the solar disc, representing the minimum phase and few days in the month of March 2000 representing the active phase of the solar cycle. We computed the various parameters of Ca-K line profile and plotted as function of latitude in Figures 4.2 and 4.3 for the minimum and active phase, respectively. The spread in the values of various parameters, represented by vertical bars (SD) in Figure 4.2, is small during the minimum phase as expected because of absence of large scale activity during this phase which generally varies by large amounts at short intervals. The values of various parameters (except intensity ratio of K_{2v} to K_{2r}) shown in Figure 4.2 increase with latitude in both the hemispheres during the minimum phase of the solar cycle. These variations are because of centre to limb effect as indicated by Athay and Skumanich (1968). Due to

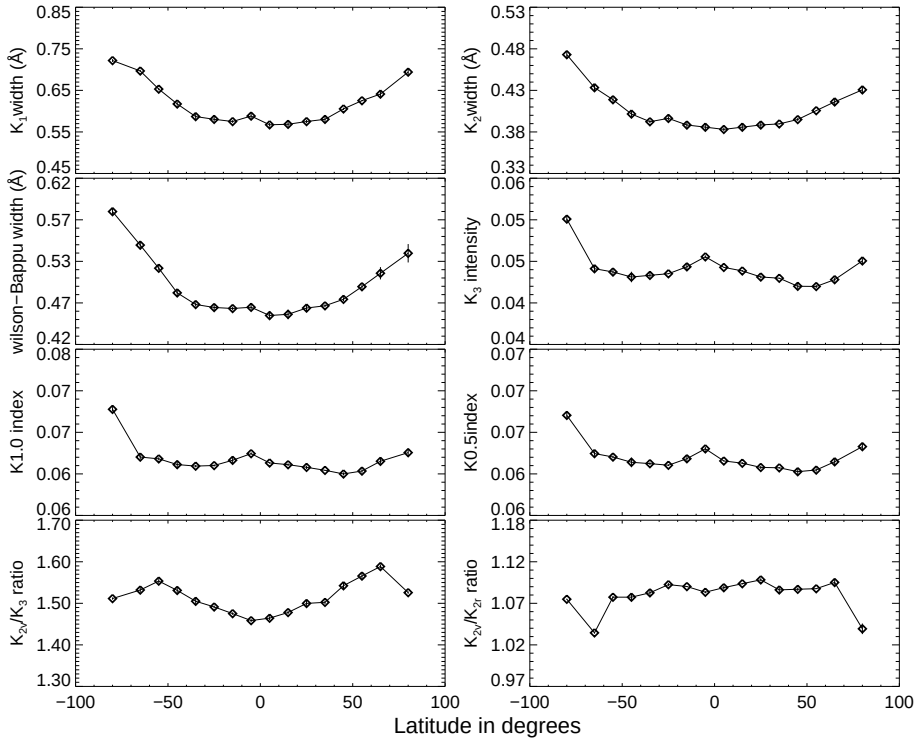

FIGURE 4.2: Average of Ca-K line parameters K_1, K_2, wilson-bappu widths, K1.0, K0.5 index, K_3 intensity and K_{2v}/K_3, K_{2v}/K_{2r} ratios for few days in March, 2007 (minimum phase of solar cycle) when no Sunspots or plages were visible. Standard deviation is shown as bars which is not due to the error but because of day to day variation in solar activity.

centre to limb effect one observes upper layers of the chromosphere near the edges of the Sun as compared to centre. The increase in temperature with height in the chromosphere causes increase in width of the Ca-K line with latitude as the Ca-K line profile originates in higher parts of the chromosphere at larger latitudes. Hence, K_1 width is expected to increase with increasing distance from the centre of the Sun as one observes higher in the chromosphere at higher temperature at larger distance from the centre. It may be noted that these variations with latitude are mostly due to line-of-sight effect only and may have marginal contribution from different activity at different latitudes, if any. Some departure from the steady increase in the values of K_1 width, K_{2v}/K_3 and K_{2v}/K_{2r} intensity ratios at high latitude around 70° may be due to anticorrelated activity in polar region with that of mid-latitudes.

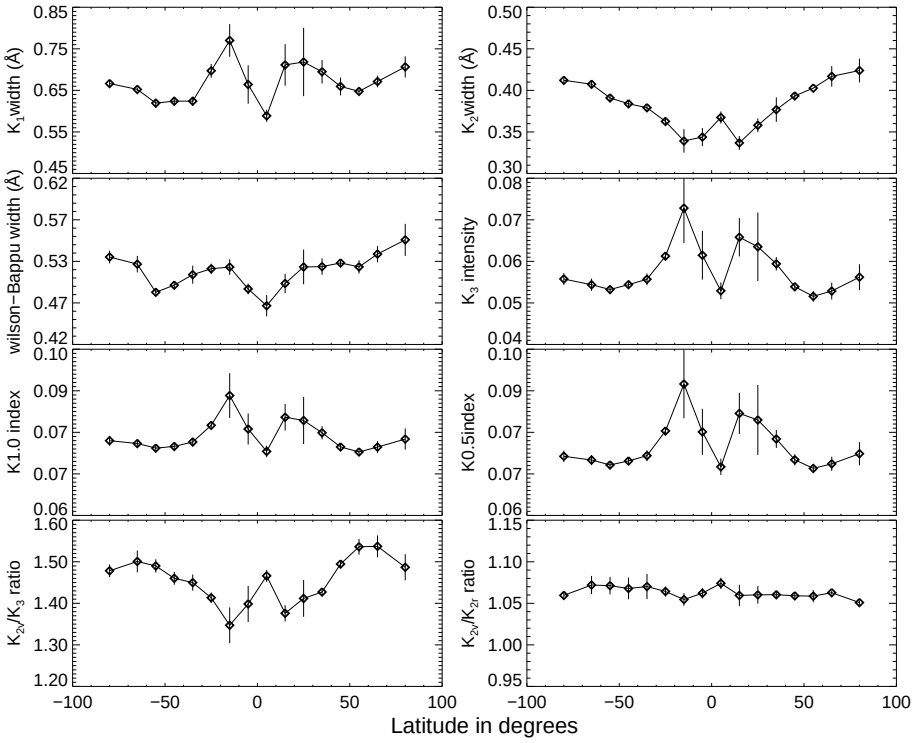

FIGURE 4.3: Average of Ca-K line parameters K_1, K_2, Wilson-Bappu widths, K1.0, K0.5 index, K_3 intensity and K_{2v}/K_3, K_{2v}/K_{2r} ratios for few days in March, 2000 (active phase of solar cycle). Standard deviation is shown as bars which is not due to the error but because of day to day variation in solar activity.

In addition Figure 4.2 shows that K_1 and W-B widths, K_3 intensity, K1.0 and K0.5-indexes have larger values at 5° southern latitude as compared to those at the adjacent latitudes. The larger values of these parameters indicate more activity around 5° latitude belt which may be due to small scale Ca-K network activity as no sunspots were seen on the solar surface during the period of observations. Further, the ratio of K_{2v} to K_3 intensity shows increase with latitude up to about 60° latitude but the value of this ratio decreases in the polar region as compared to that at 60°. Similarly, the ratio of K_{2v} to K_{2r} intensity remains more or less the same up to 60° latitude and decreases in the polar regions. In addition, all these parameters indicated sharper increase in the values with latitude in the southern hemisphere as compared to the increase in the northern hemisphere. The difference in the variations of the parameters with latitude in northern and southern hemispheres may imply that even the small scale activity in the form of networks, generally representing weak magnetic fields on the Sun, is different in both hemispheres.

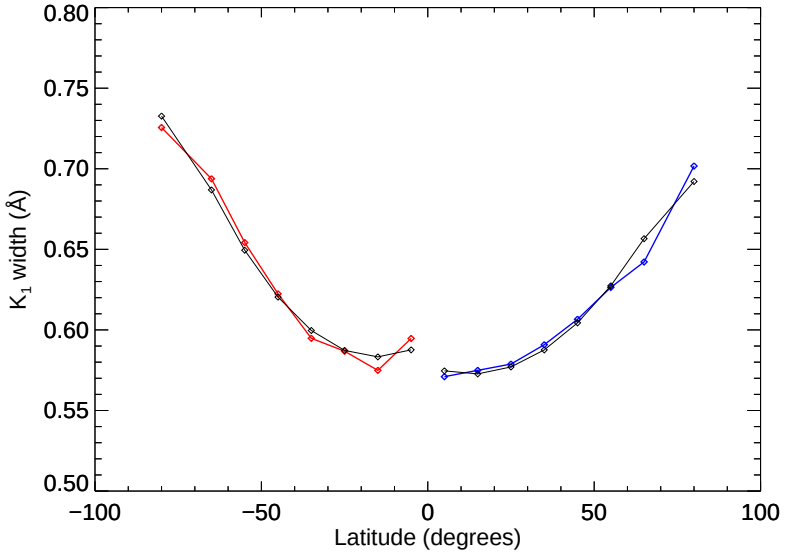

FIGURE 4.4: Figure shows average K_1 width over 10° latitude and 180° longitude as a function of latitude, separate polynomial fits to the southern and northern hemisphere is also shown in Figure.

On the other hand, the spread in the values of Ca-K line parameters represented by the vertical bars in Figure 4.3 is large, especially at the middle latitude region. Also the values of K_1 width, K_3-intensity and K-index parameters are large around 25° latitude region in both the hemispheres. Whereas K_2 width and intensity ratio of K_{2v}/K_3 show lower values around 25° latitude. Both of these properties are signature of the existence of large scale activity in the visible part of the Sun at the middle latitude region during the active phase which shows large day to day variations and also with rotation cycle. Large variation in the activity at short intervals causes large spread in these plots, especially in the middle latitude region.

4.2.2 North-South asymmetry in K_1 width during minimum phase

Figure 4.4 shows the variation of K_1 width with latitude for the quiet Sun obtained from the observations made on March 7, 2007 when there was no visible sunspot on the solar surface. Similar variations have been observed on other days of the quiet Sun. The plot of K_1 width as a function of latitude shows the asymmetry in the

variation of the width in the northern and southern part of the Sun. The K_1 width increases faster with latitude in the southern hemisphere as compared to the northern hemisphere even during the minimum phase of the solar cycle. In the southern hemisphere, the K_1 width increases by 0.15 Å from 0.58 Å at 5° latitude to 0.73 Å at 80° latitude whereas it increases by 0.12 Å from 0.58 Å in the northern hemisphere. One would have expected a symmetric behaviour of K_1 width in both the northern and southern hemispheres as these measurements are held during the minimum phase of the solar cycle. The larger values of K_1 width in southern as compared to those in the northern hemisphere and positive correlation of K_1 width with the Ca-K emission may imply that chromospheric emission from the southern part was more than that from the northern part of the Sun even during the minimum phase of the solar cycle.

4.2.3 North-South asymmetry in K_2 width during minimum phase

We plot in Figure 4.5 the variation of K_2 width as a function of latitude with separate polynomial fits for the northern and southern hemispheres for the same day March 7, 2007. The plot of K_2 width with latitude shows the asymmetry in the variation of the width in the northern and southern part of the Sun. It is expected that during the minimum (absence of activity) phase Ca-K line widths will vary symmetrically in both the hemispheres but the K_2 width increases faster with latitude in the southern hemisphere as compared to the northern hemisphere even during the minimum phase of the solar cycle. In the southern hemisphere the K_2 width increases by 0.075 Å from 0.385 Å at 5° latitude to 0.46 Å at 80° latitude whereas it increases by $\sim$ 0.04 Å from $\sim$ 0.38 Å in the northern hemisphere. These variations confirm the findings from the measurements of K_1 width showing the asymmetry and faster increase in the southern hemisphere.

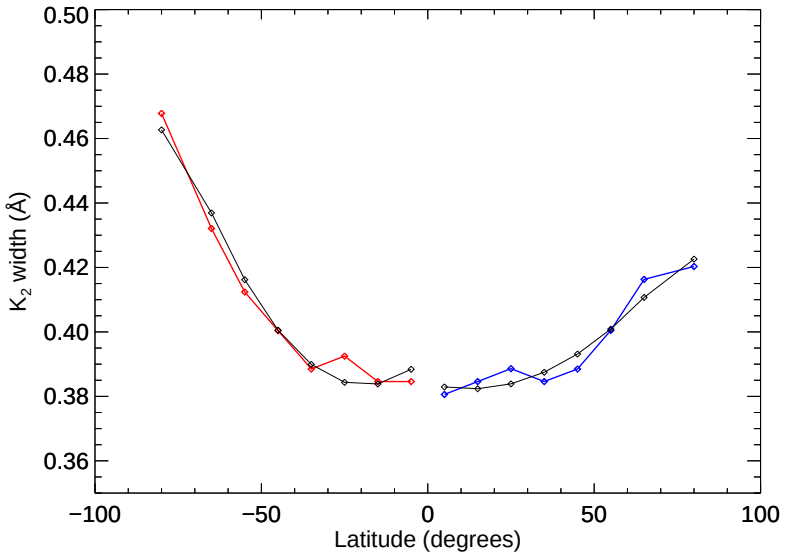

FIGURE 4.5: Figure shows average K_2 width over 10° latitude and 180° longitude as a function of latitude, separate polynomial fits to the southern and northern hemisphere is also shown in Figure.

4.3 Comparison of K_1, K_2 widths variations with other measurements

To study the variations in the line parameters with distance from the center of the Sun we have made plots of K_1 and K_2 widths, with and without integration along the longitudes. In Figure 4.6 we show K_2 widths as a function of distance from disc center in degrees by (triangles) without integration over longitudes and the widths with integration over longitudes by (diamonds). The plot shows K_2 widths for both the cases up to 65° latitude but it shows K_2 width at 75° (weighted average latitude) in case of integrated spectra over the longitudes and at 80° for spectra without integration along longitudes since we have not obtained the spectra at 75° latitude / longitude without integration. We have also compared the center-to-limb variations of K_2 widths with the variation of K_2 width as a function of longitude determined by Engvold (1966), shown by asterisks symbols in the plot. The comparison shows that the values obtained by us matches well with values obtained by Engvold (1966) at all the longitudes with a small difference of 0.002 Å upto 65° latitude. This small difference between the two could be related to the spectral resolutions of observations

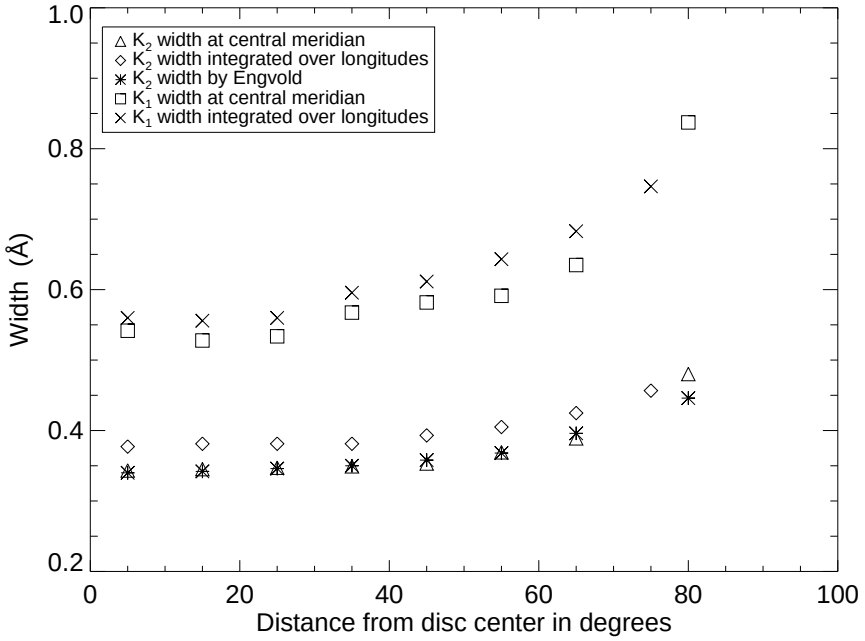

FIGURE 4.6: The figure shows the K_1 and K_2 widths of Ca-K line as a function of distance from disc center in degrees. Triangles show K_2 width at the central meridian as a function of latitude, diamonds show K_2 width for each latitude but integrated over the longitudes and asterisks indicates K_2 width determined by Engvold (1966) with longitude. K_1 width without and with integration over the longitudes are shown by squares and crosses , respectively.

or some uncertainty in measurements. The difference in K_2 width at 80° (0.03 Å) may be because of locating the spectrograph slit at the required position on the Sun's image due to large projection effect near the solar limb.

In the same plot we have also shown the variations of K_1 width as a function of latitude for both non-integrated at the central meridian by square symbol and integrated over the longitude belt by cross symbol. The comparison of K_1 and K_2 widths at respective latitude indicates that K_1 and K_2 widths increase with latitudes as expected. The values of K_1 and K_2 line width at various latitudes and integrated over visible longitudes are systematically larger than those without integration for longitudes up to 65° as seen in Figure 4.6 and the trend continues for higher latitudes. The larger values for the spectra integrated along longitudes are due to contributions from the larger longitudes where the widths will be more as compared to that of the central meridian.

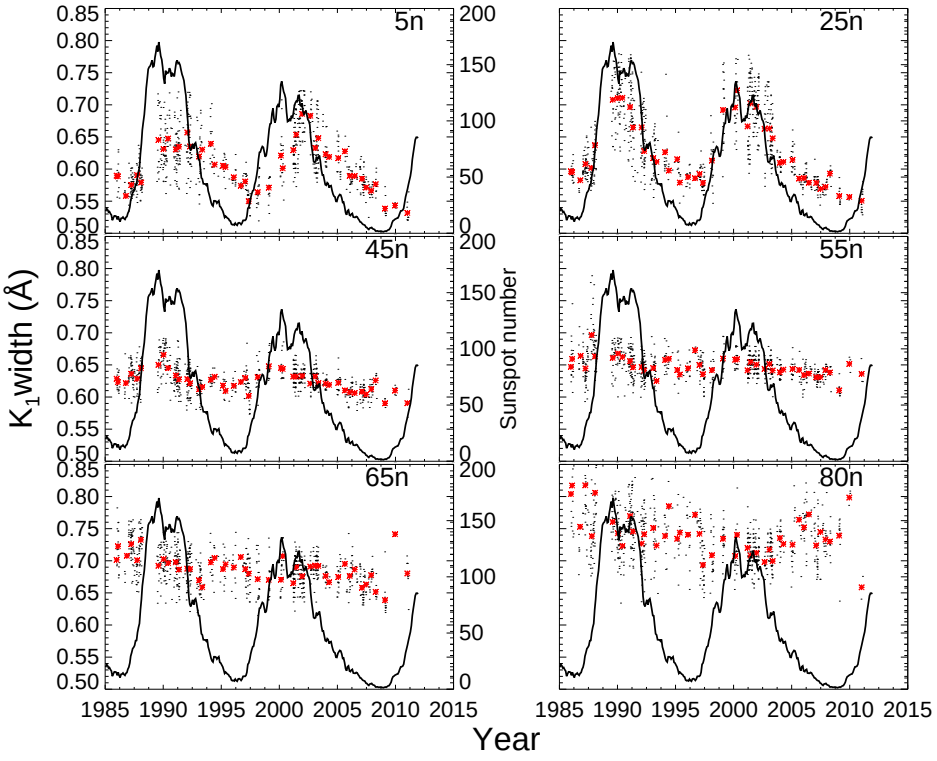

FIGURE 4.7: Variation of K_1 width of Ca-K line with time for the period of 1985 -2011 shown by dots. Over plotted are half yearly mean data (red asterisk) and half yearly averaged sunspot number (black line) for the northern hemisphere.

4.4 Variation of K_1 and K_2 widths with latitude and time

In Figure 4.7, we show the K_1 width for some representative latitudes such as 5, 25, 45, 55, 65 and 80° for northern hemisphere and in Figure 4.8 for southern hemisphere as a function of time for the period 1985 - 2011 to investigate the variation of activity with latitude and time. The figure indicates that K_1 width representing solar activity varies with the phase of the solar cycle appreciably at 25° whereas at higher latitudes its variation reduces with increasing latitude and becomes negligible around 60° latitude. Again the magnitude of variations with solar cycle increases in polar regions and becomes noticeable. The implications of these variations will be discussed in the last section.

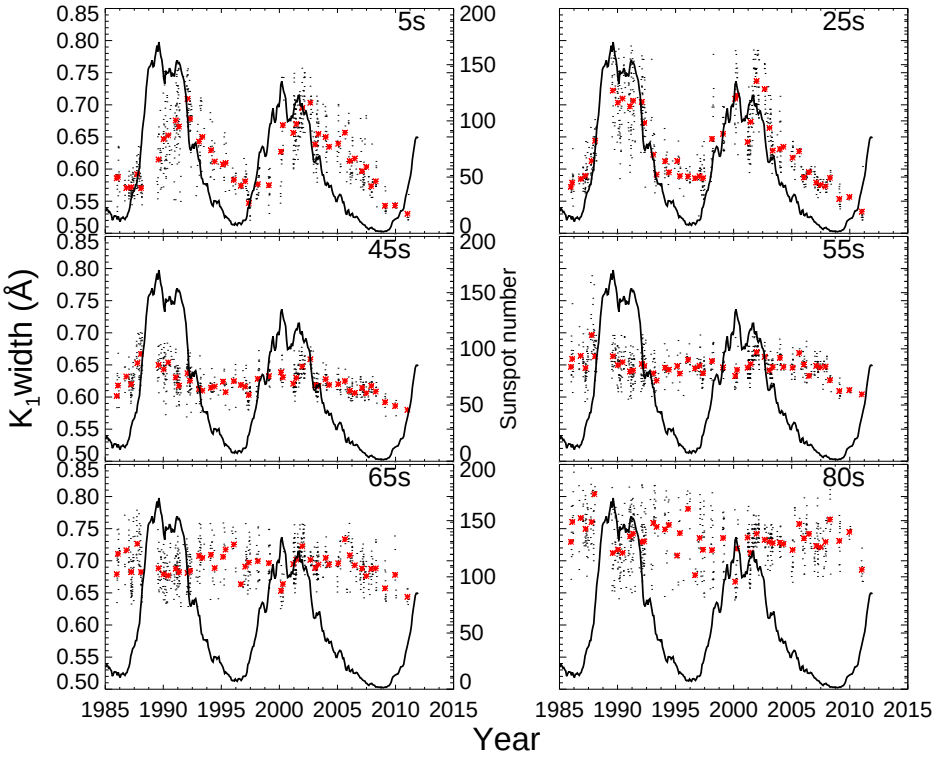

FIGURE 4.8: Same as Figure 4.7 but for the southern hemisphere.

To investigate the differences between active and minimum phase, we have divided the data in two groups one, around the active and the other, around the minimum phase of the solar cycle. The plage free data as seen from Ca-K images of the Sun during the periods of 1985-1986, 1995-97 and 2007-09 represents the minimum phase and rest of the period of observations during 1985-2011 period represents active phase of solar cycle. We have combined the data for two cycles because of data for less number of days.

In Figures 4.9 and 4.10 we plot the distribution of K_1 width for various latitudes for the active and minimum phase, respectively. The histograms in blue and red are for northern and southern hemispheres, respectively. To compute the most probable value of K_1 width and range of the distribution, we made the Gaussian fits to each distribution of K_1 widths. The Table 4.1 gives the most probable value of K_1 width defined by the peak of Gaussian and range of distribution defined by the FWHM of the Gaussian curve at each latitude for the quiet and active phases of the Sun. To have a quick look at the pattern of variations and compare the values for the two phases

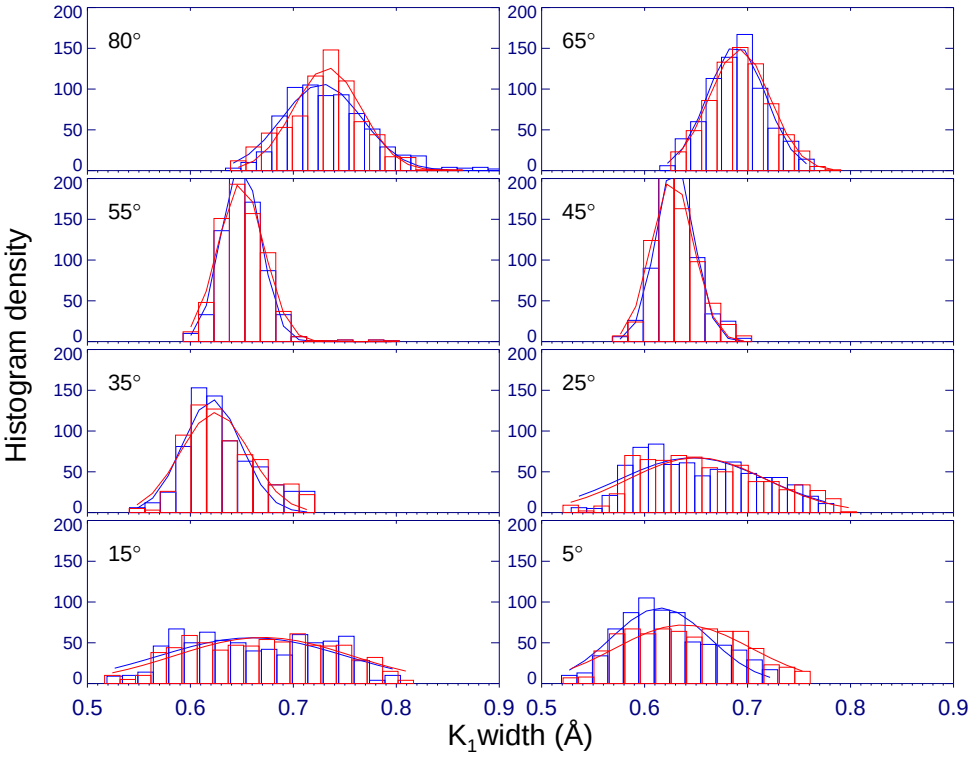

FIGURE 4.9: Distribution of K_1 width of Ca-K line profile for the active period for different latitude for both the hemispheres. Histograms in blue and red are for northern and southern hemispheres. Latitudes of histogram is noted in the top left corner of each panel.

TABLE 4.1: The most probable values of K_1 width defined by the peak of Gaussian fit to the frequency distribution of widths and range of the values defined by the FWHM of Gaussian fit for K_1 and K_2 widths for minimum and active phase as a function of latitude.

Latitude	Minimum (Peak)		Active (Peak)		Minimum (FWHM)		Active (FWHM)	
	K_1 width	K_2 width	K_1 width	K_2 width	K_1 width	K_2 width	K_1 width	K_2 width
80n	0.736	0.453	0.728	0.446	0.093	0.064	0.091	0.049
65n	0.669	0.426	0.689	0.422	0.093	0.026	0.066	0.031
55n	0.640	0.404	0.649	0.401	0.041	0.021	0.044	0.022
45n	0.615	0.391	0.629	0.389	0.036	0.015	0.043	0.019
35n	0.595	0.382	0.621	0.379	0.036	0.013	0.067	0.021
25n	0.581	0.381	0.647	0.367	0.043	0.023	0.167	0.033
15n	0.574	0.377	0.659	0.358	0.036	0.023	0.212	0.048
05n	0.571	0.375	0.615	0.359	0.038	0.023	0.112	0.037
05s	0.574	0.375	0.638	0.355	0.049	0.025	0.155	0.042
15s	0.571	0.377	0.671	0.357	0.049	0.025	0.202	0.044
25s	0.578	0.381	0.651	0.366	0.037	0.023	0.158	0.034
35s	0.591	0.382	0.624	0.379	0.031	0.018	0.079	0.025
45s	0.614	0.392	0.627	0.388	0.036	0.016	0.048	0.021
55s	0.646	0.408	0.649	0.399	0.039	0.023	0.053	0.026
65s	0.691	0.439	0.692	0.423	0.082	0.037	0.069	0.043
80s	0.739	0.467	0.733	0.446	0.111	0.033	0.078	0.050

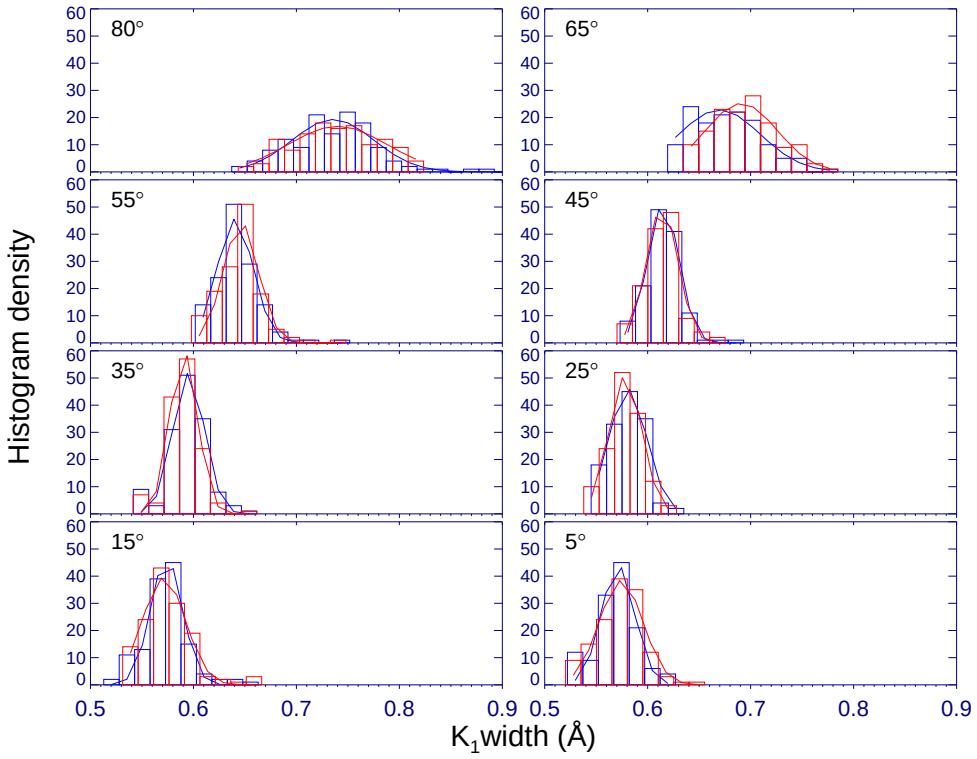

FIGURE 4.10: Same as that of figure 4.9 but for minimum phase of the solar cycle.

we have plotted the value of K_1 width (the peak of Gaussian curve) and FWHM in Figure 4.11 as a function of latitude for the active and minimum phase of the solar cycle. Similarly, we show the most probable values and range of distribution for the K_2 widths for each latitude in Figure 4.12. Table 4.1 and left side panel of Figure 4.11 show that the values of K_1 width for the active phase are larger by about 10-15% than those for the minimum phase for the equatorial region up to $\sim 35^\circ$ latitude. Then the difference in values at the active and minimum phase goes on decreasing up to 55° latitude and the values of K_1 width become similar around 65° latitude. But in the polar regions K_1 width is 1-2% smaller during the active phase than that at minimum phase indicating more activity at polar region during the minimum phase as compared to that during the active phase of solar cycle. The range of variation in K_1 width also shows the similar behaviour as the K_1 width as indicated in the right side panel of Figure 4.11. Figure 4.12 shows that pattern of variations in K_2 width and range of variations in K_2 widths is similar to K_1 variations but in the opposite direction, as K_1 width increases and K_2 width decreases with solar activity and thus support the results of K_1 variations of Ca-K line with solar cycle phase. In conclusion

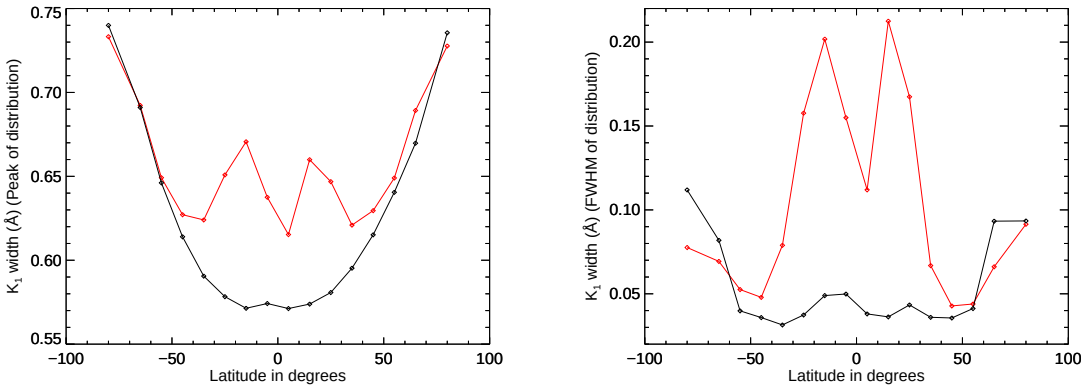

FIGURE 4.11: *Left* shows most probable value of K_1 width defined by the peak of Gaussian fit for the active phase in red and for minimum phase in black. *Right* shows range of K_1 width defined by the FWHM of the Gaussian fit to the distribution of K_1 widths.

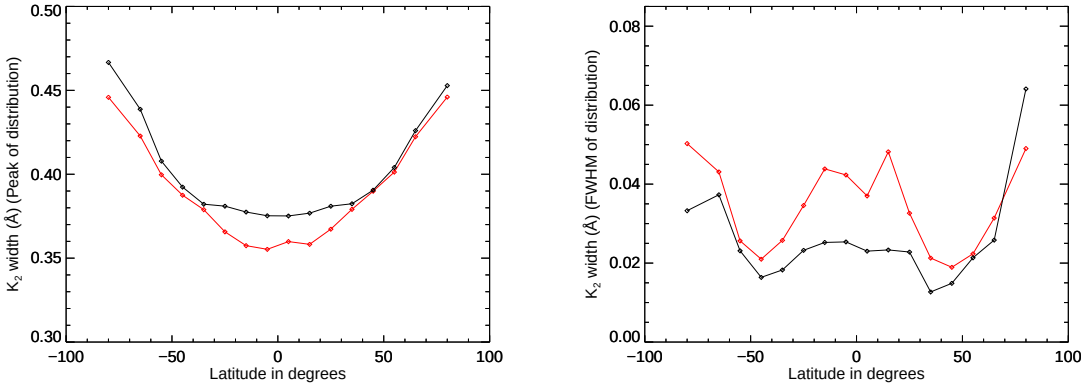

FIGURE 4.12: Same as that for figure 4.11 but for K_2 width

we may say that widths vary with the phase of solar cycle at the middle latitudes and the polar region because of the variation in the magnitude of toroidal and poloidal magnetic fields responsible for the solar activity, respectively, but these do not show any variation around 60° latitude.

It may be noted that K_1 width and range of K_1 width near the equator around 5° latitude are appreciably large during activity period as compared to that during the minimum phase. Generally a very few Ca-K plages and sunspots occur near the 5° latitude which cause the increase in the width and range of K_1. It is difficult

to quantify the contribution of plages and the network to increase in the K_1 width during the activity period because of the availability of data for less number of days. But it appears that small scale activity due to network contributes appreciably to the variation in Ca-K line parameters at this 5° latitude belt.

Further, We have attempted to see the variation in activity at different latitudes on yearly basis by plotting the mean K_1 width as a function of latitude in Figures 4.13 and 4.14 for the solar cycle numbers 22 and 23. Figures show how the activity shifts from mid latitude to lower latitudes from the beginning to the minimum phase of the solar cycle. Better resolution in latitude is needed to compute the details of the shift and time taken to shift the activity from mid to lower latitude belt which is not possible due to availability of less data for limited number of days in a year. Figures 4.13 and 4.14 show that the minimum phases of the solar cycle are $\sim$ 1 and $\sim$ 3 years for the cycle numbers 22 and 23, respectively, even though some small activity occurred during 2010 in the southern hemisphere for short duration during the cycle number 24. Observed pattern of K_1 width as a function latitude and time indicates the longer duration of the minimum phase of the Sun before the beginning of cycle 24 which agrees well with the reported extended minimum phase of the cycle number 23 (Singh *et al.* 2012; Jin and Wang 2011).

4.5 Comparison of K_1 and K_2 line widths with Ca-K plage area

The K_1 and K_2 widths of the Ca-K line are likely to change with varying day to day contribution from plage area, intensity of plage, enhanced, active and quiet networks to the Ca-K emission. The variation in the background chromospheric emission may also contribute to the solar cycle variations. The plages are the brightest among these features and thus affect widths of the line the most. The intensity of plages varies but it has been considered same, in the absence of detailed measurements of intensity, for the purpose to study the variation in the solar activity with time. The plage contribution to solar cycle variations dominates but contribution from the networks is also significant due to large number of network features. Worden *et al.* (1998); Priyal

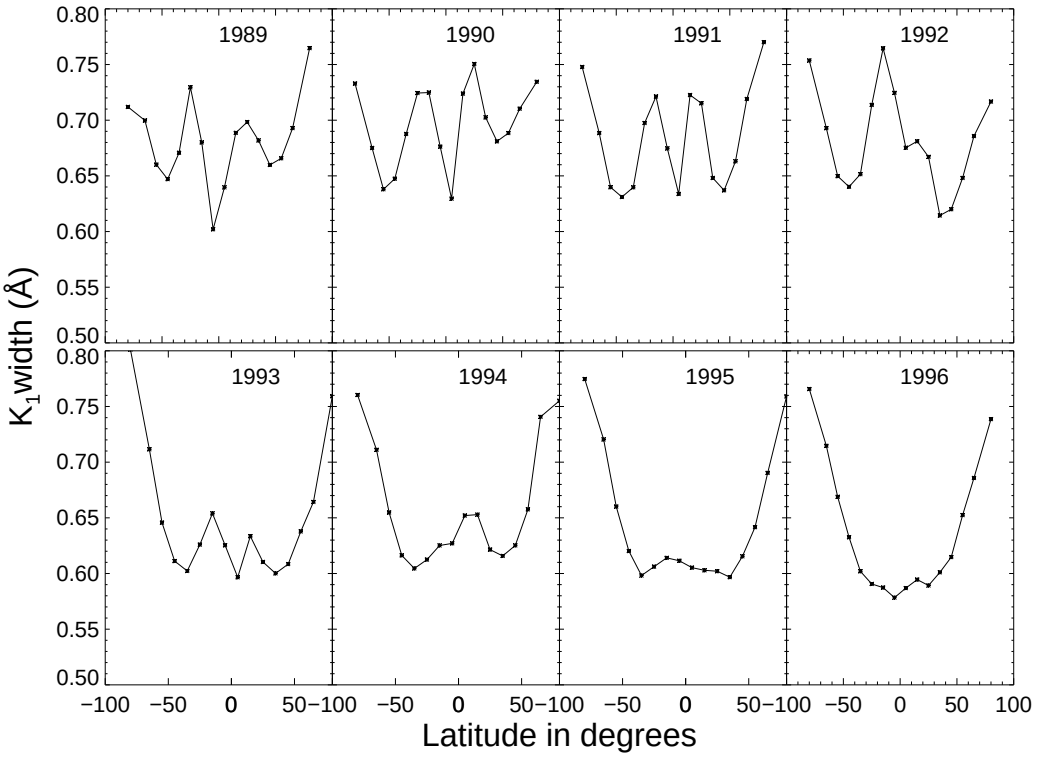

FIGURE 4.13: Mean K_1 width as a function of latitude for cycle 22 to see the yearly variation. The year for the plot is indicated in each panel.

et al. (2014) have identified these features using the threshold values of intensity contrast for each feature. They found that sunspot number is very well correlated with the derived values of plage area using this methodology. On an average the fractional plage areas vary between 0.0 to 0.08 during the solar cycle whereas the enhanced and active network together vary between 0.01 to 0.10 over the visible part of the Sun Priyal *et al.* (2014). Because of the large contribution of plages due to their intensity, to the Ca-K line profile we have chosen to compare K_1 and K_2 widths with the plage areas determined over the same region on the Sun up to 40° since most of the plages occur in this region. We have plotted K_1 width determined from the average spectra obtained over 10° in latitude and 180° in longitude versus plage areas determined from the Ca-K images in millionth of the solar disc using the methodology adopted by Priyal *et al.* (2014) for the mean latitudes of 5 - 35° at an interval of 10° for both the hemispheres as shown in Figure 4.15. The plots for each latitude indicate that K_1 width increases with plage areas although there is large amount of scatter in the plot and K_2 width decreases with increasing plage area. The scatter plots indicate a linear relationship between the K_1 widths and the plage areas. We computed least square fit

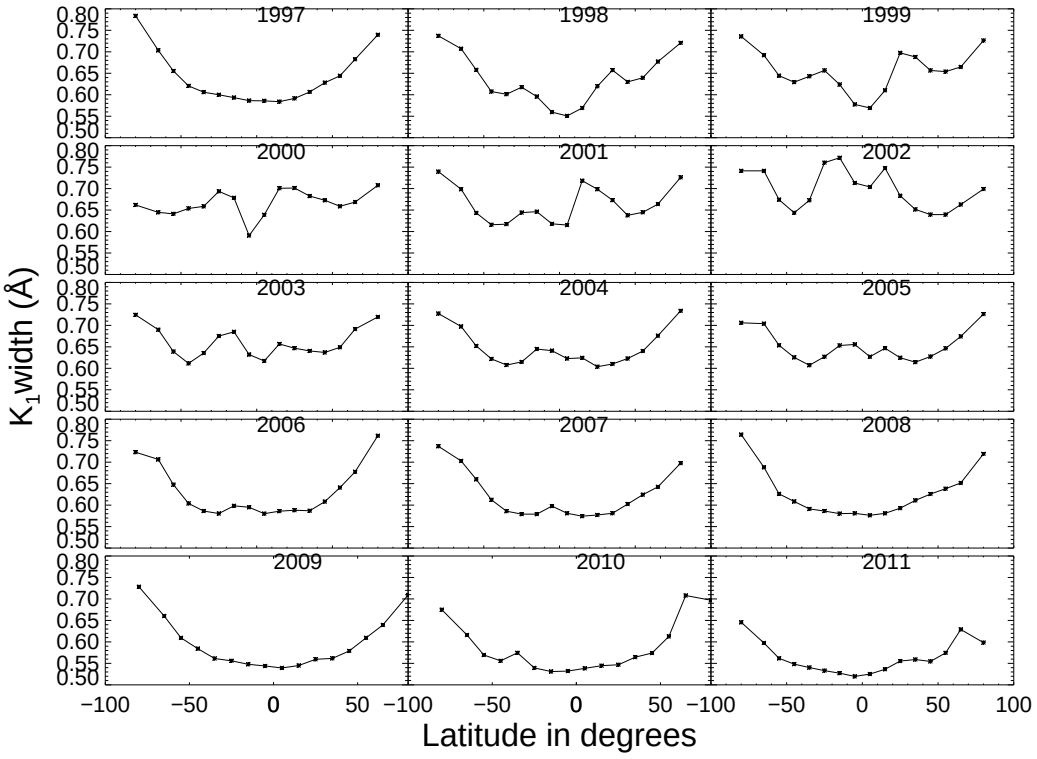

FIGURE 4.14: Same as that of figure 4.13 but for cycle 23

to determine the intercept, the value of K_1 width for the derived value of plage area as zero (hereafter called remnant K_1 width-1) for each latitude. The derived values are likely to represent K_1 width due to contribution to the emission from all networks and the background chromosphere in the absence of Ca-K plages defined by Priyal *et al.* (2014) and others. We have also determined the mean values of K_1 width (hereafter called remnant K_1 width-2) at these latitudes considering the data only for the days when there are no plages in the respective belts during the active phase to compare these values with the remnant K_1 width-1 and have listed in Table 4.2. Further, to compare the K_1 width during the active and minimum phase we have also determined the average K_1 width at these latitudes during the minimum phase when plages were not visible on the solar surface (hereafter called K_1 width-3). It may be noted that mean values of remnant K_1 width-2 derived from the days when plages were not visible in the respective latitude belts and the values of remnant K_1 width-1 derived from the intercept are the same within the standard deviation (SD) for the northern hemisphere for the active phase showing the confidence in the methodology adopted. The Table 4.2 also indicates that the remnant values of K_1 width (remnant

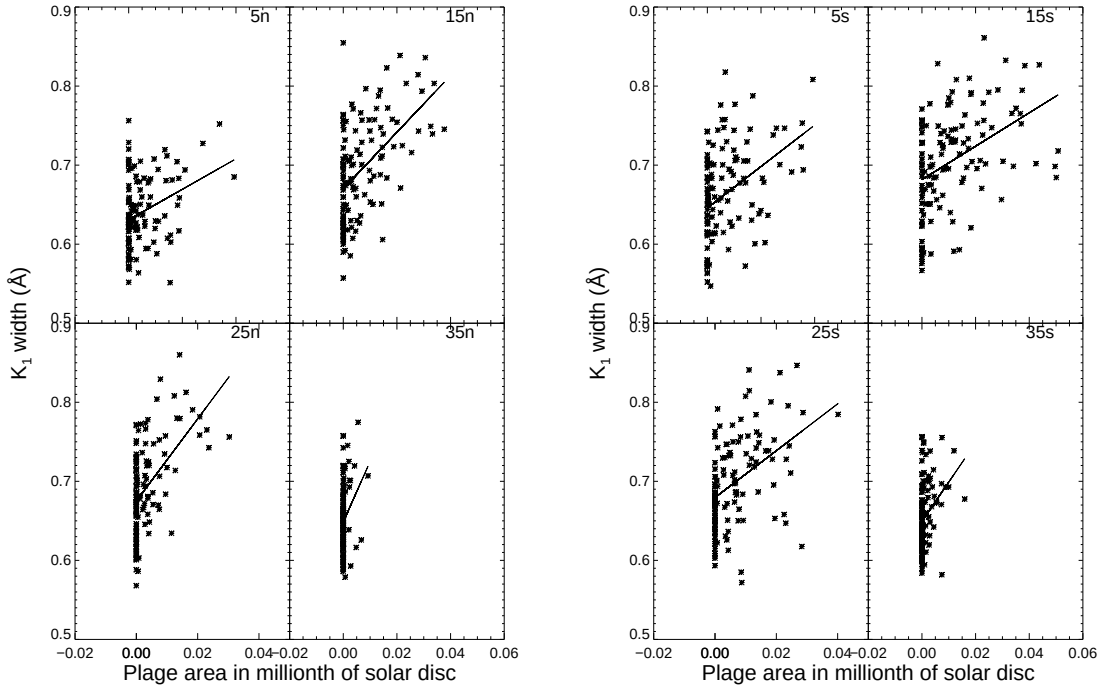

FIGURE 4.15: *Left* Plot of K_1 width vs plage area in millionth of solar disc for 5°, 15°, 25° and 35° north latitudes for the years 1989 - 1992 and 2000 - 2005 around the active phase *Right* Same for southern hemisphere

TABLE 4.2: Remnant K_1 and K_2 width representing the plage free chromosphere

Latitude	K_1 width (Active.)		K_1 width (Min.)	K_2 width (Active.)		K_2 width (Min.)
	Intercept (Remnant K_1 width-1)	Mean (Remnant K_1 width-2)	Mean (K_1 width-3)	Intercept (Remnant K_2 width-1)	Mean (Remnant K_2 width-2)	Mean (K_2 width-3)
5n	0.636±0.004	0.630	0.611	0.356±0.002	0.355	0.365
15n	0.675±0.006	0.669	0.621	0.358±0.002	0.358	0.364
25n	0.676±0.005	0.667	0.633	0.365±0.001	0.363	0.366
35n	0.649±0.004	0.644	0.608	0.379±0.001	0.380	0.378
5s	0.659±0.006	0.626	0.619	0.352±0.002	0.356	0.361
15s	0.697±0.007	0.667	0.631	0.355±0.002	0.357	0.367
25s	0.682±0.006	0.668	0.608	0.363±0.002	0.365	0.377
35s	0.648±0.004	0.639	0.601	0.375±0.001	0.377	0.379

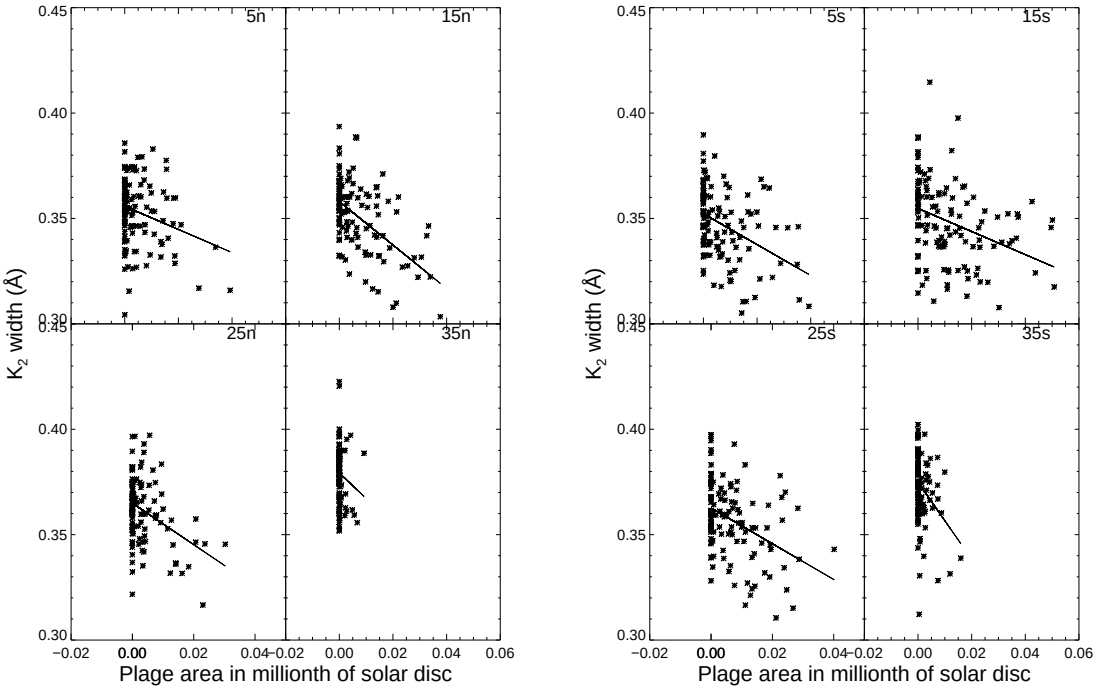

FIGURE 4.16: Same as that for Figure 4.15 but for K_2 width.

width-1 and 2) for the active phase are larger by about 3 - 7% than K_1 width-3 for the minimum phase. The larger values during the active phase may be due to extra emission from network or chromosphere during the active phase and therefore, need to be considered while modelling the variation in solar irradiance. The plot of K_2 widths versus plage areas as seen in Figure 4.16 and values of remnant K_2 widths listed in Table 4.2 follow similar trends but in the opposite direction as K_1 width increases and K_2 width decreases with activity. It may be noted that the variations in the K_1 widths with variations in activity are much more than those in K_2 widths and thus more suitable for comparing the results.

It may be noted that the large amount of scatter in the plots in Figures 4.15 and 4.16 indicates that the day to day variations in observed plage areas are not sufficient to account for the variations in the K_1 widths. Even though contribution from all the networks appears small but may be responsible for the observed scatter. Further, to establish the relation between the line widths and intensity we have plotted K_1 width versus the intensity ratio of K_{1v}/ K_{1r} for all the four latitude belts, represented by the average latitude of 5, 15, 25 and 35° in Figure 4.17. The Figure shows that

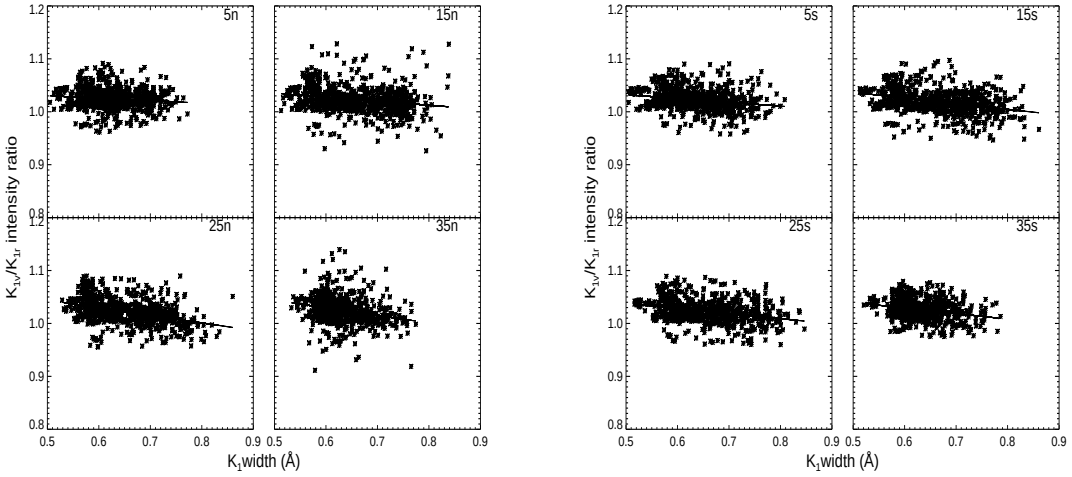

FIGURE 4.17: *Left* K_1 - width of Ca-K line versus intensity ratio of K_{1v} / K_{1r} for all the data for latitude up to 40°n at an interval of 10° for the northern hemisphere. *Right* Same for southern hemisphere

the intensity ratio and K_1 width are negatively correlated and the slope of the linear fit is larger for higher latitude belts as compared to the lower latitude belts. The scatter in these plots appears less as compared to the scatter for the plots of K_1 width versus plage area. In the plots of K_1 width versus intensity ratio, the contribution to the width and emission comes from all the Ca-K line features such as plages and network. From these comparisons it may be inferred that small scale and less bright features also contribute to the solar cycle variations.

4.6 Results and discussions

We find that remnant K_1 width at middle and lower latitudes representing the small scale (network) solar activity is more during the active than K_1 width-3 for the minimum phase of the solar cycle. Assuming a linear relation between the K_1 width and the plage area and after accounting for this variation, we find that the scatter in the values of K_1 width on the day to day basis is large. This appears to be caused by variation at different time scales as suggested by Scargle *et al.* (2013). Therefore, contribution due to variation in the small scale activity caused by the network needs

to be considered in the study of irradiance variation with solar cycle phase. More number of days data per year and better resolution in latitude are needed to confirm the variations in small scale activity during the different phases of solar cycle.

We have found that the magnitude of variations from 35° to 60° goes on decreasing with latitude during the solar cycle and becomes minimum around 60° latitude in both the hemispheres. The distribution of values of K_1 width is narrow for the 55° latitude belts for both the hemispheres during both of the minimum and active period whereas it is broader for the polar and equatorial belts. Generally it is believed that due to dynamo process the activity because of toroidal fields occurs at lower and further lower latitudes as the solar cycle progresses and the decaying fields (poloidal component) move towards polar regions from the middle latitude belt around 35°. The variation in K_1 width with time at a given latitude represents the variation in emission in Ca-K line which depends on the underlying magnetic field strength. One would expect variations in Ca-K line parameters at all the higher latitudes up to polar regions to experience a similar effect as reversal of magnetic field polarity has been observed every 22 years and the activity cycle of $\sim$ 11 years with a phase difference of $\sim$ 5.5 years with middle latitude activity cycle. Even if we assume that poloidal component of magnetic field weakens with increasing latitude, why the variations become negligible around 60° latitude and again become significant in polar regions?

The measurements of K_1 and K_2 widths of Ca-K profile with latitude and time indicate asymmetry in the northern and southern hemisphere and confirm the extended minimum phase of the solar cycle 23. We may conclude that the measurements of Ca-K profile as a function of latitude with better resolution and data obtained at higher frequency for more number of days per year is a valuable technique to study solar irradiance variation and possibly solar dynamo.

Chapter 5

Study of meridional flow

5.1 Introduction

[1] It is generally believed that solar magnetic field generated at the base of the convection zone by dynamo process leads to magnetic and solar activity on the Sun's surface. The main idea of parker's turbulent dynamo is that the poloidal and toroidal magnetic fields can sustain each other. The toroidal field arises due to differential rotation of the Sun and decay of toroidal field generates poloidal field. But this dynamo model could not be sustained because of the difficulty in twisting the very strong toroidal field by helical turbulence. The modified model by Babcock and Leighton invokes a mechanism that suggests that weak diffuse magnetic field arises from the decay of tilted bipolar sunspots and the weak fields migrate towards the polar regions by the meridional circulation. In spite of lot of work done in this direction the details of meridional flows on the Sun needs to be understood. Initially the proposed meridional flows model involved the circulation from equator to poles at the solar surface and from poles to equator in the deeper layers of the Sun. With the availability of more and accurate observations of the velocity pattern on the Sun, the model has been revised and proposes existence of multi-cells of the circulation currents.

[1]The chapter is based on the paper Sindhuja *et al.* (2014)

The observed systematic variation in the activity on the solar surface has been used to study recycling of two components of magnetic fields namely, the toroidal and poloidal components through meridional flow (Choudhuri *et al.* 1995). The flow of material in the meridional plane from the solar equator towards the Sun's poles and from the poles towards the equator deep inside the Sun to carry the dynamo wave towards the equator, plays an important role in the Sun's magnetic dynamo (Choudhuri *et al.* 1995; Charbonneau 2007). Earlier, Howard and Labonte (1981) found that formation of polar fields are due to the migration of weak magnetic field towards the pole. The observed weak fields at polar regions are due to the poloidal field generated from solar dynamo process and the poleward migration of small scale magnetic fields of decaying solar active regions. The aforesaid processes may be responsible for the reversal of polarity of the poloidal field at the polar region (Leighton 1964; Makarov and Tlatov 1999). Recent studies of dynamo models suggest that a meridional flow towards the equator, plays an important role in transporting the toroidal component of magnetic field (Hathaway *et al.* (2003) and references therein). The toroidal component of the magnetic field emerge at the surface due to buoyancy and appear as sunspots.

The weak diffused field observed outside the sunspots are known as poloidal component caused by migration of magnetic flux from decaying active regions [the Babcock - Leighton process]. The magnetic field data of the Sun has been analyzed by many researchers to study the variations in magnetic field with solar cycle (Harvey and Harvey 1974; Foukal *et al.* 1991; Jin and Wang 2011). Jin and Wang (2011) studied three categories of magnetic elements in three different flux ranges 1.5-2.9 $\times 10^{18}$Mx, 2.9-32.0 $\times 10^{18}$Mx and 4.27-38.0 $\times 10^{19}$Mx show no correlation, anticorrelation and correlation respectively. The variations in polar regions have implications for predicting the next cycle (Schatten *et al.* 1978; Choudhuri *et al.* 2007; Muñoz-Jaramillo *et al.* 2013). Analysis of low resolution magnetograph data indicated that during the minima of cycle 20 and 21 the magnetic field peaked at polar regions (Svalgaard *et al.* 1978; Wang and Sheeley 1988). Raouafi *et al.* (2007) observed that the density of magnetic elements decreases close to the polar regions. They concluded that the field strength is relatively flat at a latitude of 55° till latitudes of 75° and then decreases by more than 50% towards the pole. Jiang *et al.* (2009) argued that the observed decrease in the field in polar regions could be due to a weak equatorward

directed meridional flow at high latitudes with speed of a few m s^{-1}. However, Worden and Harvey (2000) pointed out that measurements beyond 75° latitude poorly represents flux distribution because of canopy effects and geometrical foreshortening of features. Meridional flows are very weak (10 to 20 m s^{-1}) and difficult to measure it in the presence of strong flows due to granulation, super-granulation and differential rotation on the surface of the Sun (Hathaway 1996; Hathaway and Rightmire 2010). The variations in Ca-K line profiles due to the variations in solar activity as a function of latitude with solar cycle phase are likely to be caused by meridional circulation and thus such type of study may help to understand the meridional flow and thereby the solar dynamo.

5.2 Further analysis of K_1 and K_2 widths to study meridional flow

It may be recalled that the average profile of 0-10° is referred as 5° latitude profile and similarly other profiles are referred by their average latitude. It may be noted that spectra for 70° to limb (referred as 80° spectra) has seasonal variation in the representative chromospheric area due to visibility of different polar region.

Here we are not emphasizing the variations in profiles as a function of latitude but studying the variation in profiles as a function of time, especially with solar cycle. For the quiet Sun the effect of averaging along the 10° latitude and integration along the longitudes is expected to remain constant for the chosen latitude belt over the solar cycle. The temporal variations in activity in the chosen latitude belt will cause variations in the Ca-K line profile according to the strength of the activity above the profile for quiet Sun. It may be noted that the reported results on the long-term variations in the line profile width are due to variations in the activity on the Sun and not due to averaging or centre to limb variations.

5.3 Results

5.3.1 Long term variation in K_1 and K_2widths at all latitudes

To study the variations of line widths with confidence we removed the outliers from the K_1 and K_2 widths data by restricting the values up to 2σ level. The percentage variation in K_1 width during solar cycle range between 15 to 40% for different latitudes whereas variations in K_2 width range between 5 to 15% only. Figures 5.1 and 5.2 show day to day variations of K_1 width with time for the period of 1989 - 2011 for different latitude belts at an interval of 10° for the northern and southern hemispheres, respectively. Similarly, Figures 5.3 and 5.4 show day to day variation of K_2 width. The scatter in the values is due to day to day variations due to activity and solar rotation modulation, but not because of uncertainty in measurements (Scargle *et al.* 2013). To study the long period variations, the K_1 line width has been averaged over a period of six months and is shown in Figure 5.1 and 5.2 as red coloured astericks symbol. The half yearly averaged Sunspot numbers are also plotted for comparison. The figure shows that the K_1 width varies with large amplitude in the equatorial belts as compared to that in mid latitudes and polar regions. Further, the figure shows that during the maximum activity of sunspot, the K_1 width is maximum around 25° latitude belt in northern hemisphere. Similar trend was seen in the southern hemisphere too. The mean with σ values of K_1 and K_2 widths after the removal of outliers are listed in the second and fifth column of Table 5.1, respectively.

From the table it is clear that mean values of K_1 width increases from equatorial region to mid-latitude, then onwards it decreases upto about 50° latitude and again starts increasing upto the polar regions. This trend of increase-decrease and increase has been observed in both the hemispheres.

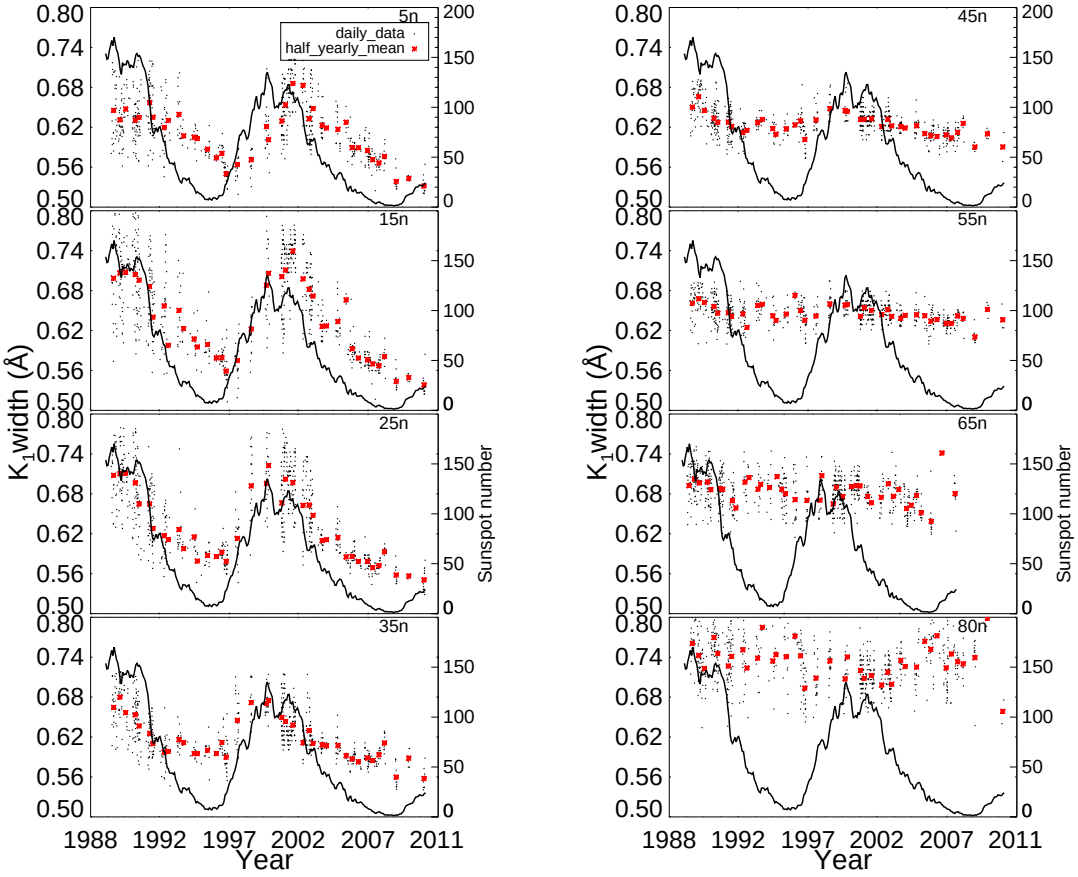

FIGURE 5.1: The K_1 widths as a function of time are plotted for all the latitudes for period of 1989 - 2011, at an interval of 10° in the northern hemisphere on day to day basis (black dots). Half yearly mean values of K_1 width are shown as red asterisks and the half yearly Greenwich averaged Sunspot numbers (solid line) are also shown for comparison. Average latitude of the data is indicated at top right side in each panel.

5.3.2 Differences in the distribution of K_1 and K_2 widths at equatorial and high latitude belts

To study the the variations in widths, we have made the histograms of K_1 and K_2 widths for each latitude belt in both the hemispheres (Figures 5.5 and 5.6). The distribution shown in red colour is for the southern and blue colour for the northern hemisphere. We could not study both the cycles separately because the data for cycle 22 is incomplete. Third and sixth column in the table list the range (Max. - Min.) of K_1 and K_2 widths, respectively. Unlike the mean value, the range of values in K_1

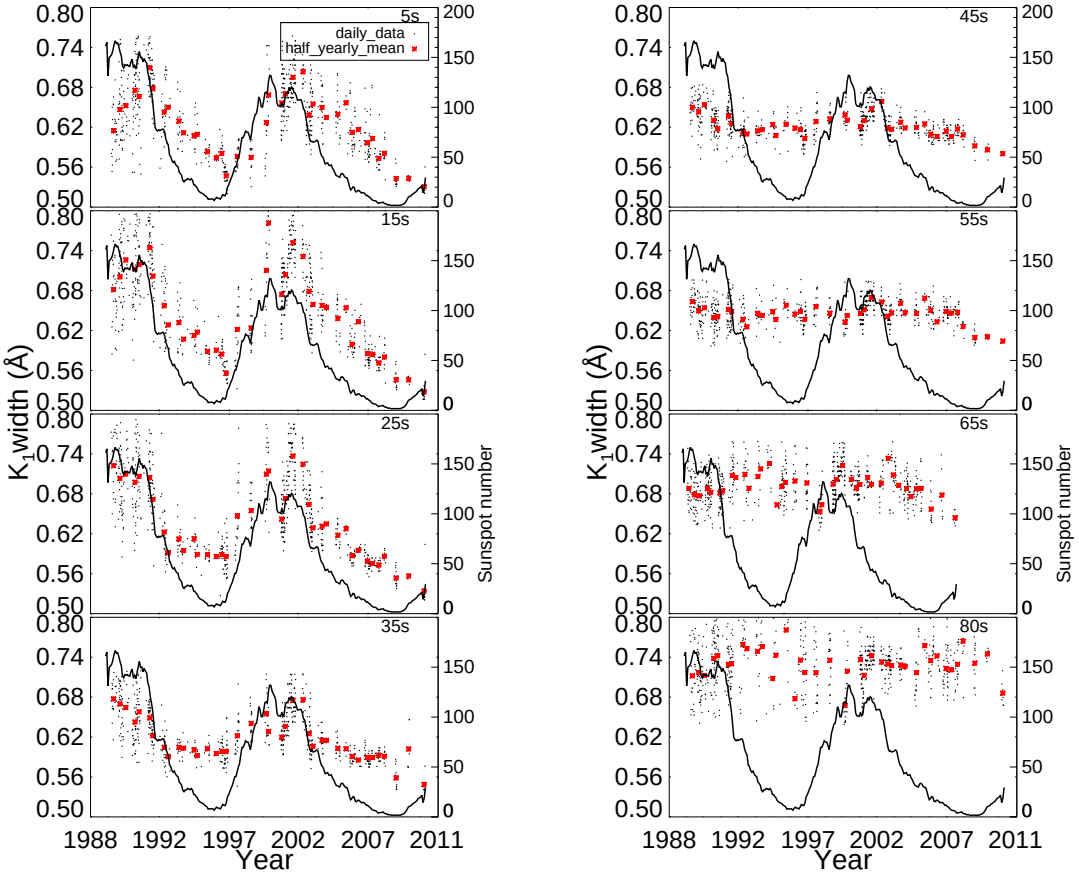

FIGURE 5.2: Same as Figure 5.1 but for the southern hemisphere.

width is distributed in a different way. At very low-latitude 5 to 25°, the width of the distribution increases and it decreases afterwards till the mid-latitude belt (55°). After 55° there is again a tendency of increase in the range of K_1 width until the polar regions. A similar trend is observed in the southern hemisphere too. The range values (max. - min.) of K_1 width at each latitude indicates the extent of variations, but to give a weightage to each value in the histogram and to uniformly compare the spread in distribution at each latitude, we have fitted Gaussian to the histogram. Fourth and seventh columns of Table 5.1 gives the values of FWHM of the distribution for K_1 and K_2 widths for various latitudes in both hemispheres. As expected the FWHM of distribution of K_1 and K_2 widths is broader for the equatorial belts up to 30° as compared to that for mid latitude belts up to 60° as seen from Figure 5.5 and Table 5.1. The K_1 width increases with latitude due to two components, one with latitude (Centre to Limb variation) and other with solar activity. Table 5.1 also shows

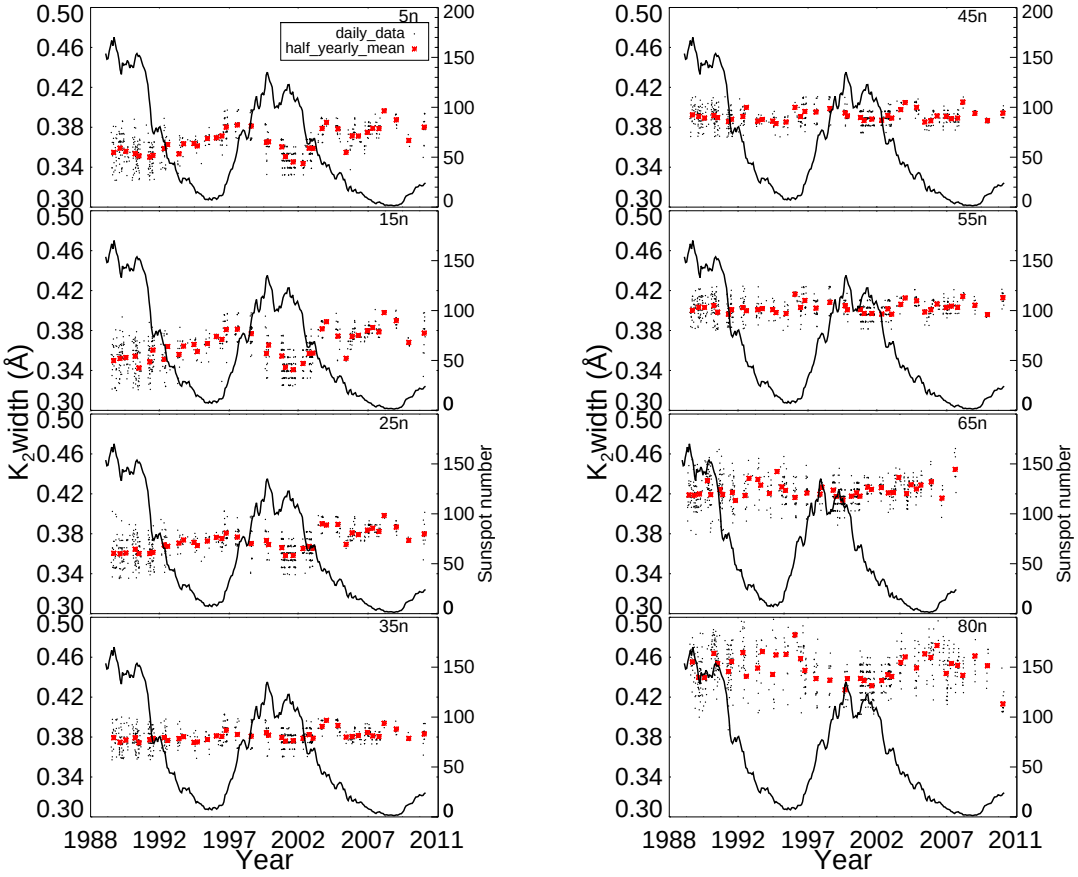

FIGURE 5.3: The K_2 widths as a function of time are plotted for all the latitudes for period of 1989 - 2011, at an interval of 10° in the northern hemisphere on day to day basis (black dots). Half yearly mean values of K_1 width are shown as red asterisks and the half yearly Greenwich averaged Sunspot numbers (solid line) are also shown for comparison. Average latitude of the data is indicated at top right side in each panel.

that FWHM of the distribution of K_1 width is maximum (~30%) in the equatorial belts up to 30° latitude and minimum (~ 6%) in the mid latitude belts 40 - 60° latitude. The FWHM of the distribution in polar regions has the intermediate value (~ 11%), almost twice the minimum value at mid latitude belts. The variations in the parameters of K_2 widths with latitude confirms the results obtained for K_1 widths.

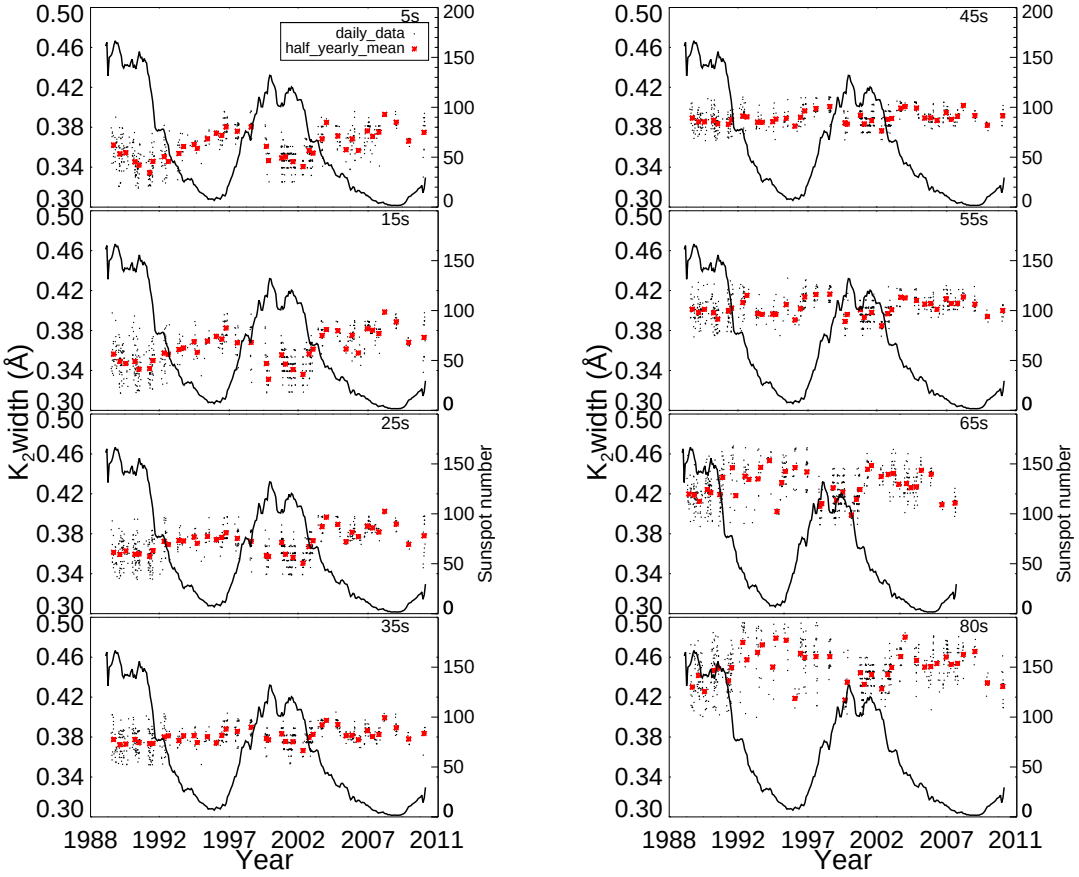

FIGURE 5.4: Same as Figure 5.3 but for the southern hemisphere.

5.3.3 Phase difference in the maximum activity at different latitude belts

Further, we computed the cross-correlations (CC) between the activity at 35° belt and at other latitude belts to understand how the activity in other belts lags or leads the 35° latitude. The 35° latitude was chosen because at the beginning of the new solar cycle, the activity is expected to begin at around 35°. The computed CC is shown in Figure 5.7 as coloured dots for various latitude belts. The top-left panel in Figure 5.7 shows the variation of CCs for 5° (blue dots), 15° (red dots), 25° (green dots), 80° (violet dots) northern latitude belts with 35° latitude belt as a function of phase difference . The bottom-left panel shows the same for 45° (blue dots), 55° (red dots) and 65° (green dots) with 35° latitude belt. Right panels show the respective

TABLE 5.1: List of mean ± σ values and range of widths (maximum - minimum) derived from daily data after removal of outliers with 2σ level cutoff and FWHM derived from the Gaussian fit to the distribution of K_1 and K_2 width for various latitudes.

	K_1 width			K_2 width		
Latitude	Mean (Å)	Range (Å)	Fwhm (Å)	Mean (Å)	Range (Å)	Fwhm (Å)
80n	0.730±0.037	0.196	0.089	0.446±0.020	0.115	0.050
65n	0.682±0.025	0.136	0.065	0.422±0.013	0.086	0.030
55n	0.647±0.018	0.095	0.042	0.402±0.009	0.044	0.021
45n	0.627±0.021	0.123	0.037	0.391±0.008	0.041	0.018
35n	0.624±0.037	0.177	0.071	0.380±0.009	0.046	0.020
25n	0.645±0.061	0.251	0.202	0.370±0.014	0.068	0.037
15n	0.653±0.070	0.284	0.244	0.361±0.019	0.081	0.055
5n	0.618±0.047	0.203	0.125	0.363±0.016	0.071	0.043
5s	0.635±0.055	0.237	0.164	0.358±0.017	0.077	0.050
15s	0.662±0.071	0.293	0.228	0.359±0.019	0.083	0.054
25s	0.650±0.064	0.271	0.187	0.370±0.015	0.070	0.040
35s	0.625±0.037	0.179	0.078	0.380±0.010	0.053	0.022
45s	0.625±0.021	0.115	0.041	0.389±0.009	0.044	0.021
55s	0.648±0.019	0.100	0.044	0.402±0.011	0.059	0.027
65s	0.693±0.027	0.133	0.067	0.426±0.017	0.081	0.046
80n	0.728±0.036	0.179	0.084	0.448±0.020	0.095	0.052

CCs for southern latitude belts.

We then experimented to fit the CC data with various degrees of polynomials to quantify the phase differences and found that 8-degree polynomial fit to be the best and shown in Figure 5.7. The values of maximum CCs, its significance values and phase differences are listed in Table 5.2. It may be noted that the values of CCs for the latitude belts > 55° are less because of small amplitude of variations in K_1 width with solar cycle at higher belts as seen in the time series. Never the less, the power spectral analysis indicate the existence of ∼ 11 year periodicity in the K_1 width at higher latitude belts too, even though the length of the data is smaller, covers about two solar cycles. Therefore, the phase differences determined for these belts are also believable. The values of phase shift indicate that in the northern hemisphere toroidal field shifted from mid latitude belts towards the equator uniformly at a rate of 1.1° / month (5.1 m s^{-1}). But, in the southern hemisphere it shifted at faster rate ∼3° / month in the beginning of the cycle and later decreased with time yielded an average speed of 1.6°/ month (7.5 m s^{-1}) towards the equator. The negative (southern) and positive (northern) phase difference between 35 and 45° latitude belts indicate that the

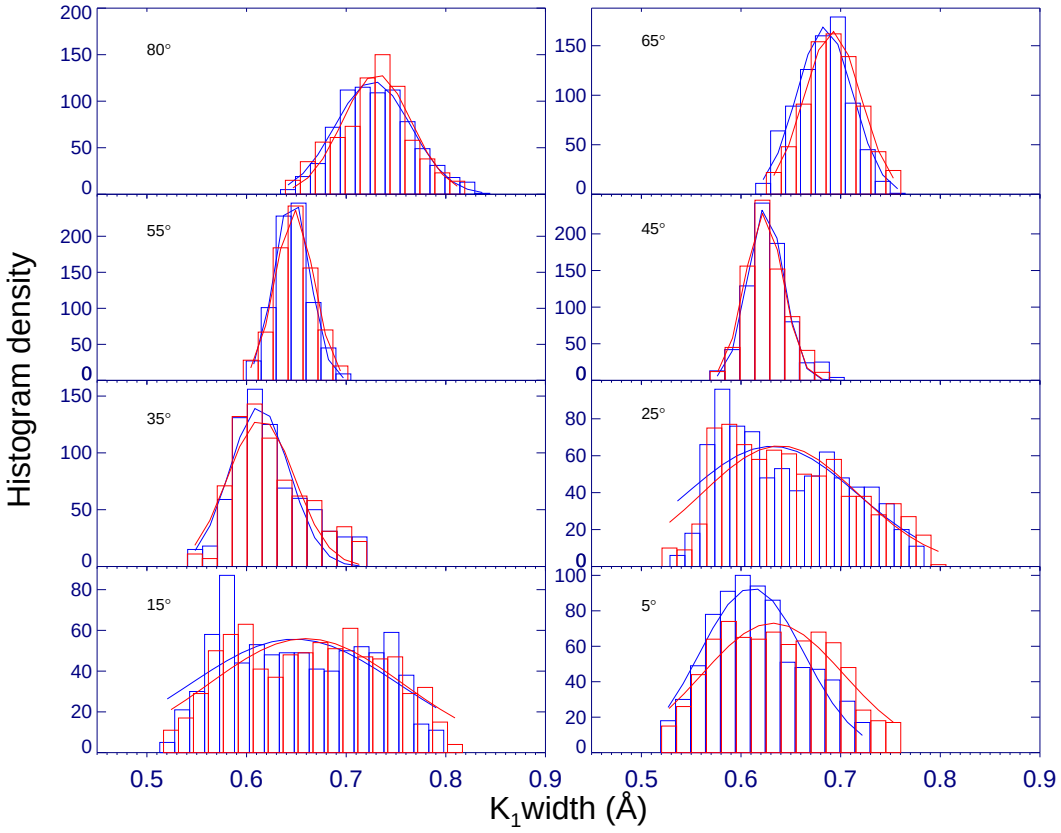

FIGURE 5.5: Histograms of the distribution of K_1 widths in blue and red are for northern and southern hemispheres respectively with bin size of 0.015 Å . Gaussian fit curves are also plotted in respective colours. The mean latitude of the distribution is shown in each panel.

activity begins at the higher latitude or earlier in southern hemisphere as compared to the northern hemisphere.

Further, the CC of 35° with polar regions yield two peaks, one for the maximum activity at polar regions for solar cycle 22 and other for cycle 23 with a significance level ~99% for northern and ~90% for the southern belts. The CCs indicate that peak in the activity at the polar region for the northern hemisphere occurred ~ 92 months before and again ~77 months after the beginning of solar cycle 23. The corresponding values for the southern hemisphere are 99 and 50 months. Thus the interval between the maximum activity at the polar region for cycle 22 and 23 is ~169 months for the northern and ~149 months for the southern hemisphere.

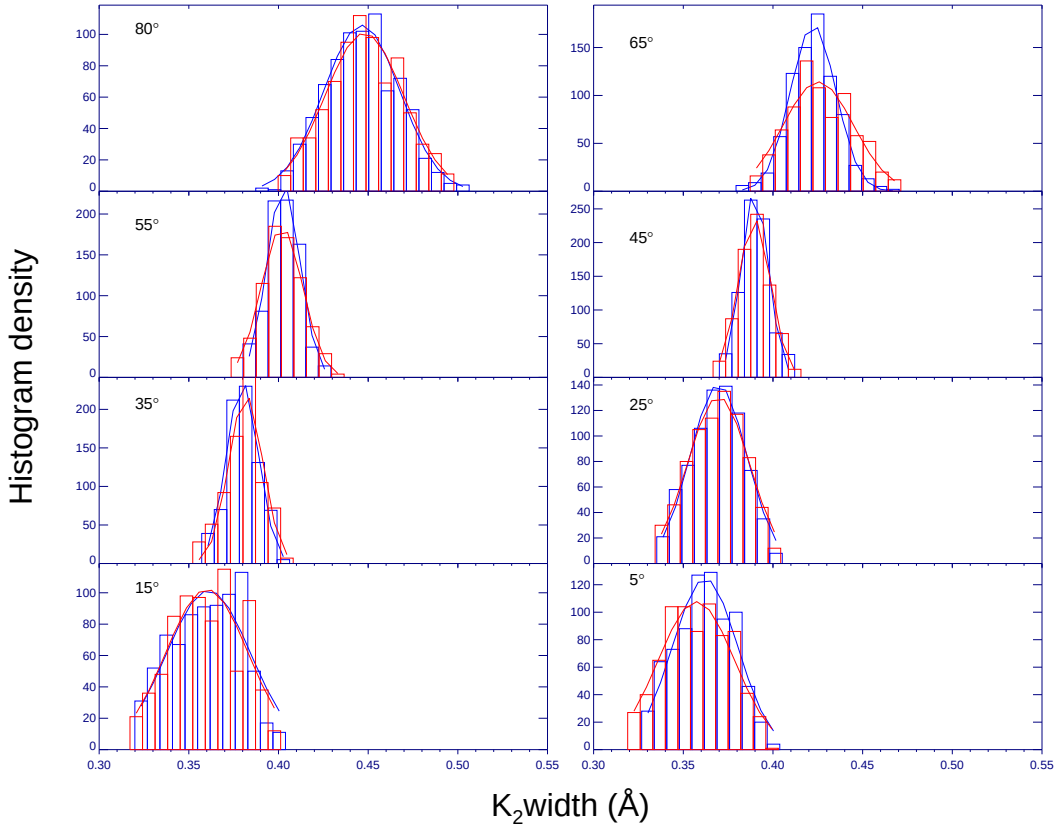

FIGURE 5.6: Histograms of the distribution of K_2 widths in blue and red are for northern and southern hemispheres respectively with bin size of 0.007 Å . Gaussian fit curves are also plotted in respective colours. The mean latitude of the distribution is shown in each panel.

To confirm the asymetry in northern and southern hemispheres and verify the change in speed we have computed the cc functions in the adjacent belts for example 35° and 25°, 25° with 15° and other belts. In Figure 5.8 we show the cc's functions for different latitude belts along with the polynomial fits to each data set. The figure indicate that the phase difference upto ~ 60° latitude can be determined easily and varies systematically but it is difficult to find out in polar regions because of large scatter in values and multiple values phase difference. In Table 5.3 we list the maximum correlation coefficient, confidence level in bracket and the phase difference in months. The table confirms that the activity shifted in the northern hemisphere with uniform rate of about ~ 5 ms^{-1} from mid latitude to equatorial belts. But in the southern hemisphere, the activity shifted from 35° to 25°s latitude belt at the rate of ~ 15 ms^{-1} from 25° to 15°s at the rate of ~ 7 ms^{-1} and from 15° to 5°s at the rate of ~ 5 ms^{-1}. Further, inspite of small values of cc's and noise in the data, the phase difference of

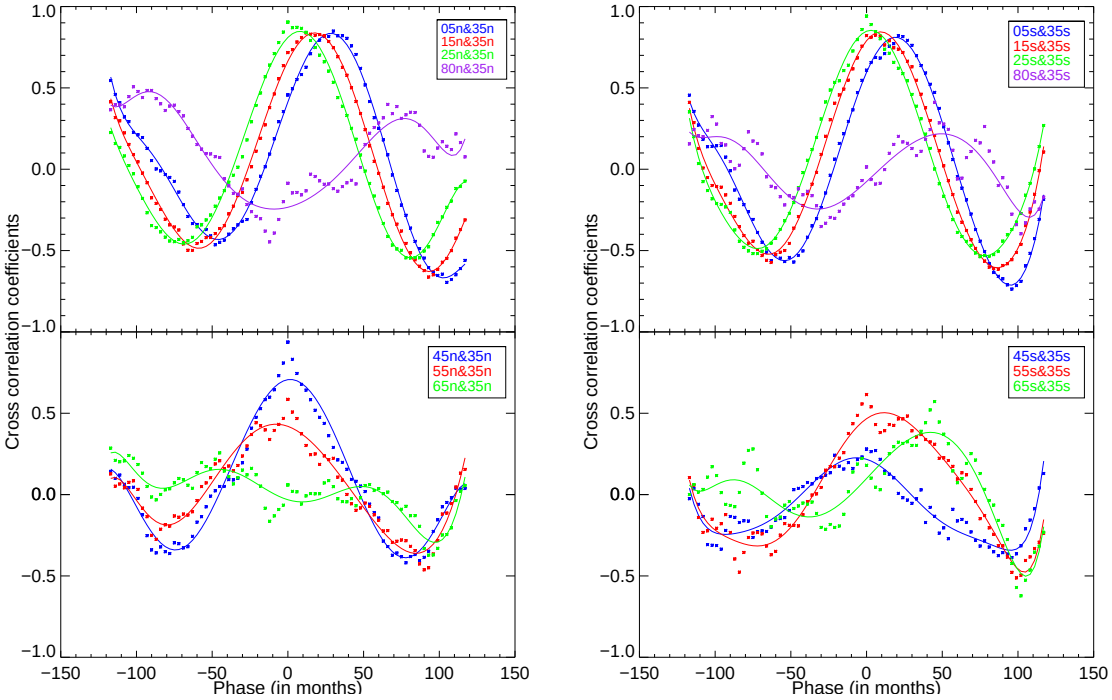

FIGURE 5.7: The cross-correlation coefficients of K_1 width at 35° latitude with that at other latitude belt as a function of phase difference. *Top left* CCs is for 5° (blue), 15° (red), 25° (green) and 80° (purple) northern belts with 35° northern latitude belt and *Bottom left* CCs is for 45° (blue), 55° (red) and 65° (green) northern latitude belts. *Top and bottom right* are for southern hemisphere. Solid curves are polynomial fits to the coefficients.

5-6 years in the activity in the polar regions and mid latitude belts is apparent.

5.4 Discussions and Conclusions

Harvey and White (1999) found a linear relation with slope 0.5, which suggests that Ca-K residual intensity is proportional to the half power of the magnetic flux density. From the comparison of Ca-K images and magnetograms it was found that plage regions are strongly associated with strong field regions (Babcock and Babcock 1955; Leighton 1959; Howard 1959). Among them Steponov was the first to study the magnetic flux vs Ca-K intensity curves. Skumanich *et al.* (1975) found a linear relation between absolute magnetic density less than 120 Mx cm^{-1} and Ca-K line intensity for

TABLE 5.2: Table lists the maximum value of cross-correlation coefficients between two belts, significance level in % and the phase difference in months.

Correlation between latitude	Maximum correlation coefficient	Phase difference in months
80n & 35n	0.48 (99.9), 0.31 (98.7)	-92.1±1.7, 77.2±1.4
65n & 35n	0.16 (82.4), 0.05 (32.34)	-47.4±4.0, 50.1±14.9
55n & 35n	0.43 (>99.9)	-7.8±1.2
45n & 35n	0.71 (>99.9)	2.1±0.8
35n & 35n	1	0
25n & 35n	0.85 (>99.9)	7.8±0.6
15n & 35n	0.84 (>99.9)	17.7±0.3
05n & 35n	0.83 (>99.9)	28.8±0.7
05s & 35s	0.81 (>99.9)	18.9±0.5
15s & 35s	0.84 (>99.9)	9±0.5
25s & 35s	0.85 (>99.9)	3±0.6
35s & 35s	1	0
45s & 35s	0.23 (96.7)	-6.9±1.5
55s & 35s	0.50 (>99.9)	12±2.4
65s & 35s	0.09 (49.8), 0.40(99.7)	-88.2±1.1, 42.6±1.5
80s & 35s	0.12(61.7), 0.22(93.7)	-99±8.7, 49.5±11.6

TABLE 5.3: Table lists the maximum value of cross-correlation coefficients between two belts, significance level in % and the phase difference in months.

Correlation between latitude	Maximum correlation coefficient	Phase difference in months
80n & 65n	0.11 (70), 0.1 (70)	-57.9±0.04, 51.9±0.04
65n & 55n	0.1 (70), 0.001 (1)	-6.3±0.04,73.5±0.05
55n & 45n	0.41 (>99.9)	11.7±0.03
45n & 35n	0.70(>99.9)	1.6±0.02
35n & 25n	0.84 (>99.9)	8.0±0.01
25n & 15n	0.89 (>99.9)	9.1±0.005
15n & 05n	0.89 (>99.9)	9.6±0.005
15s & 05s	0.89 (>99.9)	9.07±0.005
25s & 15s	0.91 (>99.9)	5.87±0.006
35s & 25s	0.85 (>99.9)	3.2±0.009
45s & 35s	0.22 (96)	6.94±0.015
55s & 45s	0.17 (87)	1.06±0.02
65s & 55s	0.33 (99.9)	4.27±0.03
80s & 65s	0.11 (70), 0.1 (70)	-0.5±0.04, -78.47±0.04

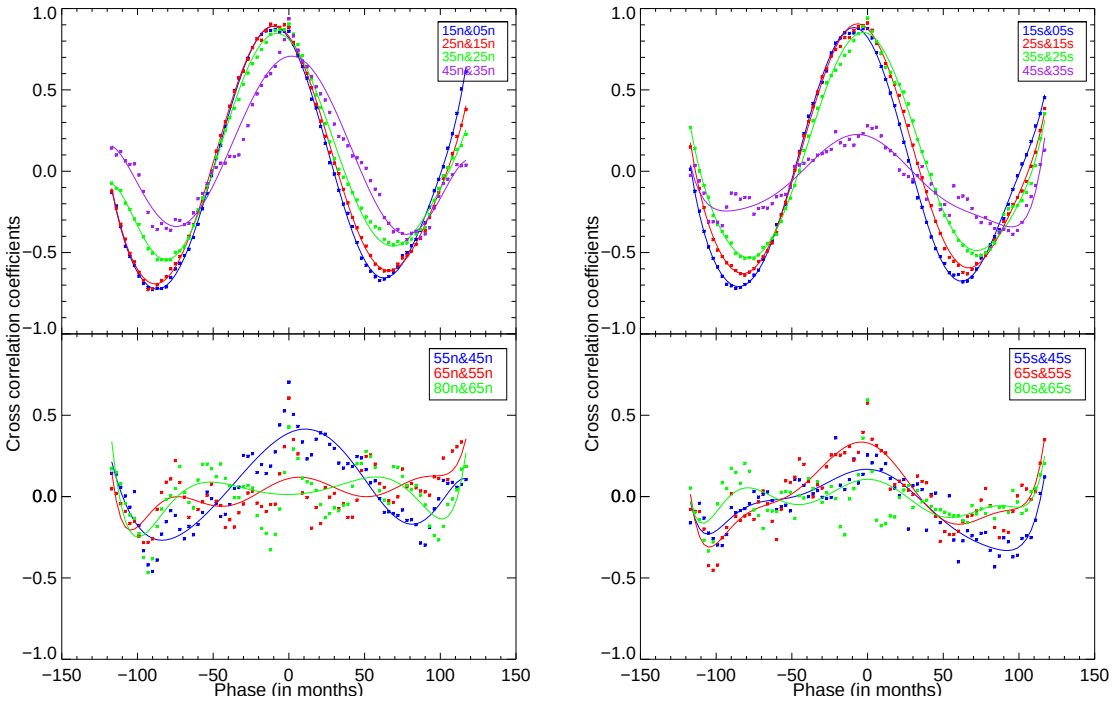

FIGURE 5.8: The cross-correlation coefficients of K_1 width for various latitudes with K_1 width at adjacent latitude belts as a function of phase difference. *Top left* is for 15° (blue), 25° (red), 35° (green) and 45° (purple) northern belts with adjacent northern latitude belt and *Bottom left* for 55° (blue), 65° (red) and 80° (green) northern latitude belts. *Top and bottom right* are for southern hemisphere respectively. Solid curves are polynomial fits to the coefficients.

quiet Sun. Schrijver (1993) measured a power law relation between Ca-K emission and magnetic fields with a slope of 0.6. The relation between the observed soft X-ray fluxes of the corona and the Ca II H and K fluxes that follows solar/stellar cycle is well known (Schrijver *et al.* 1990). A relationship between the Ca-K network brightness and the magnetic field strength was confirmed by Nindos and Zirin (1998). The study of variations in Ca-K line over the solar cycle indicate that K_1 width is larger during maximum phase implying that it increases with magnetic field (White and Livingston 1981). Therefore, the FWHM of the distribution represents the variation of magnetic field during the solar cycle at that latitude. In other words, it represents difference in magnetic field strength at the maximum and minimum phase of solar cycle. It appears that variations in the K_1 and K_2 widths occur because of variations in the toroidal magnetic field in the equatorial belts up to about 40° latitude and poloidal

magnetic field for latitude belts > 40° latitude. Therefore, it can be inferred that variations of about 30% in the K_1 width in the equatorial belts over the solar cycle are because of variations in the toroidal magnetic field that shifted with a velocity of 1.1° / month (5.1 m s^{-1}) in the northern hemisphere and 1.6° / month (7.5 m s^{-1}) in the southern hemisphere towards the equator. Muller and Roudier (1994) reported the small scale magnetic field dominated in the latitude belt of 40 - 70° which may not be correlating with the solar cycle. Raouafi *et al.* (2007) found that the magnetic field elements are relatively flat between 55 to 75° and then they decrease by more than 50% toward the pole. On the other hand, Jin and Wang (2011) restricted their analysis of solar cycle variation of magnetic field only upto 60°, but reported that detection of a fewer magnetic elements and more noise while approaching the polar regions.

If plages are due to toroidal field then it can cause about 30% variation in the K_1 line width. Then the observed 11% variation in the line width in the polar region should originate from the variation in the magnetic field at polar regions with solar cycle phase. In contradiction to the findings of Raouafi *et al.* (2007) we find that magnetic field increases in polar regions by 100% over the cycle in comparison with mid latitude belts as K_1 width is related with the strength of the magnetic field. The observed increase in activity in the polar region is anti-correlated with the equatorial regions which is in agreement with the findings of Makarov *et al.* (2004) that the cycle of Ca-K bright points at polar regions precede on average by 5.5 years with the sunspot cycle. It is difficult to interpret the shift of activity (poloidal fields) in the mid latitude belts (45° and 55°) because of the presence of positive and negative phase differences with 35° belt. The analysis of the data with resolution of 3-5° in latitude and observations for longer period may yield better understanding about the shift in activity in the mid latitude region. Finally, the large interval of about 13 years between the maximum of polar fields during the solar cycle 22 and 23 may be responsible for the extended minimum in cycle 23 and the delay in the beginning of cycle 24.

It may be recalled that phase differences in the shift of activity in the mid and equatorial latitude belts are systematic but the phase differences in both the hemispheres around 60° latitude are complicated and have values which are difficult to explain. The observed variations can be explained if we assume that probably there are two

types of meridional flows or sources of activity, one that begins at the mid latitude belts which causes stronger component to move towards equator and weaker component towards higher latitude belts and other in polar regions having boundaries around 60° latitude. In other words there are counter flows in the polar region with a phase difference of about five and half years in the solar activity in the polar and equatorial region. It may be noted that inferences about the flows derived from the variations in the Ca-K activity are at the chromospheric level. It is not clear how these are related to surface and the sub-surface level flows? It may be expected that at least in the mid latitudes and polar regions the flows derived from Ca-K activity are related with the meridional circulation at the surface and sub-surface levels derived from other observations. Using the Doppler-grams and magnetic field measurements of the Sun, Ulrich (2010) determines the circulation velocity of the solar surface along meridional planes and found a double cell structure during some solar cycles. The deduced meridional flow differed from the circulation velocities derived from magnetic pattern movements and a reversed pattern was found in polar regions during the solar minima. Further, Ulrich and Tran (2013) found the existence of small amplitude (3 - 5 G) but spatially coherent ripples with semi-regular periodicity of one to three years. The directions of those flows appear to be inconsistent with that found here. The differences between the flow patterns may be due to the type of data used for the analysis. Their results are based on the analysis of global magnetic fields of the Sun whereas our results are from the variation of total activity including strong as well as weak activity.

In conclusion we may say that (1) the Ca-K line profile observations is effective to study the latitudinal variation of solar activity and especially polar region magnetic field (2) no symmetry is found in the northern and southern hemispheres in terms of the speed of shifting toroidal field towards equator (3) no uniformity is found in the speed of movement of poloidal field towards polar regions (4) negligible variation in the poloidal field at the latitude belt $\sim 60^\circ$ as compared to those for the polar regions and (5) existence of multicells in the meridional circulation. We propose three types of cells one those transport toroidal flux from mid latitude to equatorial belts, second those transport poloidal flux from mid latitude to high latitude belts upto $\sim 60^\circ$ and the third those exists in the polar region. How these are created and function is not clear to us. These results will have very important implications on the solar dynamo and meridional flow modelling and further will be useful for polar activity studies.

Chapter 6

Ca-K line profile modelling

6.1 Introduction

The resonance lines of singly ionized calcium, the Fraunhofer H and K lines, are the two strongest lines in the optical part of the solar spectrum. The source function for the Ca-K line is controlled by collisions and thereby leads to the formation of broad wings. These lines are suitable to provide temperature diagnostics over a wide range of heights in the solar atmosphere. The shape of Ca-K line profile is an important source of information about physical conditions in layers where these lines are formed. These lines have been employed extensively in determining the temperature structure using semiempirical models (Vernazza *et al.* 1981b; Maltby *et al.* 1986; Fontenla *et al.* 1991, 1993) and in assessing the validity of chromospheric radiation-hydrodynamic models (Rammacher and Ulmschneider 1992; Carlsson and Stein 1992, 1995). A precise determination of the radiative losses in the Ca II resonance lines is a prerequisite for accurate conclusions on the structure of the chromospheric layers in both types of modeling (Uitenbroek 2001). The chromospheric temperature rise is necessary to produce a self reversed emission core. The double reversal at the center of the spatially average profiles (see Chapter 1 Figure 1.5) of the Ca-K resonance line is a phenomena due to the distribution of temperature and density with height. The asymmetries in the line, such as the slighly greater violet

peak measured on average profiles, can be explained by a slight outward motion of the emitting regions on the solar surface (Pasachoff and Zirin 1971). Most of the models of both the solar and stellar Ca-K lines have been based upon simplified assumption of CRD (Complete Redistribution) in the scattering of line photons (Shine *et al.* 1975). In CRD, source function is independent of frequency. In 1970s many researchers started using PRD (Partial ReDistribution) where the source function is dependent on frequency. PRD is a realistic way of treating the line profile modelling. It leads to an improved agreement with observation. It is well known that the H and K lines have to be treated with the partial frequency redistribution (PRD) formalism for diagnostic purposes e.g., (Shine *et al.* 1975; Uitenbroek 1989). Compared to complete frequency redistribution (CRD), which is sufficiently accurate for most weaker lines, PRD adds considerable complexity to radiative line transfer because the emission-profile coefficient depends on the radiation field directly through the population numbers. This increases the nonlinearity of the transfer function. The added complexity may even be greater in dynamic atmospheres, where the coupling between angles and frequencies introduced by macroscopic velocities could require the use of angle-dependent PRD instead of the computationally simpler angle-averaged variant (Uitenbroek 2001).

6.2 Method

In the past many researchers have tried to model the centre to limb variation of line profiles, an important property that provides information about the physical characteristics of the plasma. Engvold (1966) assuming an optically thin atmospheric model. He showed that centre to limb variation of the $\Delta\lambda$ (K_1 width or FWHM) of Ca-K line or (Fraunhoffer lines) profiles is due to variation in optical depth with variation in μ ie $\cos\theta$. However Athay and Skumanich (1968) found that the $\Delta\lambda$ variation is independent. Shine *et al.* (1975) modelled the centre to limb variation of $\Delta\lambda$ and intensity both in PRD and CRD. They found that PRD model yields more realistic line profiles. It has been found that in quiet regions the core of the Ca-K line reveal the limb darkening. It looks the same in both the absorption and emission parts of Ca-K line profiles (Zirker 1967). The presence of the limb darkening in the Ca-K

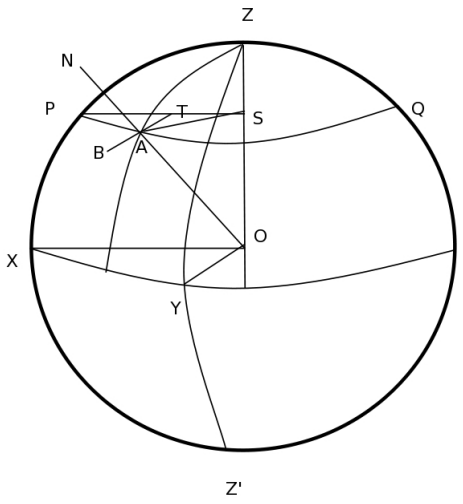

FIGURE 6.1: figure illustrating the geometry of the observing system.

line yields a unique opportunity to verify the radiative transfer theory while calculating chromospheric line profiles. The computations based on the CRD assumption provide the limb brightening in the K_1 and K_2 parts e.g., (Milkey and Mihalas 1973). Considering the frequency dependence of PRD model made it possible to reproduce properly the observed limb darkening in the K line when spatially averaged redistribution functions were used along with quiet-Sun chromosphere model. We have used the observed data as described in Chapter 2 for comparison purposes. The observations of Ca-K line profile are taken at different latitudes integrated over the visible 180° longitude. So we need to model the observed profile taken from each latitude strip of 10° interval with the model profile. In order to do that, we have to get the model profile also from integrated latitude strip instead of getting rays at different cosθ values, so we have to convert that to latitude profiles. In order to do this we need to calculate the path length of each latitude strip. R is the radius of the solar disc taken as 1 in the following analysis.

Figure 6.1 shows the geometry of the Sun and observations where OY is the line of sight direction. A is one of the point of observation. OAN is the local normal. θ is the angle between local normal and the line of sight. Using theory we calculate I(θ) ie

the specific intensity as a function of θ (TAB || OY). OX, OY, OZ are the orthogonal directions. OY $\perp$ OX similarly TAB $\perp$ STP AS = PS = r = radius of small circle PAQ. OAN is along the radial direction from the center O to point A. It is the local normal to the spherical surface at A. The distance between two points in the small circle is

$$(\psi 1 - \psi 2) cos\chi \tag{6.1}$$

Where $\psi 2$ and $\psi 2$ are the longitudinal difference between those two points measured in radians.

$$Flux = 2\Delta\chi \int_{\theta=\chi}^{\chi = latitude,\ 90} I(\theta) sin\theta cos\theta \quad d\theta \tag{6.2}$$

$\Delta\chi$ is 10° in our case. This is the modified flux after multiplying the path length of the particular latitude. Following the procedure, we can get the intensity profiles as a function of latitude considering all longitude angles, ie., integrating along the 180° visible longitude.

6.3 Results and Discussions

6.3.1 Model

In 1990 Fontenla, Avrett and Loeser (FAL) constructed four atmospheric models named as FALA, FALC, FALF and FALP, in which the first three FALA, FALC, FALF are components of quiet Sun namely faint cell center area, and average intensity area and a bright area of the network respectively (Fontenla *et al.* 1993). The fourth one corresponds to a plage area of medium brightness. The quiet Sun models of photosphere and chromosphere are those of VAL model (named after the authors

Vernazza, Avrett and Loeser) modified by Avrett (1985) in the temperature minimum region and by Maltby *et al.* (1986) in the photosphere. The plage model photosphere and chromosphere is based on a modification of the model by Lemaire *et al.* (1981). The four atmospheric models were of increasing order of UV emission. For atmospheric models FALA and FALC low and moderate activity full disk average is applied as representative local values. For FALF and FALP three times the moderate activity values were used. The models include photospheric layers in which the temperature decreases outwards (ie., decreases with decreasing column mass). A minimum temperature is reached at a height of $\sim$ 500 km above the τ_{5000} =1 level (Column mass $\sim$0.05 g cm^{-2}). Then the temperature rises rapidly up to a chromospheric plateau where the temperature gradually increases with height over a distance of $\sim$ 1500 km. The temperatures of the chromospheric plateau are different for the various models. The change in the column mass of the chromosphere in the various models is mainly due to the increase of temperature for the brighter models, which increases the density scale height and allows higher densities in the chromosphere. The energy balance in FAL model includes the diffusion of hydrogen atoms and protons, expressed in terms of ambipolar diffusion velocity, ie., the diffusion velocity of atoms relative to protons. In FAL models line emission is computed consistently (including diffusion) and should be compared to the observed intensity. Another atmospheric model which explores the formation of the lines of other elements such as C and O including corresponding diffusion effects is model FALXCO which represents cell interior of quiet Sun. The Variation of temperature and electron density with respect to column mass are given in Figure 6.2. The results of various models and the observations are plotted for comparison in Figure 6.3 for latitudes 5, 25, 45, 65°. From this Figure 6.3 we can say that models FALC & FALXCO and models FALF & FALXCO were combined in different % to obtain the resultant profile closer to the observation. Quiet Sun is defined as a combination of network and cell interior or intranetwork. Intranetwork is smaller in size covers the whole solar disc and has lower magnetic field than the network regions (Worden *et al.* 1998). Therefore the % contribution of the models were assumed keeping this in mind and also by performing several trials.

To compute profiles at different latitudes, we have used the numerical radiative transfer code based on the MALI (Multi-level Approximate Lambda Iteration) formalism of Rybicki and Hummer (1991, 1992) developed by Uitenbroek. The code solves the

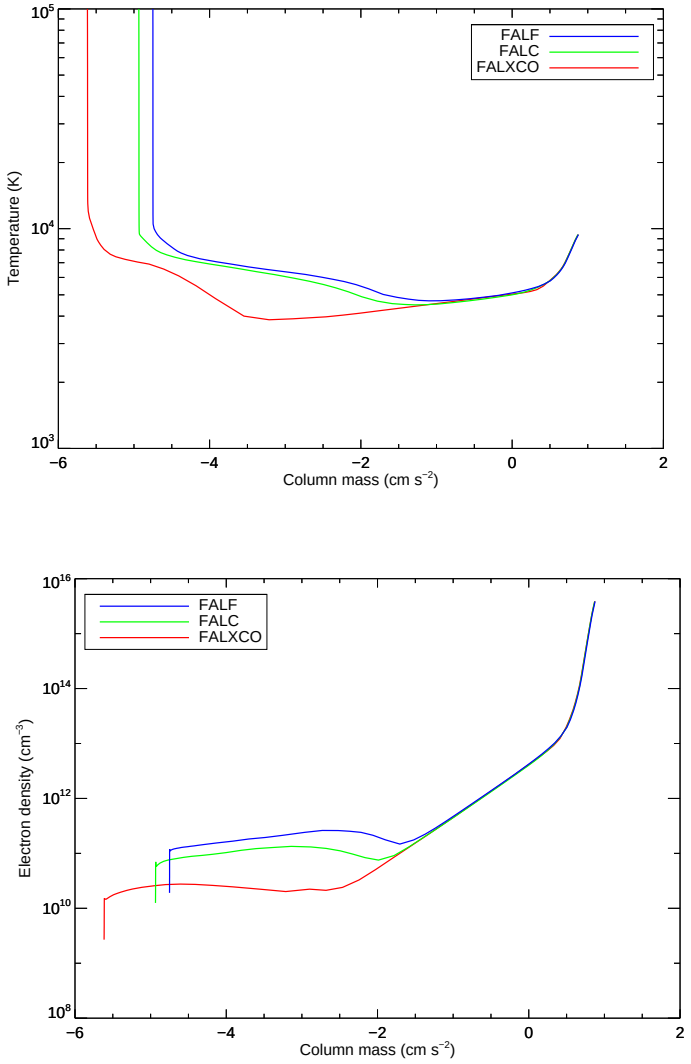

FIGURE 6.2: *Top*: Temperature vs Column mass in log scale for the different models C, F and XCO *Bottom*: Similarly Electron density vs Column mass

combined equations of statistical equilibrium and radiative transfer for multi-level atoms and molecules in a given plasma under general Non-LTE conditions. Many semi empirical atmospheric models (Vernazza *et al.* 1981b; Fontenla *et al.* 1993, 2006, 2009) are there which use proxies or observations of solar magnetic activity to describe the evolution of the sun's surface by different types of solar features like quiet Sun, plages, faculae etc. We have tried to model the quiet Sun profile observed on March, 08 2007. According to the data from Silso data center there is no sunspot on that day. Therefore the variation along the latitude will be purely because of the

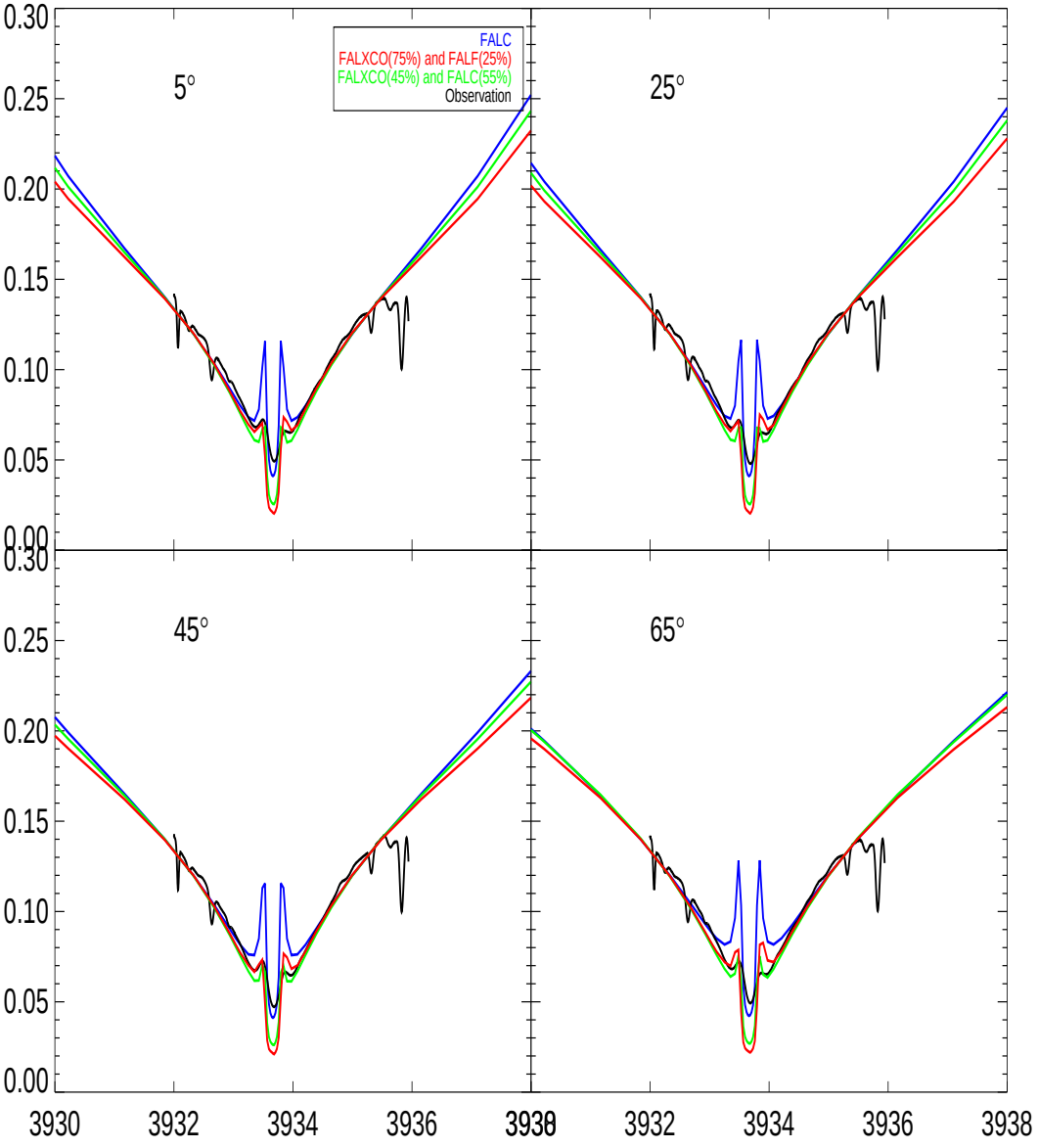

FIGURE 6.3: comparison of computed profile for different models with observed profile shown in different colours

TABLE 6.1: The Table shows the computed K_{2v}/K_{1v} ratio and K_{2v}/K_3 ratio from the model profile, the fifth row of the table shows the ratios for observed profile

Model	K_2/K_1 ratio	K_2/K_3 ratio
B	1.194	4.75
FALC	1.601	2.777
FALC (vturb=2.5km/s)	1.891	4.579
FALC (vturb=4.5km/s)	2.182	7.178
FaLXCO (75%) and FALF (25%)	1.067	3.383
observation on march 08,2007	1.055	1.459

latitudinal effect. We have used quite sun model FALC (an average intensity quiet sun area), model B (quiet sun internetwork) and FALF (a bright area of network) and FALXCO (quiet sun cell interior) and FALC with depth dependent turbulent velocity (2.5 km/s and 4.5 km/s). Table 6.1 lists the model and K_2/K_1 & K_2/K_3 ratio of Ca-K line model profile, also listed are the ratios for the observation. We empirically attempted to compute the profile by assuming different contribution from different features and compare it with the observed profile. From the table it is understood that K_2/K_1 ratio of FALXCO (75%) + FALF (25%) model matches the observation. Though there is still a discrepancy in the K_2/K_3 ratio. This may be due to small amount of scattering in the observed line profile. Further from Figure 6.4, K_1 width measured from model profile for all latitudes were compared with K_1 width from observed profile. K_1 width of FALXCO (75%) + FALF (25%) model nearly matches with the observation and also with the latitudinal variation.

6.3.2 Active network contribution

Using the new technique of observation (See chapter 2) and model profile, active network contribution can be measured at each latitude. This can be done with the help of Ca-K spectroheliograms to measure the contribution of plages. Contribution of active network at each latitudes can be measured by,
% contribution of plages × plage model + % assumed contribution of quiet network × quiet Sun model → model profile (M)
and observed profile (O).
Y=O-M, This Y is the active network component. The observed line profile at each

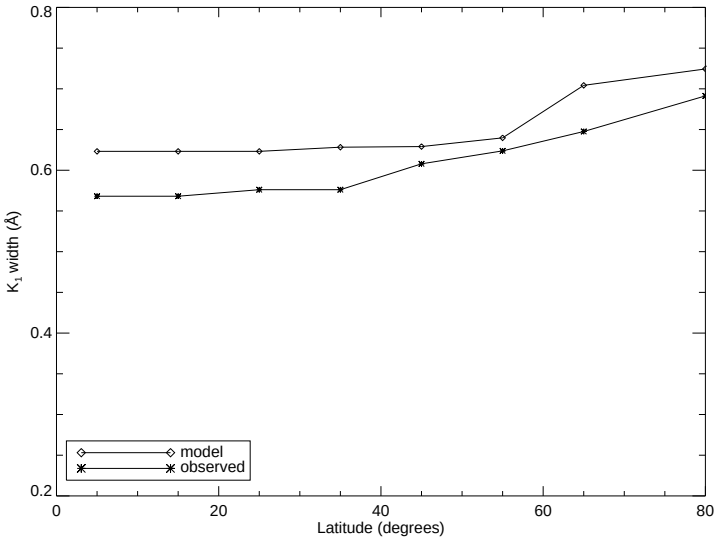

FIGURE 6.4: Variation of K_1 width with latitude for model (FALXCO (75%) + FALF (25%)) and observed line profiles

latitude will have contribution of all features like quiet network, Plages and active network. This is the main advantage of Ca-K spectroscopy. Whereas in Ca-K images the features were identified and the identification depends on the algorithm used by different researchers.

The excess of intensity in this profile is active network contribution. In order to measure the active network contribution at each latitude, we have to measure the plages at each latitude using the Ca-K spectroheliogram and the quiet network contribution (cell & network) is obtained from the model. By doing this the discrepancy in measuring active network regions can be resolved. The discrepancy in modelling the solar irradiance can also be overcome. We have measured the plage contribution at each latitude upto 35° (since most of the plages are identified upto this latitudes) with 10° interval from the kodaikanal Ca-K images. Then the contribution of cell and network features were assumed to be 75% and 25% from the rest excluding plages.

Observations taken on Febraury 12, 2003 were compared with the model profile. For Active Sun plage model FALP is used apart from quiet network models as already discussed FALXCO (75%) & FALF (25%). Table 6.2 shows the different models and their contribution used at each latitude. In Table 6.3 the results of K_1 width for observed and model Ca-K line profiles for 5-35° northern and southern latitudes and the difference (active network contribution) were shown. From Table 6.3 one can

TABLE 6.2: Contribution of model used

Latitude	FALP	FALXCO	FALF
5n	0.05	0.71	0.24
15n	0.06	0.7	0.24
25n	0.0	0.75	0.25
35n	0.0	0.75	0.25
5s	0.001	0.75	0.25
15s	0.04	0.72	0.24
25s	0.01	0.74	0.25
35s	0.0	0.75	0.25

TABLE 6.3: Calculated active network contribution using K_1 width (in Å)

Latitude	Observation	Model	Active network contribution
35	0.658	0.625	0.033
25	0.658	0.625	0.033
15	0.686	0.630	0.056
5	0.630	0.627	0.003
-5	0.651	0.625	0.026
-15	0.722	0.627	0.095
-25	0.714	0.625	0.089
-35	0.637	0.625	0.012

say that active network component also follows the plages. But however we need to measure the variation of active network contribution over solar cycle phase for different latitudes. This will give a clear picture of the active network component's behaviour over solar cycle phase at different latitudes. But to do this we need more number of data points. We have only 142 days of observation matching both Ca-K spectra and Ca-K images with huge data gaps. So it is difficult to study the active network contribution over solar cycle. Observations of both Ca-K spectra and Ca-K images have to be obtained simultaneously to achieve this studies.

Chapter 7

Conclusion and Future work

Synoptic observations of the Sun are very important in studying the long term variation of the solar magnetic field and its effect on space weather and climate. The large and small scale structures observed on the Sun contribute to the solar irradiances by different magnitudes at different times of the solar cycle (Worden *et al.* 1998). The small scale network structures can be observed at the chromospheric level and above in the solar atmosphere. The contrast between the network structures is large in the Ca-K wavelength band. Ca-H and K images have been identified as useful for identifying regions of chromospheric activity on the solar surface. There is a correlation between Ca-K emission and magnetic field (Ortiz and Rast 2005). Results indicate that more than 60% of the observed TSI solar cycle variability occurs between 150 and 400 nm. To understand the solar chromospheric variability the observations of the Sun as a star in Ca-K line profile were started in 1970's on day to day basis. Also, the areas occupied by plages and networks in the Ca-K line images were measured on day to day basis to study the solar surface variability. But, there remains some uncertainty in determining the areas of plages and networks due to fixing the intensity contrast empirically. Further, large amount of geometrical foreshortening effect in features near the solar limb causes large uncertainty in the measurements of areas of plages and networks. Due to the uncertainty in areas measurement of features to study the solar variability and in an attempt to find the 'active network' contribution during the maximum phase introduced by Skumanich *et al.* (1984) to explain

the excess in parameters of Ca-K line during the active phase, the new technique of observing the Sun as a function of latitude and integrated over visible longitudes was started in 1986 on daily basis at Kodaikanal tunnel telescope. These observations can be used to study the contribution to the variation in polar regions and quiet regions with solar cycle phase. These observations as a function of latitude and time will yield the information about latitudinal drift of activity and hence the meridional flow in the Sun, which can be used for the modelling of solar dynamo.

7.1 Important Results

We have made observations of the Ca-K line profiles on a day to day basis as a function of latitudes and integrated over the visible longitudes. These data can be used to study the variations in the various parameters of Ca-K line with latitude and solar cycle phase for about two solar cycles. The analysis of the data was done to derive the K_1 and K_2 widths of the Sun as a star using the values of K_1 and K_2 widths computed for different latitudes at an interval of 10°. The values of K_1 and K_2 widths of Sun as a star obtained at KO shows good correlation with those obtained at KPNO and NSO/Sac Peak. It may be noted that the average value of K_1 width during the maximum phase of the solar cycle 22 is 0.673 Å and 0.672 Å for cycle 23 (as obtained from the yearly mean data after outlier's removal). But the average values are lower and different during the minimum phases of cycle 22 and 23. Generally it has been observed that occurrence of Sunspots and related chromospheric activity such as Ca-K plages cause variations in the irradiance and Ca-K line parameters. But we find that yearly mean of K_1 width is larger (0.58 ± 0.01 Å) during the minimum phase of cycle 22 as compared to the average value (0.55 ± 0.01 Å) during the minimum phase of cycle 23 (after removal of outliers from the data). The smaller value of K_1 width during the cycle 23 may be because of the extended minimum phase of this cycle. We speculate that the extended minimum phase may lead to lower temperature of the chromosphere or lower small scale chromospheric activity causing the K_1 width to be smaller as compared to that for cycle 22. It may be noted that standard deviation (SD) is 0.01 Å whereas the difference in mean values at two minima is 0.03 Å and large variations are not expected during the minimum phase as seen in the residual plot

of Figure 3.7. K_2 width does not show a significant variations during the minimum phases of cycle 22 and 23. Further, the ratios of K_1/K_2 width are 1.54 and 1.45 during the minimum phase of cycle 22 and 23 respectively, confirm the above mentioned scenario. The plot of K_2 width versus plage areas indicate that K_2 decreases with increasing activity but it shows only $\sim$ 10% variation in the width as compared to $\sim$ 20% variation in K_1 width during these two solar cycles. On an average both K_1 width and plage areas are more during the maximum phase as compared to those during the minimum phase of the solar cycle. But day to day variations in the K_1 and K_2 widths and plage areas do not occur with similar magnitude and thus cause large amount of scatter in the plot of K_1 width versus plage areas. This implies that irradiance variations may occur not only due to large scale solar activity but also because of variations in small scale activity due to enhanced, active and intra-network in quiet regions of the Sun. These finds support from the fact that in 2010-11 when the sunspot activity has started appearing with sunspot number around 25, the K_1 width continues to be minimum implying less chromospheric emission in Ca-K. The effect of extended minimum on the emission in Ca-K line agrees well with the results obtained from the analysis of Ca-K images obtained at Kodaikanal by Singh *et al.* (2012).

We find that remnant K_1 width at middle and lower latitudes representing the small scale (network) solar activity is more during the active phase than that during the minimum phase of the solar cycle. Assuming a linear relation between the K_1 width and the plage area and after accounting for this variation, we find that the scatter in the values of K_1 width on the day to day basis is large. This appears to be caused by variation with different time scales as listed by (Scargle *et al.* 2013). Therefore, contribution due to variation in the small scale activity caused by the network need to be considered in the study of irradiance variation with solar cycle phase. More number of days data per year and analysis with better resolution in latitude are needed to confirm the variations in small scale activity during the different phases of solar cycle. We have found that the magnitude of variations from 35° to 60° goes on decreasing with latitude during the solar cycle and becomes minimum around 60° latitude in both the hemispheres. The distribution of values of K_1 width is narrow for the 55° latitude belts for both the hemispheres during both of the minimum and active period whereas it is broader for the polar and equatorial belts. Generally it is believed that due to dynamo process, the activity because of toroidal field occurs at lower and

further lower latitudes as the solar cycle progresses and the decaying fields (poloidal component) move towards polar regions from the middle latitude belt around 35°.

In the histogram distribution of K_1 width, the FWHM of the distribution is likely to represent the variation of magnetic field during the different phases of solar cycle at that latitude. In other words, it represents difference in magnetic field strength at the maximum and minimum phase of solar cycle. It appears that variations in the K_1 and K_2 widths occur because of variations in the toroidal magnetic field in the equatorial belts up to about 40° latitude and poloidal magnetic field for latitude belts > 40° latitude. Therefore, it can be inferred that variations of about 30% in the K_1 width in the equatorial belts over the solar cycle are because of variations in the toroidal magnetic field that shifted with an average velocity of 1.1° / month (5.1 m s^{-1}) in the northern hemisphere and 1.6° / month (7.5 m s^{-1}) in the southern hemisphere towards the equator. If plages are due to toroidal field those cause about 30% variation in the K_1 line width, then the observed 11% variation in the line width in the polar region should originate from the variation in the magnetic field at polar regions with solar cycle phase.

We may conclude that (1) the Ca-K line profile observations are effective to study the latitudinal variation of solar activity and especially polar region magnetic field (2) no symmetry is found in the northern and southern hemispheres in terms of the speed of shifting toroidal field towards equator (3) no uniformity is found in the speed of movement of poloidal field towards polar regions and (4) less variation in the poloidal field at the middle latitude belts (40 - 60°) as compared to those for the polar regions. These results will have very important implications on the solar dynamo and meridional flow modelling and will be useful for polar activity studies. These findings indicate that continuation of these observations with improved methodology by using a cylindrical lens as an objective to focus the image of the Sun along the latitude direction alone on the slit of the spectrograph to obtain the spectra of Ca-K line will be very valuable data in understanding the drift of activity with latitude, especially in polar regions

We have used rhcode by Uitenbroek to model the observed line profile taken with the new technique of observation at Kodaikanal observatory. After several trials the

combination of Model F and Model XCO, models of bright network and cell interior respectively, developed by fontenla in 1993 where found to be the best model that matches the quiet Sun observed line profile. The Ca-K line parameters like K_1 width, K_2 width, the intensity ratios like K_{2v}/K_3 and K_{2v}/K_{2r} were matching very well with the observed line parameters for this model. Therefore, we planned to use this model, Ca-K line observation and Ca-K features identified from Ca-K images at each latitude to measure the active network component. This will help in solar irradiance modelling. The measurements of K_1 and K_2 widths of Ca-K profile with latitude and time indicate asymmetry in the Northern and Southern hemisphere and confirm the extended minimum phase of the solar cycle 23. We may conclude that the measurements of Ca-K profile as a function of latitude with better resolution and data obtained at higher frequency for more number of days per year is a valuable technique to study solar irradiance variation and possibly solar dynamo.

7.2 Future direction

Meridional flow, is the flow of material along meridian lines from the equator towards the poles at the surface and from the poles to the equator below surface, is the key component of solar dynamo model. But it is difficult to interpret the shift of activity (poloidal fields) in the mid latitude belts (45° and 55°) because of the presence of positive and negative phase differences with 35° belt. The analysis of the data with resolution of 3-5° in latitude and observations for longer period may yield better understanding about the shift in activity in the mid latitude region. This data taken at different latitudes and integrated over visible longitudes can be used further for the modelling solar dynamo. One can feed this data as input in any of the standard dynamo model to understand the Sun's magnetic field generation. Some of the questions raised from the results of Chapter 4, for example, why there are less solar cycle variations in the poloidal field at the mid-latitude belts ($\sim 60°$) as compared to those for the polar region? The detailed confirmation of these findings will have important contribution to the meridional flow modelling.

The flux transport models those include differential rotation, super granular diffusion

and meridional flow (Wang *et al.* 1989; Schrijver *et al.* 2002; Baumann *et al.* 2004) have been used to simulate the evolution, dispersion and cancellation of large-scale magnetic flux at the solar surface. The importance of the meridional flow in determining the structure (DeVore *et al.* 1984; Sheeley *et al.* 1989) and the strength (Wang *et al.* 2002; Schrijver and Liu 2008) of polar fields has been emphasized in such studies. Dikpati *et al.* (2004) included the temporal variations of the subsurface meridional flow and a high-latitude reverse cell in a flux transport dynamo to model the polar reversal in cycle 23. Helioseismology also has indicated strong variations and the appearance of a subsurface, countercell flow developing at high-latitudes (Haber *et al.* 2002; González Hernández *et al.* 2006). Likewise, theory and global convection simulation suggest multiple cells (Durney 1996; Brun and Toomre 2002). In view of the above models, it is important to study in more details the variations in the shift of activity with latitude and time for different solar cycle and invoke the varying flow pattern found for the first time by us, to investigate the reasons for the variations in the magnitude of solar cycles.

Bibliography

Athay, R. G. and Skumanich, A., 1968, "Emission Cores in H and K Lines. IV: Center-to-Limb Variation", *Solar Phys.*, **4**, 176–184. [DOI], [ADS]

Athay, R. G. and Thomas, R. N., 1961, *Physics of the solar chromosphere*. [ADS]

Avrett, E. H., 1985, "Recent thermal models of the chromosphere", in *Chromospheric Diagnostics and Modelling*, (Ed.) Lites, B. W., [ADS]

Babcock, H. W. and Babcock, H. D., 1955, "The Sun's Magnetic Field, 1952-1954.", *Astrophys. J.*, **121**, 349. [DOI], [ADS]

Baumann, I., Schmitt, D., Schüssler, M. and Solanki, S. K., 2004, "Evolution of the large-scale magnetic field on the solar surface: A parameter study", *Astron. Astrophys.*, **426**, 1075–1091. [DOI], [ADS]

Brun, A. S. and Toomre, J., 2002, "Turbulent Convection under the Influence of Rotation: Sustaining a Strong Differential Rotation", *Astrophys. J.*, **570**, 865–885. [DOI], [ADS], [astro-ph/0206196]

Carlsson, M. and Stein, R. F., 1992, "Non-LTE radiating acoustic shocks and CA II K2V bright points", *Astrophys. J. Lett.*, **397**, L59–L62. [DOI], [ADS]

Carlsson, M. and Stein, R. F., 1995, "Does a nonmagnetic solar chromosphere exist?", *Astrophys. J. Lett.*, **440**, L29–L32. [DOI], [ADS], [astro-ph/9411036]

Cebula, R. P. and Deland, M. T., 1998, "Comparisons of the NOAA-11 SBUV/2, UARS SOLSTICE, and UARS SUSIM MG II Solar Activity Proxy Indexes", *Solar Phys.*, **177**, 117–132. [DOI], [ADS]

Chapman, G. A., 1987, "Solar variability due to sunspots and faculae", *J. Geophys. Res.*, **92**, 809–812. [DOI], [ADS]

Charbonneau, P., 2007, "Cross-hemispheric coupling in a Babcock Leighton model of the solar cycle", *Advances in Space Research*, **40**, 899–906. [DOI], [ADS]

Choudhuri, A. R., Schussler, M. and Dikpati, M., 1995, "The solar dynamo with meridional circulation.", *Astron. Astrophys.*, **303**, L29. [ADS]

Choudhuri, A. R., Chatterjee, P. and Jiang, J., 2007, "Predicting Solar Cycle 24 With a Solar Dynamo Model", *Physical Review Letters*, **98**(13), 131103. [DOI], [ADS], [astro-ph/0701527]

DeVore, C. R., Boris, J. P. and Sheeley, Jr., N. R., 1984, "The concentration of the large-scale solar magnetic field by a meridional surface flow", *Solar Phys.*, **92**, 1–14. [DOI], [ADS]

Dikpati, M., de Toma, G., Gilman, P. A., Arge, C. N. and White, O. R., 2004, "Diagnostics of Polar Field Reversal in Solar Cycle 23 Using a Flux Transport Dynamo Model", *Astrophys. J.*, **601**, 1136–1151. [DOI], [ADS]

Durney, B. R., 1996, "On the Influence of Gradients in the Angular Velocity on the Solar Meridional Motions", *Solar Phys.*, **169**, 1–32. [DOI], [ADS]

Engvold, O., 1966, "On the center-limb variation of the H- and K-line of Ca II.", *Astrophysica Norvegica*, **10**, 101. [ADS]

Ermolli, I., Berrilli, F. and Florio, A., 1999, "Solar Irradiance Variations Associated to Quiet Network", in *Magnetic Fields and Solar Processes*, (Eds.) Wilson, A., et al., ESA Special Publication, 448, [ADS]

Ermolli, I., Berrilli, F. and Florio, A., 2003, "A measure of the network radiative properties over the solar activity cycle", *Astron. Astrophys.*, **412**, 857–864. [DOI], [ADS]

Ermolli, I., Marchei, E., Centrone, M., Criscuoli, S., Giorgi, F. and Perna, C., 2009a, "The digitized archive of the Arcetri spectroheliograms. Preliminary results from the analysis of Ca II K images", *Astron. Astrophys.*, **499**, 627–632. [DOI], [ADS]

Ermolli, I., Solanki, S. K., Tlatov, A. G., Krivova, N. A., Ulrich, R. K. and Singh, J., 2009b, "Comparison Among Ca II K Spectroheliogram Time Series with an Application to Solar Activity Studies", *Astrophys. J.*, **698**, 1000–1009. [DOI], [ADS]

Fligge, M. and Solanki, S. K., 2000a, "Properties of Flux Tubes and the Relation with Solar Irradiance Variability", *Journal of Astrophysics and Astronomy*, **21**, 275. [DOI], [ADS]

Fligge, M. and Solanki, S. K., 2000b, "The solar spectral irradiance since 1700", *Geophys. Res. Lett.*, **27**, 2157–2160. [DOI], [ADS]

Floyd, L. E., Reiser, P. A., Crane, P. C., Herring, L. C., Prinz, D. K. and Brueckner, G. E., 1998, "Solar Cycle 22 UV Spectral Irradiance Variability: Current Measurements by SUSIM UARS", *Solar Phys.*, **177**, 79–87. [DOI], [ADS]

Fontenla, J. M., Avrett, E. H. and Loeser, R., 1991, "Energy balance in the solar transition region. II - Effects of pressure and energy input on hydrostatic models", *Astrophys. J.*, **377**, 712–725. [DOI], [ADS]

Fontenla, J. M., Avrett, E. H. and Loeser, R., 1993, "Energy balance in the solar transition region. III - Helium emission in hydrostatic, constant-abundance models with diffusion", *Astrophys. J.*, **406**, 319–345. [DOI], [ADS]

Fontenla, J. M., Avrett, E., Thuillier, G. and Harder, J., 2006, "Semiempirical Models of the Solar Atmosphere. I. The Quiet- and Active Sun Photosphere at Moderate Resolution", *Astrophys. J.*, **639**, 441–458. [DOI], [ADS]

Fontenla, J. M., Curdt, W., Haberreiter, M., Harder, J. and Tian, H., 2009, "Semiempirical Models of the Solar Atmosphere. III. Set of Non-LTE Models for Far-Ultraviolet/Extreme-Ultraviolet Irradiance Computation", *Astrophys. J.*, **707**, 482–502. [DOI], [ADS]

Foukal, P. and Lean, J., 1988, "Magnetic modulation of solar luminosity by photospheric activity", *Astrophys. J.*, **328**, 347–357. [DOI], [ADS]

Foukal, P., Harvey, K. and Hill, F., 1991, "Do changes in the photospheric magnetic network cause the 11 year variation of total solar irradiance?", *Astrophys. J. Lett.*, **383**, L89–L92. [DOI], [ADS]

Foukal, P., Fröhlich, C., Spruit, H. and Wigley, T. M. L., 2006, "Variations in solar luminosity and their effect on the Earth's climate", *Nature*, **443**, 161–166. [DOI], [ADS]

Foukal, P., Bertello, L., Livingston, W. C., Pevtsov, A. A., Singh, J., Tlatov, A. G. and Ulrich, R. K., 2009, "A Century of Solar Ca ii Measurements and Their Implication for Solar UV Driving of Climate", *Solar Phys.*, **255**, 229–238. [DOI], [ADS]

Froehlich, C., Foukal, P. V., Hickey, J. R., Hudson, H. S. and Willson, R. C., 1991, "Solar irradiance variability from modern measurements", in *The Sun in Time*, (Eds.) Sonett, C. P., Giampapa, M. S., Matthews, M. S., [ADS]

Fröhlich, C. and Lean, J., 1998, "The Sun's total irradiance: Cycles, trends and related climate change uncertainties since 1976", *Geophys. Res. Lett.*, **25**, 4377–4380. [DOI], [ADS]

González Hernández, I., Komm, R., Hill, F., Howe, R., Corbard, T. and Haber, D. A., 2006, "Meridional Circulation Variability from Large-Aperture Ring-Diagram Analysis of Global Oscillation Network Group and Michelson Doppler Imager Data", *Astrophys. J.*, **638**, 576–583. [DOI], [ADS]

Haber, D. A., Hindman, B. W., Toomre, J., Bogart, R. S., Larsen, R. M. and Hill, F., 2002, "Evolving Submerged Meridional Circulation Cells within the Upper Convection Zone Revealed by Ring-Diagram Analysis", *Astrophys. J.*, **570**, 855–864. [DOI], [ADS]

Haigh, J. D. and Blackburn, M., 2006, "Solar Influences on Dynamical Coupling Between the Stratosphere and Troposphere", *Space Sci. Rev.*, **125**, 331–344. [DOI], [ADS]

Hale, G. E., 1919, "Preliminary results of a comparative test of the 60-inch and 100-inch telescopes of the Mount Wilson Observatory (abstract)", *Popular Astronomy*, **27**, 563. [ADS]

Harvey, K. and Harvey, J., 1974, "A Statistical Study of Ephemeral Active Regions in 1970 and 1973", in *Bulletin of the American Astronomical Society*, Bulletin of the American Astronomical Society, 6, [ADS]

Harvey, K. L. and White, O. R., 1999, "What is solar cycle minimum?", *J. Geophys. Res.*, **104**, 19 759–19 764. [DOI], [ADS]

Hathaway, D. H., 1996, "Doppler Measurements of the Sun's Meridional Flow", *Astrophys. J.*, **460**, 1027. [DOI], [ADS]

Hathaway, D. H. and Rightmire, L., 2010, "Variations in the Sun's Meridional Flow over a Solar Cycle", *Science*, **327**, 1350–. [DOI], [ADS]

Hathaway, D. H., Nandy, D., Wilson, R. M. and Reichmann, E. J., 2003, "Evidence That a Deep Meridional Flow Sets the Sunspot Cycle Period", *Astrophys. J.*, **589**, 665–670. [DOI], [ADS]

Howard, R., 1959, "Observations of Solar Magnitic Fields.", *Astrophys. J.*, **130**, 193. [DOI], [ADS]

Howard, R. and Labonte, B. J., 1981, "Surface magnetic fields during the solar activity cycle", *Solar Phys.*, **74**, 131–145. [DOI], [ADS]

Jewell, L. E., 1896, "The Coincidence of Solar and Metallic Lines. a Study of the Appearence of Lines in the Spectra of the Electric Arc and the Sun.", *Astrophys. J.*, **3**, 89. [DOI], [ADS]

Jiang, J., Cameron, R., Schmitt, D. and Schüssler, M., 2009, "Countercell Meridional Flow and Latitudinal Distribution of the Solar Polar Magnetic Field", *Astrophys. J. Lett.*, **693**, L96–L99. [DOI], [ADS]

Jin, C. and Wang, J., 2011, "Vector Magnetic Fields of A Solar Polar Region", *Astrophys. J.*, **732**, 4. [DOI], [ADS]

Kariyappa, R. and Pap, J. M., 1996, "Contribution of Chromospheric Features to UV Irradiance Variability from Spatially-Resolved CA II K Spectroheliograms,", *Solar Phys.*, **167**, 115–123. [DOI], [ADS]

Keil, S. L. and Worden, S. P., 1984, "Variations in the solar calcium K line 1976-1982", *Astrophys. J.*, **276**, 766–781. [DOI], [ADS]

Krivova, N. A. and Solanki, S. K., 2005, "Reconstruction of solar UV irradiance", *Advances in Space Research*, **35**, 361–364. [DOI], [ADS]

Krivova, N. A., Balmaceda, L. and Solanki, S. K., 2007, "Reconstruction of solar total irradiance since 1700 from the surface magnetic flux", *Astron. Astrophys.*, **467**, 335–346. [DOI], [ADS]

Kumara, S. T., Kariyappa, R., Zender, J. J., Giono, G., Delouille, V., Chitta, L. P., Damé, L., Hochedez, J.-F., Verbeeck, C., Mampaey, B. and Doddamani, V. H., 2014,

"Segmentation of coronal features to understand the solar EUV and UV irradiance variability", *Astron. Astrophys.*, **561**, A9. [DOI], [ADS]

Lean, J., 1989, "Contribution of ultraviolet irradiance variations to changes in the sun's total irradiance", *Science*, **244**, 197–200. [DOI], [ADS]

Lean, J., 1997, "The Sun's Variable Radiation and Its Relevance For Earth", *Ann. Rev. Astron. Astrophys.*, **35**, 33–67. [DOI], [ADS]

Lean, J. L., Cook, J., Marquette, W. and Johannesson, A., 1998, "Magnetic Sources of the Solar Irradiance Cycle", *Astrophys. J.*, **492**, 390. [DOI], [ADS]

Leighton, R. B., 1959, "Observations of Solar Magnetic Fields in Plage Regions.", *Astrophys. J.*, **130**, 366. [DOI], [ADS]

Leighton, R. B., 1964, "Transport of Magnetic Fields on the Sun.", *Astrophys. J.*, **140**, 1547. [DOI], [ADS]

Leighton, R. B., Noyes, R. W. and Simon, G. W., 1962, "Velocity Fields in the Solar Atmosphere. I. Preliminary Report.", *Astrophys. J.*, **135**, 474. [DOI], [ADS]

Lemaire, P., Gouttebroze, P., Vial, J. C. and Artzner, G. E., 1981, "Physical properties of the solar chromosphere deduced from optically thick lines. I - Observations, data reduction, and modelling of an average plage", *Astron. Astrophys.*, **103**, 160–176. [ADS]

Liu, S.-Y. and Smith, E. V. P., 1972, "Characteristics of the Ca ii K-line profiles in the quiet Sun", *Solar Phys.*, **24**, 301–309. [DOI], [ADS]

Livingston, W., Wallace, L., White, O. R. and Giampapa, M. S., 2007a, "Sun-as-a-Star Spectrum Variations 1974-2006", *Astrophys. J.*, **657**, 1137–1149. [DOI], [ADS], [arXiv:astro-ph/0% 612554]

Livingston, W., Wallace, L., White, O. R. and Giampapa, M. S., 2007b, "Sun-as-a-Star Spectrum Variations 1974-2006", *Astrophys. J.*, **657**, 1137–1149. [DOI], [ADS], [astro-ph/0612554]

Makarov, V. I. and Tlatov, A. G., 1999, "On the Large-Scale Magnetic Field and Sunspot Cycles", in *Magnetic Fields and Solar Processes*, (Eds.) Wilson, A., et al., ESA Special Publication, 448, [ADS]

Makarov, V. I., Tlatov, A. G. and Callebaut, D. K., 2004, "Long-Term Changes of Polar Activity of the Sun", *Solar Phys.*, **224**, 49–59. [DOI], [ADS]

Maltby, P., Avrett, E. H., Carlsson, M., Kjeldseth-Moe, O., Kurucz, R. L. and Loeser, R., 1986, "A new sunspot umbral model and its variation with the solar cycle", *Astrophys. J.*, **306**, 284–303. [DOI], [ADS]

Milkey, R. W. and Mihalas, D., 1973, "Resonance-Line Transfer with Partial Redistribution: a Preliminary Study of Lyman a in the Solar Chromosphere", *Astrophys. J.*, **185**, 709–726. [DOI], [ADS]

Morrill, J. S., Floyd, L. and McMullin, D., 2011, "The Solar Ultraviolet Spectrum Estimated Using the Mg ii Index and Ca ii K Disk Activity", *Solar Phys.*, **269**, 253–267. [DOI], [ADS]

Muñoz-Jaramillo, A., Balmaceda, L. A. and DeLuca, E. E., 2013, "Using the Dipolar and Quadrupolar Moments to Improve Solar-Cycle Predictions Based on the Polar Magnetic Fields", *Physical Review Letters*, **111**(4), 041106. [DOI], [ADS], [arXiv:1308.2038 [astro-ph.SR]]

Muller, R. and Roudier, T., 1994, "Latitude and cycle variations of the photospheric network", *Solar Phys.*, **152**, 131–137. [DOI], [ADS]

Nindos, A. and Zirin, H., 1998, "Properties and Motions of Ellerman Bombs", *Solar Phys.*, **182**, 381–392. [DOI], [ADS]

Oranje, B. J., 1983, "The CA II K emission from the sun as a star. II - The plage emission profile", *Astron. Astrophys.*, **124**, 43–49. [ADS]

Ortiz, A. and Rast, M., 2005, "How good is the Ca II K as a proxy for the magnetic flux?", *Mem. Soc. Astron. Ital.*, **76**, 1018. [ADS]

Ortiz, A., Solanki, S. K., Domingo, V., Fligge, M. and Sanahuja, B., 2002, "On the intensity contrast of solar photospheric faculae and network elements", *Astron. Astrophys.*, **388**, 1036–1047. [DOI], [ADS], [astro-ph/0207008]

Pap, J. M., Floyd, L., Lee, R. B., Parker, D., Puga, L., Ulrich, R., Varadi, F. and Viereck, R., 1997, "Long-Term Variations in Total Solar and UV Irradiances", in *Correlated Phenomena at the Sun, in the Heliosphere and in Geospace*, (Ed.) Wilson, A., ESA Special Publication, 415, [ADS]

Pasachoff, J. M. and Zirin, H., 1971, "On K-Line Central Reversals", *Solar Phys.*, **18**, 27–28. [DOI], [ADS]

Pevtsov, A. A., Bertello, L. and Uitenbroek, H., 2013, "On Possible Variations of Basal Ca II K Chromospheric Line Profiles with the Solar Cycle", *Astrophys. J.*, **767**, 56. [DOI], [ADS]

Priyal, M., Singh, J., Ravindra, B., Priya, T. G. and Amareswari, K., 2014, "Long Term Variations in Chromospheric Features from Ca-K Images at Kodaikanal", *Solar Phys.*, **289**, 137–152. [DOI], [ADS]

Rammacher, W. and Ulmschneider, P., 1992, "Acoustic waves in the solar atmosphere. IX - Three minute pulsations driven by shock overtaking", *Astron. Astrophys.*, **253**, 586–600. [ADS]

Raouafi, N.-E., Harvey, J. W. and Henney, C. J., 2007, "Latitude Distribution of Polar Magnetic Flux in the Chromosphere Near Solar Minimum", *Astrophys. J.*, **669**, 636–641. [DOI], [ADS]

Rybicki, G. B. and Hummer, D. G., 1991, "An accelerated lambda iteration method for multilevel radiative transfer. I - Non-overlapping lines with background continuum", *Astron. Astrophys.*, **245**, 171–181. [ADS]

Rybicki, G. B. and Hummer, D. G., 1992, "An accelerated lambda iteration method for multilevel radiative transfer. II - Overlapping transitions with full continuum", *Astron. Astrophys.*, **262**, 209–215. [ADS]

Scargle, J. D., Keil, S. L. and Worden, S. P., 2013, "Solar Cycle Variability and Surface Differential Rotation from Ca II K-line Time Series Data", *Astrophys. J.*, **771**, 33. [DOI], [ADS], [arXiv:1303.6303 [astro-ph.SR]]

Schatten, K. H., Scherrer, P. H., Svalgaard, L. and Wilcox, J. M., 1978, "Using dynamo theory to predict the sunspot number during solar cycle 21", *Geophys. Res. Lett.*, **5**, 411–414. [DOI], [ADS]

Schmidt, H. and Brasseur, G. P., 2006, "The Response of the Middle Atmosphere to Solar Cycle Forcing in the Hamburg Model of the Neutral and Ionized Atmosphere", *Space Sci. Rev.*, **125**, 345–356. [DOI], [ADS]

Schrijver, C. J., 1993, "Relations between the photospheric magnetic field and the emission from the outer atmosphere of cool stars. III - The chromospheric emission from individual flux tubes", *Astron. Astrophys.*, **269**, 395–402. [ADS]

Schrijver, C. J. and Liu, Y., 2008, "The Global Solar Magnetic Field Through a Full Sunspot Cycle: Observations and Model Results", *Solar Phys.*, **252**, 19–31. [DOI], [ADS]

Schrijver, C. J., Giommi, P., Dobson, A. K. and Radick, R. R., 1990, "The relationship between EXOSAT soft X-ray and Mt. Wilson CA II H+K flux densities", in *Cool Stars, Stellar Systems, and the Sun*, (Ed.) Wallerstein, G., Astronomical Society of the Pacific Conference Series, 9, [ADS]

Schrijver, C. J., De Rosa, M. L. and Title, A. M., 2002, "What Is Missing from Our Understanding of Long-Term Solar and Heliospheric Activity?", *Astrophys. J.*, **577**, 1006–1012. [DOI], [ADS]

Sheeley, N. R., Wang, Y.-M. and Harvey, J. W., 1989, "The effect of newly erupting flux on the polar coronal holes", *Solar Phys.*, **119**, 323–340. [DOI], [ADS]

Sheeley, Jr., N. R., 1967, "The Average Profile of the Solar K-Line during the Sunspot Cycle", *Astrophys. J.*, **147**, 1106. [DOI], [ADS]

Shine, R. A., Milkey, R. W. and Mihalas, D., 1975, "Resonance line transfer with partial redistribution. VI - The CA II K-line in solar-type stars", *Astrophys. J.*, **201**, 222–224. [DOI], [ADS]

Sindhuja, G. and Singh, J., 2015, "Temporal Variation of Ca-K Line Profile of the Sun during the Solar Cycle 22 and 23", *Journal of Astrophysics and Astronomy*, **36**, 81–101. [DOI], [ADS]

Sindhuja, G., Singh, J. and Ravindra, B., 2014, "Study of Meridional Flow Using Ca-K Line Profiles during Solar Cycles 22 and 23", *Astrophys. J.*, **792**, 22. [DOI], [ADS]

Sindhuja, G., Singh, J. and Priyal, M., 2015, "Chromospheric variations with solar cycle phase using imaging and spectroscopic studies", *Mon. Not. Roy. Astron. Soc.*, **448**, 2798–2809. [DOI], [ADS]

Singh, J, 1989, "A new technique to study the variability of the Sun", *Kodaikanal Obs. Bull*, **9**, 159–164

Singh, J. and Bappu, M. K. V., 1981, "A dependence on solar cycle of the size of the Ca/+/ network", *Solar Phys.*, **71**, 161–168. [DOI], [ADS]

Singh, J., Gholami, I. and Muneer, S., 2004, "Variation in the network flux as derived from the Calcium K-line profiles as function of latitude and solar cycle phase", *Advances in Space Research*, **34**, 265–268. [DOI], [ADS]

Singh, J., Belur, R., Raju, S., Pichaimani, K., Priyal, M., Gopalan Priya, T. and Kotikalapudi, A., 2012, "Determination of the chromospheric quiet network element area index and its variation between 2008 and 2011", *Research in Astronomy and Astrophysics*, **12**, 201–211. [DOI], [ADS]

Sivaraman, K. R., 1984, "CA II K bright points and the solar cycle", *Solar Phys.*, **94**, 235–238. [DOI], [ADS]

Sivaraman, K. R. and Livingston, W. C., 1982, "CA II K2V spectral features and their relation to small-scale photospheric magnetic fields", *Solar Phys.*, **80**, 227–231. [DOI], [ADS]

Sivaraman, K. R., Singh, J., Bagare, S. P. and Gupta, S. S., 1987, "Chromospheric CA II K-line variations in the sun as a star over a solar cycle", *Astrophys. J.*, **313**, 456–462. [DOI], [ADS]

Skumanich, A., Smythe, C. and Frazier, E. N., 1975, "On the statistical description of inhomogeneities in the quiet solar atmosphere. I - Linear regression analysis and absolute calibration of multichannel observations of the Ca/+/ emission network", *Astrophys. J.*, **200**, 747–764. [DOI], [ADS]

Skumanich, A., Lean, J. L., Livingston, W. C. and White, O. R., 1984, "The sun as a star - Three-component analysis of chromospheric variability in the calcium K line", *Astrophys. J.*, **282**, 776–783. [DOI], [ADS]

Smith, E. V. P., 1960, "Emission Cores in the CA II Lines in Plages.", *Astrophys. J.*, **132**, 202. [DOI], [ADS]

Solanki, S. K. and Fligge, M., 2002, "How much of the solar irradiance variations is caused by the magnetic field at the solar surface?", *Advances in Space Research*, **29**, 1933–1940. [DOI], [ADS]

Solanki, S. K. and Krivova, N. A., 2006, "Solar Variability of Possible Relevance for Planetary Climates", *Space Sci. Rev.*, **125**, 25–37. [DOI], [ADS]

Solanki, S. K. and Unruh, Y. C., 1998, "A model of the wavelength dependence of solar irradiance variations", *Astron. Astrophys.*, **329**, 747–753. [ADS]

Solanki, S. K., Fligge, M. and Unruh, Y. C., 2001, "Variations of the Solar Spectral Irradiance", in *Recent Insights into the Physics of the Sun and Heliosphere: Highlights from SOHO and Other Space Missions*, (Eds.) Brekke, P., Fleck, B., Gurman, J. B., IAU Symposium, 203, [ADS]

Svalgaard, L., Duvall, Jr., T. L. and Scherrer, P. H., 1978, "The strength of the sun's polar fields", *Solar Phys.*, **58**, 225–239. [DOI], [ADS]

Thuillier, G., 2004, "Variation of the solar diameter: a proxy for solar activity", in *35th COSPAR Scientific Assembly*, (Ed.) Paillé, J.-P., COSPAR Meeting, 35, [ADS]

Tlatov, A. G., Pevtsov, A. A. and Singh, J., 2009, "A New Method of Calibration of Photographic Plates from Three Historic Data Sets", *Solar Phys.*, **255**, 239–251. [DOI], [ADS]

Uitenbroek, H., 1989, "Operator perturbation method for multi-level line transfer with partial redistribution", *Astron. Astrophys.*, **213**, 360–370. [ADS]

Uitenbroek, H., 2001, "Multilevel Radiative Transfer with Partial Frequency Redistribution", *Astrophys. J.*, **557**, 389–398. [DOI], [ADS]

Ulrich, R. K., 2010, "Solar Meridional Circulation from Doppler Shifts of the Fe I Line at 5250 Å as Measured by the 150-foot Solar Tower Telescope at the Mt. Wilson Observatory", *Astrophys. J.*, **725**, 658–669. [DOI], [ADS], [arXiv:1010.0487 [astro-ph.SR]]

Ulrich, R. K. and Tran, T., 2013, "The Global Solar Magnetic FieldIdentification of Traveling, Long-lived Ripples", *Astrophys. J.*, **768**, 189. [DOI], [ADS], [arXiv:1304.1249 [astro-ph.SR]]

Verbeeck, C., Delouille, V., Mampaey, B. and De Visscher, R., 2014, "The SPoCA-suite: Software for extraction, characterization, and tracking of active regions and coronal holes on EUV images", *Astron. Astrophys.*, **561**, A29. [DOI], [ADS]

Vernazza, J. E., Avrett, E. H. and Loeser, R., 1981a, "Structure of the solar chromosphere. III - Models of the EUV brightness components of the quiet-sun", *Astrophys. J. Suppl.*, **45**, 635–725. [DOI], [ADS]

Vernazza, J. E., Avrett, E. H. and Loeser, R., 1981b, "Structure of the solar chromosphere. III - Models of the EUV brightness components of the quiet-sun", *Astrophys. J. Suppl.*, **45**, 635–725. [DOI], [ADS]

Walton, S. R., Preminger, D. G. and Chapman, G. A., 2003, "The Contribution of Faculae and Network to Long-Term Changes in the Total Solar Irradiance", *Astrophys. J.*, **590**, 1088–1094. [DOI], [ADS]

Wang, Y.-M. and Sheeley, Jr., N. R., 1988, "The solar origin of long-term variations of the interplanetary magnetic field strength", *J. Geophys. Res.*, **93**, 11 227–11 236. [DOI], [ADS]

Wang, Y.-M., Nash, A. G. and Sheeley, Jr., N. R., 1989, "Evolution of the sun's polar fields during sunspot cycle 21 - Poleward surges and long-term behavior", *Astrophys. J.*, **347**, 529–539. [DOI], [ADS]

Wang, Y.-M., Sheeley, Jr., N. R. and Lean, J., 2002, "Meridional Flow and the Solar Cycle Variation of the Sun's Open Magnetic Flux", *Astrophys. J.*, **580**, 1188–1196. [DOI], [ADS]

White, O. R., 1996, "Determination of Contributions to Irradiances from Plages, Network and the Quiet Solar Atmosphere", in *Solar Drivers of the Interplanetary and Terrestrial Disturbances*, (Eds.) Balasubramaniam, K. S., Keil, S. L., Smartt, R. N., Astronomical Society of the Pacific Conference Series, 95, [ADS]

White, O. R. and Livingston, W., 1978, "Solar luminosity variation. II - Behavior of calcium H and K at solar minimum and the onset of cycle 21", *Astrophys. J.*, **226**, 679–686. [DOI], [ADS]

White, O. R. and Livingston, W. C., 1981, "Solar luminosity variation. III - Calcium K variation from solar minimum to maximum in cycle 21", *Astrophys. J.*, **249**, 798–816. [DOI], [ADS]

White, O. R. and Suemoto, Z., 1968, "A Measurement of the Solar H and K Profiles", *Solar Phys.*, **3**, 523–530. [DOI], [ADS]

Willson, R. C., 1989, "Space based solar irradiance measurements.", in *New Developments and Applications in Optical Radiometry*, (Eds.) Fox, N. P., Nettleton, D. H., [ADS]

Willson, R. C. and Hudson, H. S., 1988, "Solar luminosity variations in solar cycle 21", *Nature*, **332**, 810–812. [DOI], [ADS]

Withbroe, G. L., 2006, "Quiet Sun Contribution to Variations in the Total Solar Irradiance", *Solar Phys.*, **235**, 369–386. [DOI], [ADS]

Woods, T. N., Prinz, D. K., Rottman, G. J., London, J., Crane, P. C., Cebula, R. P., Hilsenrath, E., Brueckner, G. E., Andrews, M. D., White, O. R., VanHoosier, M. E., Floyd, L. E., Herring, L. C., Knapp, B. G., Pankratz, C. K. and Reiser, P. A., 1996, "Validation of the UARS solar ultraviolet irradiances: Comparison with the ATLAS 1 and 2 measurements", *J. Geophys. Res.*, **101**, 9541–9570. [DOI], [ADS]

Worden, J. and Harvey, J., 2000, "An Evolving Synoptic Magnetic Flux map and Implications for the Distribution of Photospheric Magnetic Flux", *Solar Phys.*, **195**, 247–268. [DOI], [ADS]

Worden, J. R., White, O. R. and Woods, T. N., 1998, "Plage and Enhanced Network Indices Derived from CA II K Spectroheliograms", *Solar Phys.*, **177**, 255–264. [DOI], [ADS]

Zirin, H., 1974, "Studies of K line filtergrams", *Solar Phys.*, **38**, 91–108. [DOI], [ADS]

Zirker, J. B., 1967, "On the Motions of Chromospheric Fine-Structure in a Weak Plage", *Solar Phys.*, **1**, 204–215. [DOI], [ADS]